

Phosphoric Acid-Catalyzed Formation of Hydrogen-Bonded ortho-Quinone Methides. Enantioselective Cycloaddition with #-Dicarbonyl Compounds toward Benzannulated Oxygen Heterocycles

Fabian Göricke, Stefan Haseloff, Michael Laue, Maximilian Schneider, Thomas Brumme, and Christoph Schneider

J. Org. Chem., **Just Accepted Manuscript** • DOI: 10.1021/acs.joc.0c01375 • Publication Date (Web): 10 Aug 2020

Downloaded from pubs.acs.org on August 11, 2020

Just Accepted

“Just Accepted” manuscripts have been peer-reviewed and accepted for publication. They are posted online prior to technical editing, formatting for publication and author proofing. The American Chemical Society provides “Just Accepted” as a service to the research community to expedite the dissemination of scientific material as soon as possible after acceptance. “Just Accepted” manuscripts appear in full in PDF format accompanied by an HTML abstract. “Just Accepted” manuscripts have been fully peer reviewed, but should not be considered the official version of record. They are citable by the Digital Object Identifier (DOI®). “Just Accepted” is an optional service offered to authors. Therefore, the “Just Accepted” Web site may not include all articles that will be published in the journal. After a manuscript is technically edited and formatted, it will be removed from the “Just Accepted” Web site and published as an ASAP article. Note that technical editing may introduce minor changes to the manuscript text and/or graphics which could affect content, and all legal disclaimers and ethical guidelines that apply to the journal pertain. ACS cannot be held responsible for errors or consequences arising from the use of information contained in these “Just Accepted” manuscripts.

Phosphoric Acid-Catalyzed Formation of Hydrogen-Bonded *ortho*-Quinone Methides. Enantioselective Cycloaddition with β -Dicarbonyl Compounds toward Benzannulated Oxygen Heterocycles

Fabian Göricke,[†] Stefan Haseloff,[†] Michael Laue,[†] Maximilian Schneider,[†] Thomas Brumme,^{‡,§} and Christoph Schneider^{*,†}

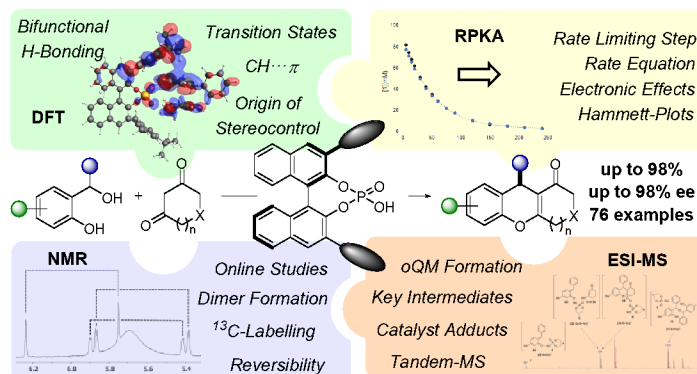
[†]Institut für Organische Chemie, Universität Leipzig, Johannisallee 29, 04103 Leipzig, Germany

[‡]Wilhelm-Ostwald-Institut für Physikalische und Theoretische Chemie, Linnéstraße 2, 04103, Leipzig, Germany.

[§]Theoretische Chemie, Technische Universität Dresden, Bergstraße 66c, 01062 Dresden, Germany.

Supporting Information Placeholder

KEYWORDS: Asymmetric synthesis · mechanistic studies · chromene · quinone methide · chiral phosphoric acid · xanthenone



ABSTRACT: A full account of the Brønsted acid-catalyzed, enantioselective synthesis of *4H*-chromenes and *1H*-xanthen-1-ones from *ortho*-hydroxyl benzyl alcohols and β -dicarbonyl compounds is provided. The central step of our strategy is the BINOL-phosphoric acid-catalyzed, enantioselective cycloaddition of β -diketones, β -keto nitriles, and β -keto esters to in situ generated, hydrogen-bonded *ortho*-quinone methides. Upon acid-promoted dehydration the desired products were obtained with generally excellent yields and enantioselectivity. Detailed mechanistic studies including online-NMR- and ESI-MS-measurements were conducted to identify relevant synthetic intermediates. A reversible formation of a dimer from the starting alcohol and the reactive *ortho*-quinone methide in an off-cycle equilibrium was observed providing a reservoir from which the *ortho*-quinone methide can be regenerated and introduced into the catalytic cycle again. Reaction progress kinetic analysis was utilized to determine kinetic profiles and rate constants of the reaction uncovering *ortho*-quinone methide formation as the rate limiting step. In combination with Hammett plots these studies document the relationship between *ortho*-quinone methide stabilization by electronic effects provided by the substituents and the reaction rate of the described process. In addition, DFT-calculations reveal a concerted, yet highly asynchronous [4+2]-cycloaddition pathway and an attractive CH- π -interaction between the catalyst's *t*Bu-group and the *ortho*-quinone methide as important stereochemical control element.

INTRODUCTION

Ortho-quinone methides featuring a dearomatized 2-alkylidene cyclohexadienone system were first proposed as transient intermediates by Fries in 1906.^{1a} A few members of the related, but more stable *ortho*-naphthoquinone

methides were even isolated as crystalline solids at the time.^{1b} Their strong tendency to undergo cycloaddition reactions with themselves thereby producing dimers and trimers, however, has prevented their synthetic use for much of the remainder of the century. Nature, on the other

hand, beautifully relies on the facile formation and reactivity of *ortho*-quinone methides for the biological activity of vitamins E and K as well several medicinally relevant natural products such as the anthracycline antibiotics and mitomycin.²

It was not until 1959 that Gardner et al. obtained the first spectroscopic proof of an isolated *ortho*-quinone methide, albeit in an impure state.³ In 1986 the first x-ray structure of a stable *ortho*-quinone methide was reported by Pochini et al. which additionally proved the *E*-configuration of the methide substituent.⁴ Subsequently, Amouri and coworkers prepared various transition metal- π -complexes with *ortho*-quinone methides acting as diene ligands from which they obtained crystal structure analyses.⁵

As highly polarized, electronpoor 1-oxabutadienes *ortho*-quinone methides primarily engage electronrich 2π -systems in cycloaddition and conjugate addition reactions both of which lead to the reconstitution of the aromatic π -system. A broad range of methods have been developed to access *ortho*-quinone methides in situ from stable precursors and comprehensive review articles on their preparation and reactions are available in the literature.⁶ In particular, the first account by Pettus et al. describing the state of the art in 2002 sparked the interest of the chemical community and laid the foundation for the further development of the field.^{6a}

In addition to methodology studies, natural product syntheses have relied heavily on the use of *ortho*-quinone methide intermediates in recent years.⁷ In most cases, hetero Diels-Alder reactions conducted both in intra- and intermolecular fashion have been employed to forge otherwise difficult bond constructions in sterically highly congested situations. A notable and very instructive example in this respect is the synthesis of the central tricyclic 6-5-5-ring system of the naphthohydroquinone dimer rubioncolin B by the Trauner group.⁸

Only in the previous decade or so have catalytic, enantioselective transformations of *ortho*-quinone methides been reported both with chiral metal and organocatalysts. Prior to 2014 the groups of Sigman,⁹ Lectka,¹⁰ Schaus,¹¹ Ye¹² and Scheidt¹³ developed Palladium-, cinchona alkaloid-, BINOL-, and *N*-heterocyclic carbene-catalyzed, enantioselective processes, respectively.

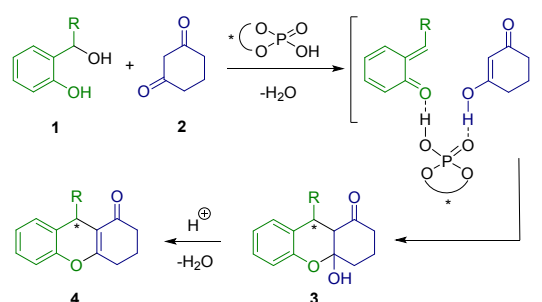
More recently, chiral Rhodium,¹⁴ Scandium,¹⁵ and Palladium¹⁶ complexes have emerged as powerful transition metal catalysts for asymmetric reactions of *ortho*-quinone methides. In the area of enantioselective organocatalysis, squareamides,¹⁷ (thio)ureas,¹⁸ biphenols,¹⁹ phosphines,²⁰ amines,²¹ *N*-heterocyclic carbenes²² and oxazaborolidinium ions²³ have been established as chiral catalysts since 2014.

Brønsted acid-catalyzed strategies starting out from *ortho*-hydroxy benzyl alcohols as substrates were first developed by the groups of Bach and Rueping in 2011 although the formation of *ortho*-quinone methides was not fully recognized at the time. Thus, Bach et al. established a phosphoric acid-catalyzed, enantioselective addition of indoles producing arylindolylmethanes with moderate enantioselectivity,²⁴ whereas Rueping developed a catalytic

6π -electrocyclization reaction furnishing *2H*-chromenes with exceptional enantioselectivity.²⁵

Our concept which we initially reported in 2014 followed the same logic and built on the Brønsted acid-catalyzed in situ generation of *ortho*-quinone methides from the corresponding *ortho*-hydroxy benzyl alcohols **1** and subsequent reaction with 1,3-cyclohexanedione (**2a**) (Scheme 1).²⁶ We speculated that a chiral phosphoric acid would easily dehydrate the benzyl alcohol and produce a hydrogen-bonded *ortho*-quinone methide intermediate which would engage the enol tautomer of **2a** in a highly ordered transition state via bifunctional activation. Ensuing [4+2]-cycloaddition with 1,3-cyclohexanedione (**2a**) would then produce lactol **3** which was likely to be dehydrated to *1H*-xanthen-1-one **4** either in situ or with added external acid.

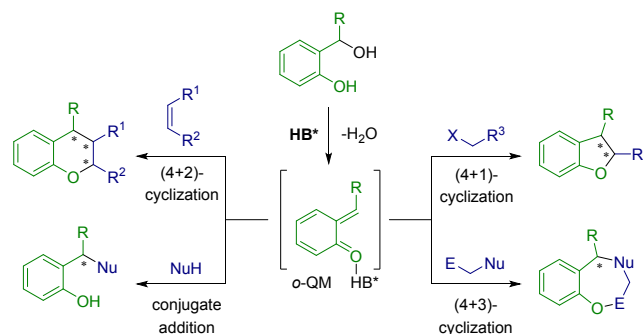
Scheme 1. Conceptualization of the Synthesis of *1H*-Xanthen-1-ones **4**.



This concept was then successfully put into practice and *1H*-xanthen-1-ones **4** were obtained with good chemical yields and enantioselectivities across a limited substrate scope.²⁶ Interestingly, the Rueping group published very similar results a little later.²⁷ Moreover, Sun and co-workers reported phosphoric acid-catalyzed conjugate addition reactions of Hantzsch esters and indoles to β,β -disubstituted *ortho*-quinone methides independently.²⁸

Subsequent to these initial discoveries a stream of additional studies on Brønsted acid-catalyzed reactions of *ortho*-quinone methides was published thus establishing a general platform for the enantioselective synthesis of five-, six- and seven-membered benzannulated oxygen heterocycles (Scheme 2).^{29,30}

Scheme 2. Enantioselective, Brønsted Acid-Catalyzed Reactions of *Ortho*-Quinone Methides.



Herein we now present a full account of our investigations on the phosphoric acid-catalyzed, enantioselective cycloaddition of *ortho*-quinone methides with various β -dicarbonyl compounds including a much expanded

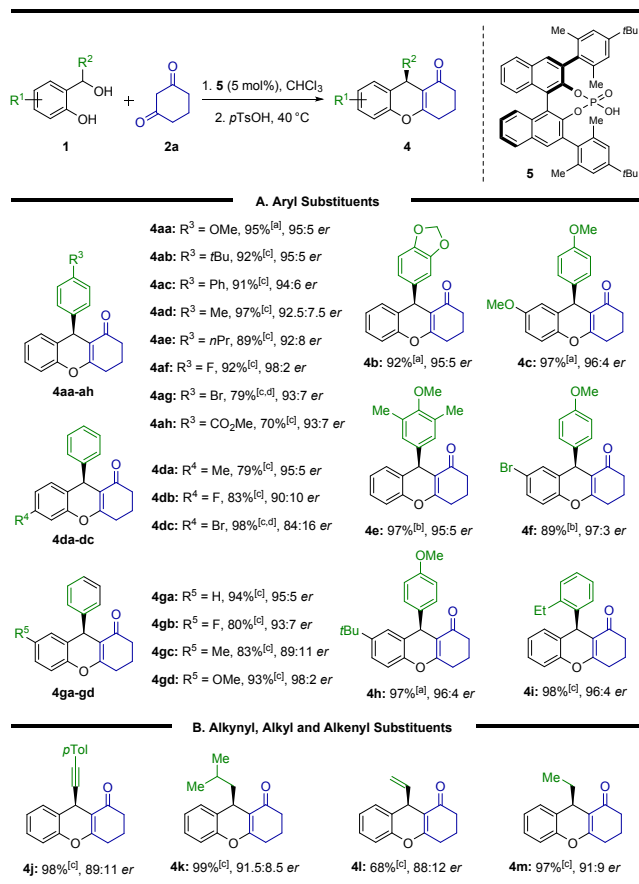
substrate scope and a detailed mechanistic analysis on the basis of spectroscopic, kinetic, and theoretical data.

RESULTS AND DISCUSSION

Our optimized procedure for the catalytic, enantioselective reaction of *ortho*-hydroxy benzyl alcohols **1** and 1,3-cyclohexanedione (**2a**) generally required 5 mol% of phosphoric acid **5** in chloroform at temperatures between 0°C and rt with subsequent addition of *para*-toluenesulfonic acid to effect the dehydration to 1*H*-xanthen-1-ones **4** (Scheme 3).²⁶

The parent substrate **1aa** delivered 9-*para*-methoxyphenyl-1*H*-xanthen-1-one **4aa** with 95% yield and 95:5 *er*. A large variety of differently substituted *ortho*-hydroxy benzhydryl alcohols **1ab-i** was then subjected to these reaction conditions and delivered xanthenones **4ab-i** with equally good yields and excellent enantioselectivity. These examples clearly show that there is a large tolerance with respect to the substitution in both aryl groups. Alkyl-, aryl-, alkoxy-, carboxy- and halogen-substitution was well tolerated and did not deteriorate yield or enantioselectivity. As will be discussed later, there was, however, an effect on the reaction rate. Electron-rich substrates reacted faster than electron-poor substrates. The bromo-substituted xanthenone **4f** gave crystals suitable for X-ray crystallography which proved the absolute configuration of the reaction products.^{26,31} In addition to aryl groups one can as well substitute the β -methide position with alkynyl, alkenyl and even simple alkyl groups which gave rise to products **4j-m** with good to excellent yields and moderate to good enantioselectivities (Scheme 3B).

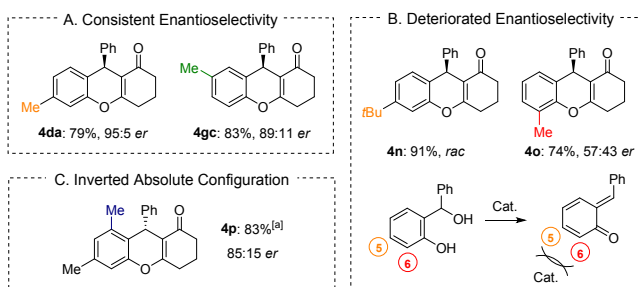
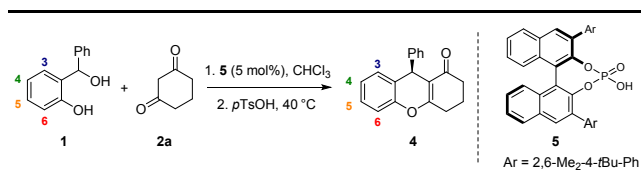
Scheme 3. Phosphoric Acid Catalyzed, Enantioselective Synthesis of 1*H*-xanthen-1-ones.



Reaction conditions: 0.20 mmol (1.0 equiv.) *ortho*-hydroxy benzyl alcohol **1**, 0.30 mmol (1.5 equiv.) 1,3-cyclohexanedione (**2a**), catalyst **5** (5 mol%), 1.60 mL CHCl₃, 24 h. Reaction temperature: [a] 0°C, [b] 10°C, [c] RT. [d] Increased reaction times. *er* values were determined by HPLC on a chiral stationary phase (see supporting information).

Substrate Binding and Enantioselectivity. Adding a methyl group to various positions within the phenol moiety revealed some interesting insights. Whereas substrates **1da** and **1gc** with either 4- or 5-methyl groups delivered products **4da** and **4gc** with yields and enantioselectivities similar to the previous examples (Scheme 4A), substrate **1o** carrying a 6-methyl substituent (*ortho* to the phenol) furnished xanthenone **4o** with 74% yield, albeit as almost a racemic mixture. Likewise, xanthenone **4n** with R⁵ = *t*Bu was isolated as racemic mixture. Apparently, any substituent adjacent to the forming carbonyl group of the *ortho*-quinone methide and even a very large substituent in the next position prevented efficient binding of the phosphoric acid catalyst to the carbonyl group and deteriorated the enantioselectivity accordingly (Scheme 4B).

Scheme 4. Substitution Pattern in the *ortho*-Quinone Methide Fragment and Enantioselectivity.



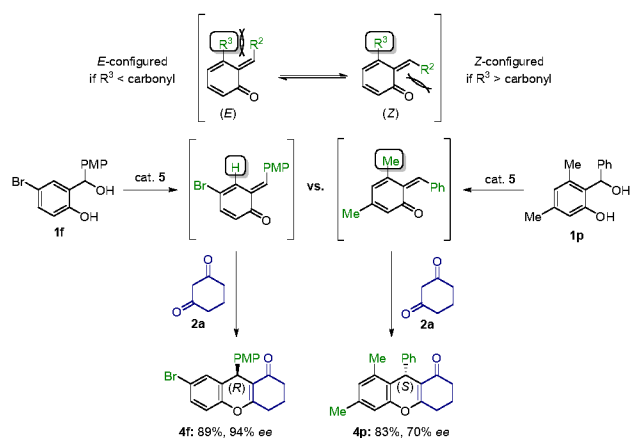
15
16
17
18
19
20

Reaction conditions: 0.20 mmol (1.0 equiv.) *ortho*-hydroxy benzyl alcohol **1**, 0.30 mmol (1.5 equiv.) 1,3-cyclohexanedione (**2a**), catalyst **5** (5 mol%), 1.60 mL CHCl₃, 24 h. [a] Reaction time: 4 d. *er* values were determined by HPLC on a chiral stationary phase (see supporting information).

21
22
23
24
25
26
27
28
29
30

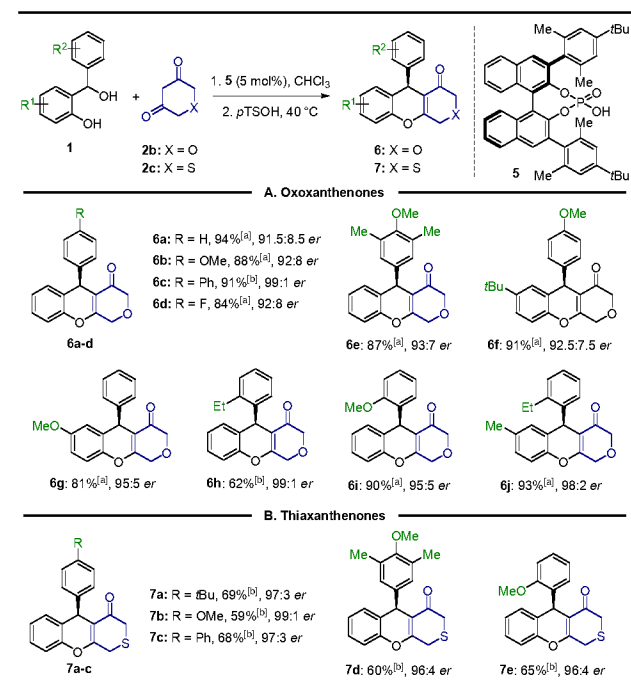
E/Z-Equilibrium and Absolute Configuration. Even more intriguing was the outcome of the reaction of benzhydryl alcohol **1p** (R³ = Me) which furnished product **4p** with moderate enantioselectivity, but an inverted absolute configuration (Scheme 4C).³¹ This is clear indication that the configuration of the forming methide double bond has been inverted from the typical *E*-configuration into a *Z*-configuration due to the steric hindrance imposed by the adjacent methyl substituent (Scheme 5).

Scheme 5. Influence of E/Z-Configuration of the *Ortho*-Quinone Methide on the Absolute Configuration.



Extension to Other β -Dicarbonyls. To further broaden the scope of the process other β -dicarbonyl compounds were employed in this reaction under the optimized reaction conditions as well. Using 3,5-pyridandione (**2b**) and 3,5-thiapyridandione (**2c**) as nucleophiles the corresponding oxa- and thioxanthenones **6a-j** and **7a-e**, respectively, were obtained in yields and enantioselectivities similar to the reactions employing 1,3-cyclohexanedione (**2a**) (Scheme 6).

Scheme 6. Phosphoric Acid Catalyzed, Enantioselective Synthesis of 3-Heteroxanthenones **6** and **7**.

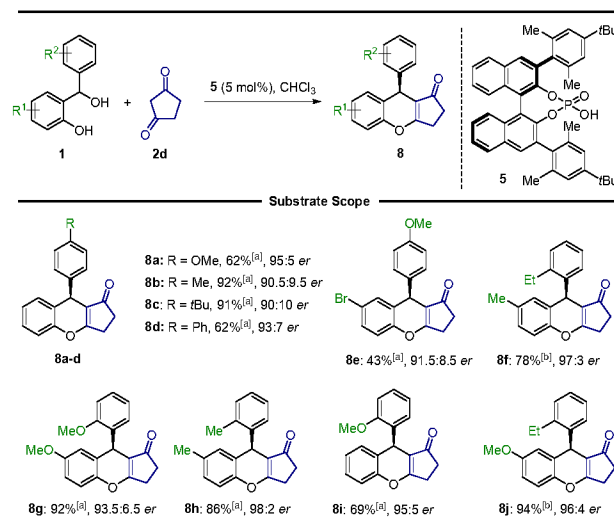


Reaction conditions for **6**: 0.10 mmol (1.0 equiv.) *ortho*-hydroxy benzyl alcohol **1**, 0.15 mmol (1.5 equiv.) 3,5-pyridandione **2b**, catalyst **5** (5mol%), 0.8 mL CHCl₃, 24 h. Reaction conditions for **7**: 0.20 mmol (1.0 equiv.) *ortho*-hydroxy benzyl alcohol **1**, 0.24 mmol (1.2 equiv.) 3,5-thiapyridandione **2c**, catalyst **5** (5mol%), 1.0 mL CHCl₃, 36 h. Reaction temperature: [a] 0°C, [b] rt. *er* values were

determined by HPLC on a chiral stationary phase (see supporting information).

Excellent results were also obtained by utilizing 1,3-cyclopentanone (**2d**) as reaction partner and the cyclopenta[*b*]benzopyranones **8a-j** were isolated with good yields and enantioselectivities (Scheme 7). It is noteworthy that in the latter cases the dehydration of the initially formed lactols occurred rapidly without the necessity to add *para*-toluenesulfonic acid which as we assume is the result of the higher Brønsted acidity of 1,3-cyclopentanone (**2d**). Fortunately, however, **2d** did apparently not compete with the chiral phosphoric acid to catalyze an unselective background reaction.

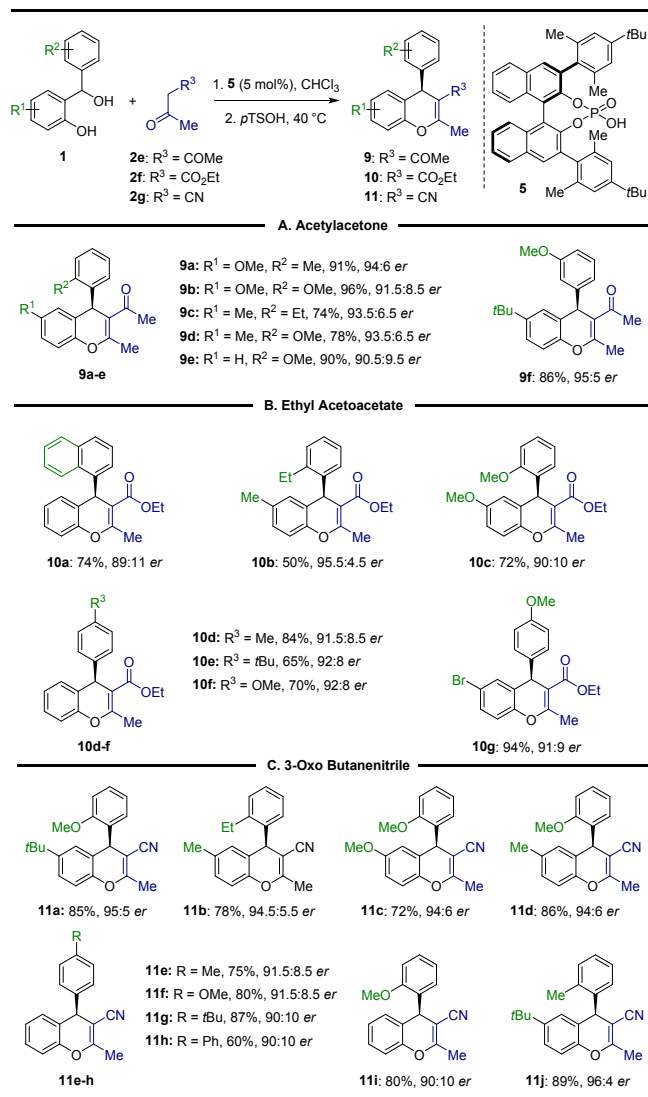
Scheme 7. Phosphoric Acid Catalyzed, Enantioselective Synthesis of Cyclopenta[*b*]benzopyranones **8**.



Reaction conditions: 0.10 mmol (1.0 equiv.) *ortho*-hydroxy benzyl alcohol **1**, 0.15 mmol (1.5 equiv.) 1,3-cyclopentanone **2d**, catalyst **5** (5 mol %), 0.8 mL CHCl₃, 24 h. Reaction temperature: [a] 0°C, [b] rt. *er* values were determined by HPLC on a chiral stationary phase (see supporting information).

Acyclic 1,3-dicarbonyl compounds could be employed as reaction partners as well and delivered the corresponding 4*H*-chromenes as products (Scheme 8). Acetylacetone (**2e**), ethyl acetoacetate (**2f**), and 3-oxo butanenitrile (**2g**) all successfully underwent the reaction and furnished the products **9-11** in generally good yields and enantioselectivities.

Scheme 8. Phosphoric Acid Catalyzed, Enantioselective Synthesis of 4*H*-Chromenes **9-11**.



36
37
38
39

40
41
42

Mechanistic Investigations. We first carried out a number of simple control experiments to shed some initial light on the reaction mechanism.

43
44
45
46
47
48

There was no product formation when benzhydryl alcohols **12a** and **12b** lacking a free phenol moiety were treated with 1,3-cyclohexanedione (**2a**) under the optimized reaction conditions underlining the importance of an in situ generated *ortho*-quinone methide for a successful reaction (Scheme 9A).

49
50
51
52
53
54
55
56
57

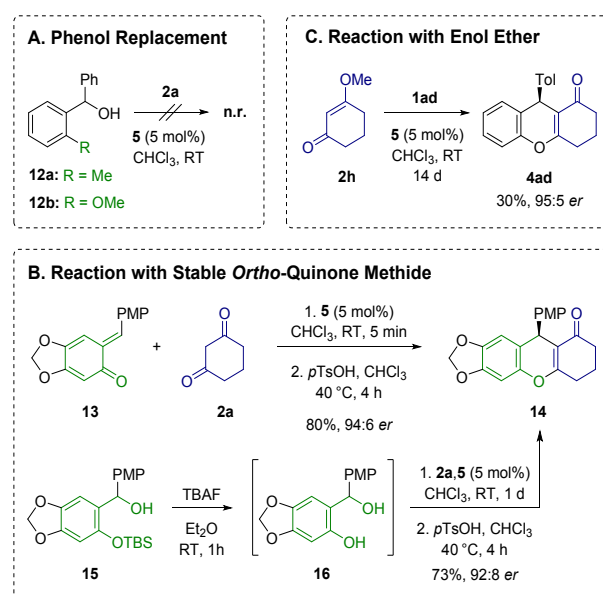
We also synthesized the stable *ortho*-quinone methide **13**³² which furnished xanthenone **14** in 80% yield and 94:6 *er* in direct analogy to the reactions with the benzhydryl alcohols as starting materials (Scheme 9B). Almost identical results were obtained when the presumed precursor of **13**, the free phenol **16**, was subjected to the reaction with 1,3-cyclohexanedione (**2a**) under our standard conditions. For that purpose *ortho*-silyloxy benzhydryl alcohol **15** was employed as starting material and was desilylated with

58
59
60

tetra-*n*-butyl ammonium fluoride to the highly sensitive phenol **16** which had to be isolated quickly and with minimal workup to avoid decomposition. Xanthenone **14** was obtained in yield and enantioselectivity comparable to that observed for the stable *ortho*-quinone methide **13** strongly suggesting that the *ortho*-quinone methide was indeed the central intermediate of the reaction (Scheme 9B).

Finally, we carried out a reaction with enol ether **2h** which gave rise to the formation of xanthenone **4ad** in only 30% yield after 14 d at rt, but the same enantiomeric ratio as for **2a** (Scheme 9C). This result suggests that the enol ether **2h** was unreactive under the reaction conditions. Instead it was slowly hydrolyzed to 1,3-cyclohexanedione (**2a**) with adventitious water under acid catalysis before this then underwent the reaction to furnish the product with the identical enantioselectivity as shown below.

Scheme 9. Control Experiments



61
62
63
64
65
66
67
68
69
70

Kinetic Studies. In order to provide thorough mechanistic information about the turnover-limiting step and the nature of kinetically relevant intermediates, we carried out a detailed kinetic profiling of the catalytic [4+2]-cycloaddition of *ortho*-quinone methides based on Reaction Progress Kinetic Analysis (RPKA).³³

Rate studies were executed under synthetically relevant conditions with **1da** as representative substrate. The experimental data for the concentration of **1da** vs time (Figure 1A, black points) were replotted as reaction rate vs [1da] (Figure 1B). The reaction displayed overall first-order kinetics in *ortho*-hydroxy benzyl alcohol **1da** with a rate constant of $k' = 0.019 \text{ min}^{-1}$. "Different excess" experiment (Figure 1A, red points) with altered initial concentration of **2a** revealed a zero-order dependence on [2a]. The order in catalyst was elucidated with a normalized time scale

analysis.³⁴ The adjustment of the time scale of **[1da]**/t for different catalyst loadings exhibited a reaction order in catalyst of less than 1 (see supporting information). The kinetic modeling of all the experimental data was used to derive an empirical rate law for the reaction of **1da** with **2a** given by the following equations:

$$\text{rate} = k \cdot [\mathbf{1da}] \cdot [\mathbf{5}]^{0.85} = k' \cdot [\mathbf{1da}] \quad (1)$$

$$\text{with } k' = k \cdot [\mathbf{5}]^{0.85} = 0.019 \text{ min}^{-1} \quad (2)$$

The first-order kinetics in **[1da]** and zero-order kinetics in **[2a]** can be rationalized with a rate-limiting formation of the *ortho*-quinone methide.

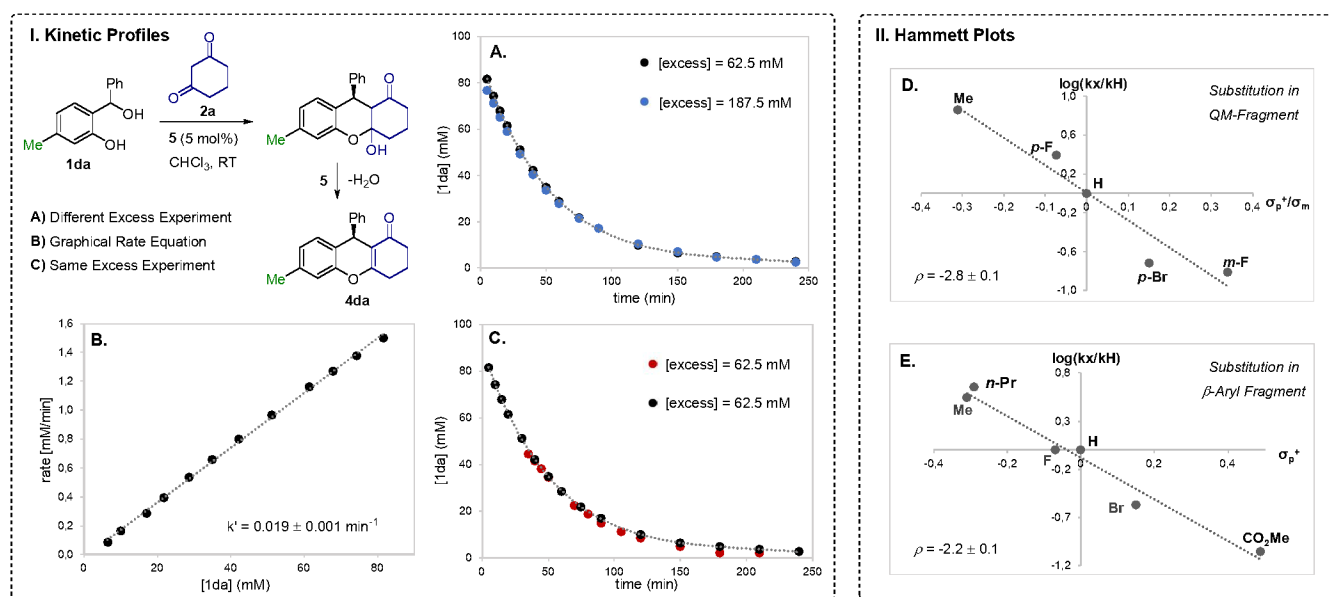


Figure 1. I. Kinetic profiles from the reaction of **1da** and **2a** with **5** under synthetically relevant conditions. **A.** **[1da]** vs time for different excess experiments. **B.** rate vs **[1da]** for standard conditions. The slope of the linear fit represents the rate constant $k' = 0.019 \pm 0.001 \text{ min}^{-1}$. **C.** **[1da]** vs time for same excess experiments. **II** Hammett plots for the reaction of substituted *ortho*-hydroxy benzyl alcohols **1** with **2a** and **5**. **D.** Hammett plot for **1da-dc** and **1ga-gb** with $\rho = -2.8 \pm 0.1$. **E.** Hammett plot for **1ad-ah** and **1ga** with $\rho = -2.2 \pm 0.1$.

We attribute the small deviation from a first-order rate dependence on **[5]** to some degree of dimerization of the phosphoric acid catalyst.³⁵ Moreover, “same excess” experiments confirmed consistent kinetic behavior throughout the course of the entire reaction and revealed the lack of significant catalyst deactivation and the absence of product inhibition (Figure 1C).³³

Hammett Plots. The kinetic data suggests the formation of the *ortho*-quinone methide to be the rate-determining step. Thus, the transition state will be characterized by an increase of positive charge and faster rates are expected for substrates that better stabilize the electron-deficient nature of the *ortho*-quinone methide. We measured the rates of the chiral phosphoric acid-catalyzed addition of **2a** to differently substituted *ortho*-hydroxy benzyl alcohols **1da-dc** and **1ga-gb** with *meta*- and *para*-substituents in the *ortho*-quinone methide fragment. The corresponding Hammett plot reveals a moderate negative value of $\rho = -2.8$ (Figure 1D) which is consistent with a substantial positive charge build-up near the aromatic ring and a loss of aromatic conjugation in the transition state as expected for *ortho*-quinone methide formation.³⁶ Electron donating substituents should exert a stabilizing and accelerating effect whereas electron withdrawing substituents lower the reaction rates by further destabilization of the already electron deficient *ortho*-quinone methide. In addition, the corresponding Hammett relation for *ortho*-hydroxy benzyl

alcohols **1ad-ah** and **1ga** with *para*-substituents in the β -aryl ring reveals comparable results with a value of $\rho = -2.2$ (Figure 1E). The slightly less negative ρ -value coincides with our synthetic observation that substituents in the β -aryl ring have a comparably less pronounced effect on the reaction rate than electronic effects in the *ortho*-quinone methide fragment.

Online NMR Studies. We then turned our attention to NMR investigations to gain spectroscopic evidence for a generated *ortho*-quinone methide. The reaction of *ortho*-hydroxy benzyl alcohol **1da** with **2a** was monitored by ¹H-NMR spectroscopy under the catalytic reaction conditions. ¹H-NMR spectra were recorded after the indicated reaction times important parts of which are displayed in Figure 2. Representative signals are assigned to the reaction partners and intermediates. Both starting materials **1da** and enol-**2a** were rapidly consumed whereas the lactol **18** was formed and gradually converted to xanthenone **4da** with much slower rate. Two additional signals at about 5.64–5.67 ppm immediately emerged after the reaction start and then slowly decreased in the course of the reaction. The same signals were observed in NMR-experiments recorded with **1da** and phosphoric acid **5** in the absence of **2a** suggesting an acid-catalyzed byproduct formation. In an attempt to isolate this compound, we always obtained mixtures of benzhydryl alcohol **1da** and a dimer **17** which was clearly identified by mass spectrometry (see below).

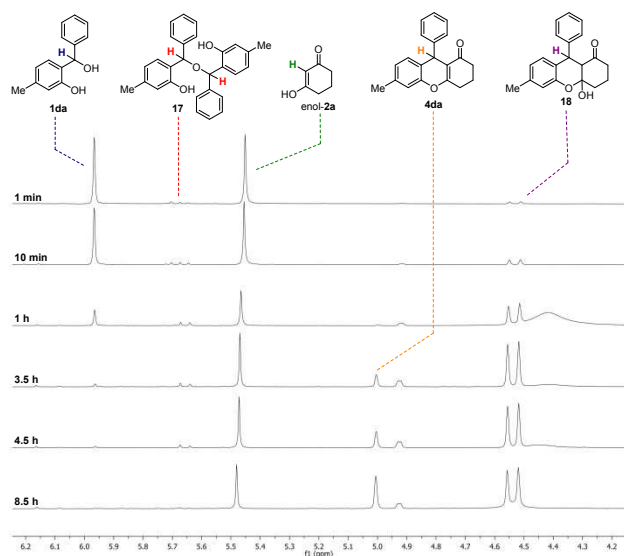


Figure 2. Online ^1H -NMR studies from the reaction of **1da** (1.0 equiv.) and **2a** (1.5 equiv.) with **5** (5 mol%) in CDCl_3 . ^1H -NMR spectra were recorded after 1 min, 10 min, 1 h, 3.5 h, 4.5 h and 8.5 h and partially displayed. Representative signals are assigned to the reaction partners and intermediates.

Dimer Formation and Reversibility. In principle, dimer formation may occur via conjugate addition of either the benzyl alcohol or the phenolic moiety toward the *ortho*-quinone methide leading to two different structures **17a** and **17b**. In order to distinguish between both possibilities, we synthesized a ^{13}C -labelled *ortho*-hydroxy benzyl alcohol **19** and performed NMR studies in the presence of phosphoric acid **5** (Figure 3). The benzyl proton signal of **19** emerged as doublet with $J = 145$ Hz (^{13}C -H-coupling) at 6.02 ppm in ^1H -NMR due to the ^{13}C -labelling. In the presence of phosphoric acid **5**, two additional sets of signals at 5.62 ppm and 5.63 ppm were detected for the readily formed dimer. Both signals appeared as doublet of doublets with identical coupling constants of $J = 145$ Hz and $J = 2.5$ Hz each of which can be attributed to ^1J - and ^3J - ^{13}C -H-couplings, respectively, between the benzyl protons and the labelled benzyl carbon atoms. This scenario is fully consistent with the formation of dimer **17a** and rules out the existence of dimer **17b**. The observed two sets of signals are caused by the two diastereomers of **17a** (C_2 -symmetric chiral and meso).

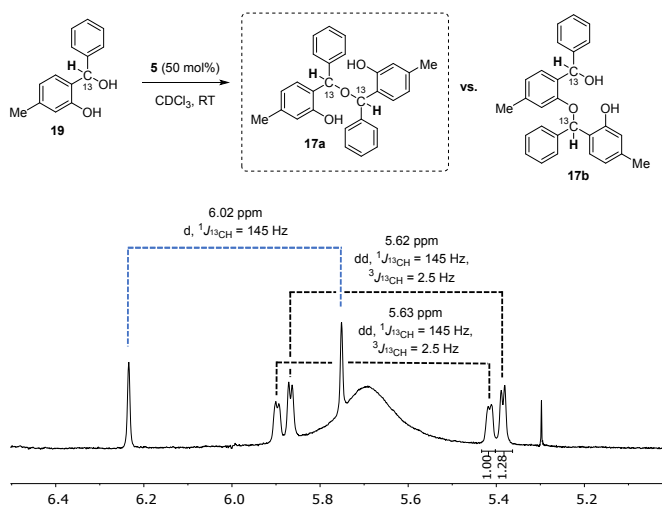
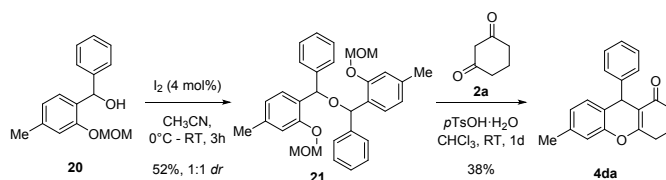


Figure 3. Structural elucidation of dimer with NMR-studies on ^{13}C -labelled *ortho*-hydroxy benzyl alcohol **19** with **5** (50 mol%) in CDCl_3 . ^1H -NMR spectrum was recorded after 30 min and is partially displayed. Chemical shifts and J -values are assigned for **19** and **17a**.

The dimer formation is a reversible process as already confirmed with online NMR studies. As a further important proof, we synthesized a MOM-protected dimer **21** from benzyl alcohol **20** with catalytic amounts of iodine and subjected it to the reaction in place of the *ortho*-hydroxy benzyl alcohol **1** (Scheme 10). Phenol protection was indispensable here to prevent decomposition. Due to insufficient acidity of the chiral phosphoric acid **5** for complete MOM-deprotection, we used *para*-toluene sulfonic acid as Brønsted acid to eventually convert **21** back to the corresponding *ortho*-quinone methide that reacted with **2a** to the desired xanthenone **4da** in moderate yield. This observation clearly proves an acid-catalyzed equilibrium between the *ortho*-quinone methide and the dimer. This dimer presumably provides a reservoir for the unstable and highly reactive *ortho*-quinone methide in the course of the reaction.

Scheme 10. Proof of Reversibility of Dimer Formation



Characterization of Key Intermediates with Mass Spectrometry. We carefully investigated the reaction of *ortho*-hydroxy benzyl alcohol **1da** and 1,3-cyclohexanedione (**2a**) in the presence of chiral phosphoric acid **5** under catalytic conditions using ESI-MS. These studies enabled us to identify all critical intermediates of the proposed catalytic cycle as sodium adducts. A representative spectrum is depicted in Figure 4 and shows the expected signals for the *ortho*-hydroxy benzyl alcohol **1da** (m/z 237), lactol **18** (m/z 331) and product **4da** (m/z 313). The characteristic signal at m/z 433 is caused by the previously elucidated dimer **17** and disappears in the course of the reaction confirming its reversible formation.

Moreover, the signals at m/z 197 and m/z 219 are ascribed to the *ortho*-quinone methide once as H-adduct and once as sodium adduct, which are formed during the reaction and the ionization process.

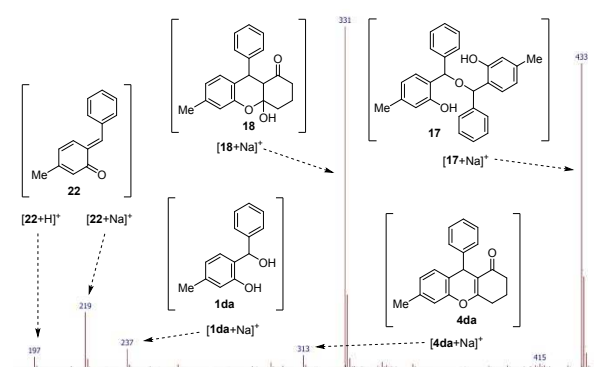


Figure 4. Partial ESI-MS spectrum (positive mode) from the reaction of **1da** and **2a** with **5** (5 mol%) after 30 min. Detection of Na-adducts of reaction intermediates are presented in the spectrum.

Moreover, we could also detect the corresponding catalyst adducts (Figure 5). The peak at m/z 887 corresponds to the phosphoric acid catalyst coordinated to the *ortho*-quinone methide $[22\cdot5+Na]^+$. The affinity of the phosphoric acid to the dimer **17** and their predicted off-cycle equilibrium was supported with a peak at m/z 1101. Furthermore, the peak at m/z 999 is indicative of a complex of phosphoric acid **5** with the lactol product $[18\cdot5+Na]^+$. The same mass charge ratio can as well be ascribed to a trimeric complex with the catalyst bound to both the *ortho*-quinone methide and the nucleophile $[22\cdot2a\cdot5+Na]^+$.

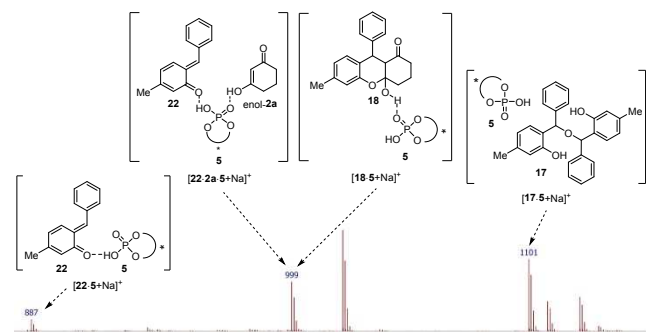


Figure 5. Partial ESI-MS spectrum (positive mode) from the reaction of **1da** (1.0 equiv.) and **2a** (1.5 equiv.) with **5** (5 mol%) after 30 min. Detection of Na-adducts of reaction intermediates in complex with **5** are presented in the spectrum.

For a more detailed analysis, CID studies in positive mode were performed. Relatively low collisional energy of 10 eV leads to fragmentation into $[5+Na]^+$ (m/z 691) and with much lower intensity for $[5\cdot22+Na]^+$ (m/z 887) and $[5\cdot2a+H]^+$ (m/z 781) (Figure 6). The latter ions can only be formed by dissociation of either **2a** or **22** from the precursor m/z 999. The poor stability of precursor m/z 999 and its fragmentation pattern leads us to conclude that a trimeric structure $[22\cdot2a\cdot5]$ is indeed a feasible assumption. It would confirm our underlying working hypothesis of a ternary complex of the phosphoric acid

bound to both substrates in a bifunctional manner. The ESI-MS studies were confirmed with accurate mass data using a quadrupole-time-of-flight instrument (ESI-Q-TOF, see Supporting Information).

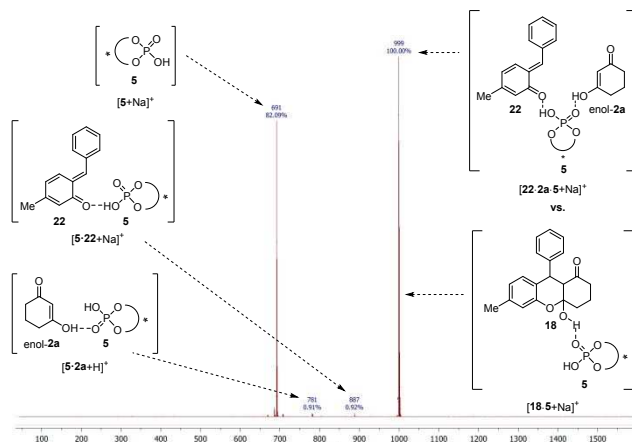


Figure 6. ESI-MS/MS spectrum (positive mode) of m/z 999 at collisional energy of 10 eV.

DFT-Calculations

In order to obtain a deeper insight into the reaction mechanism and to shed light on the origin of the enantioselectivity of the process, computational studies using *ortho*-hydroxy benzhydryl alcohol **1**, 1,3-cyclohexanedione (**2a**) and the complete catalyst **5** were performed. Theoretical studies were carried out at the PBE0-D3(BJ)/TZP + COSMO-(CHCl₃)/PBE-D3(BJ)/TZP + COSMO-(CHCl₃) level of theory³⁷ using ADF.2018.107.³⁸ Transition states were located by employing the Climbing Image Nudged Elastic Band (CI-NEB) method³⁹ starting from relaxed ground state structures of the reactants using a reduced basis set size (DZP) before further refinement via TZP (see supporting information for further details).

Figure 7 shows the relative Gibbs free energy profile of the reaction with respect to the *ortho*-hydroxy benzhydryl alcohol **1**. The reaction pathway can be divided into three parts with *ortho*-quinone methide formation representing the first step. Direct formation of an *ortho*-quinone methide in the absence of any Brønsted acid-catalyst featured a high activation energy ($\Delta G^\ddagger = +25.8$ kcal/mol) and thus, generation of the *ortho*-quinone methide is unlikely to occur in the absence of a suitable catalyst. Furthermore, the configuration of the exocyclic double bond was investigated. According to the relative Gibbs free energies of both double bond isomers, the *E*-isomer of the *ortho*-quinone methide is strongly favored giving an *E/Z*-ratio of 99:1 (at $T = 298.15$ K). This coincides well with our experimental results (see Scheme 5) and recently published gas phase vibrational spectroscopy studies.³¹

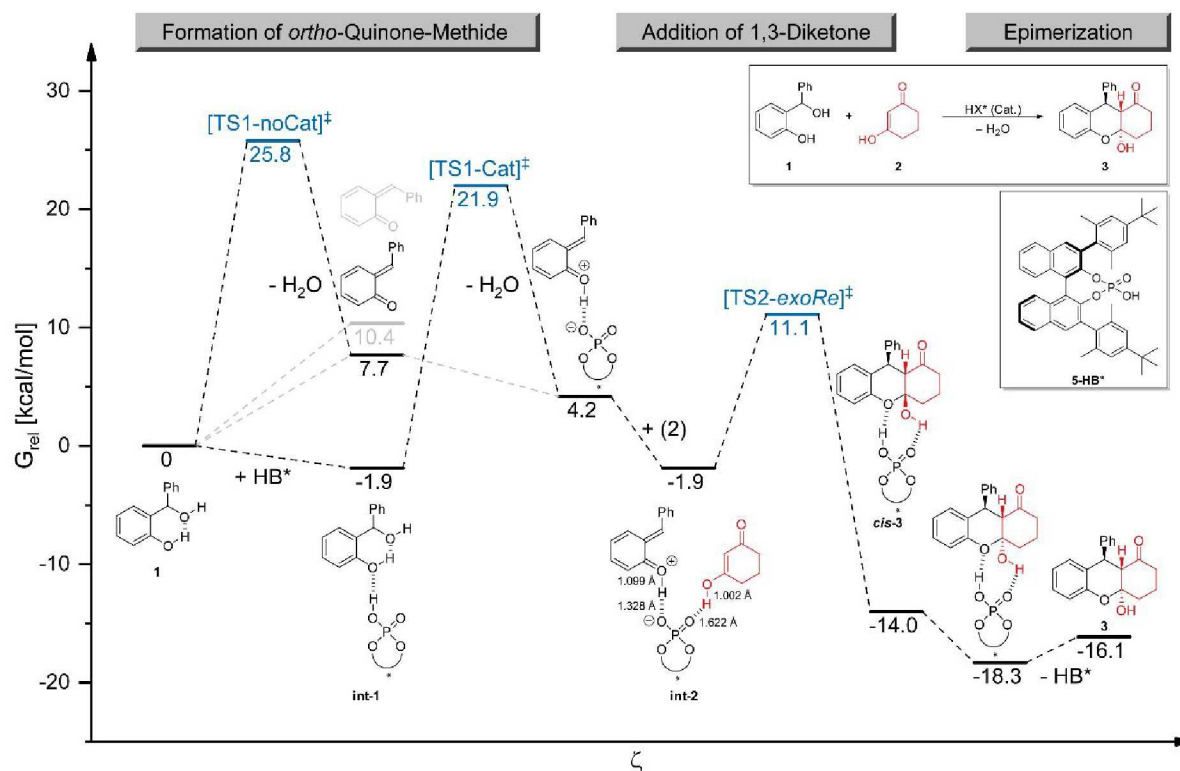


Figure 7 Computational studies and proposed reaction mechanism (Gibbs free energies at the PBE0-D3(BJ)/TZP + COSMO-(CHCl₃)/PBE-D3(BJ)/TZP + COSMO-(CHCl₃) level).

Coordination of **1** to the BINOL-phosphoric acid catalyst **5** via hydrogen bond formation was shown to be an exergonic process ($\Delta G_{\text{rel}} = -1.9$ kcal/mol). The resulting complex readily undergoes dehydration to form the phosphoric acid-bound *ortho*-quinone methide which was also confirmed by our HR-MS studies. The activation energy for this process was lowered by coordination to the catalyst and calculated to be $\Delta G^\ddagger = +23.8$ kcal/mol. A closer look at the structure of the phosphoric acid-bound *ortho*-quinone methide reveals that the O-H distance towards the acidic proton is significantly shorter for the *ortho*-quinone methide-oxygen (1.09 Å) than for the oxygen atom of BINOL-phosphoric acid **5** (1.33 Å). Despite the formation of **int-1** being an overall endergonic process, the following coordination of the enol tautomer of **2** is again exergonic ($\Delta G_{\text{rel}} = -$

6.1 kcal/mol) giving rise to the trimeric complex **int-2** which was previously detected in our HR-MS experiments.

The second part of the reaction pathway comprises the addition of **2** to the *ortho*-quinone methide in an apparently highly ordered transition state in which both reactants are activated by the catalyst in a bifunctional fashion. We have calculated activation energies for all four different transition state assemblies, i.e. *exo* and *endo*-structures and a *Re*/*Si*-face attack, respectively. Importantly, a closer inspection of the individual reaction pathways reveals no evidence for a stepwise mechanism (vide infra).

Figure 8 depicts the structures of all transition states and their relative Gibbs free activation energies ($\Delta\Delta G^\ddagger$) with respect to the energetically most favorable transition state ([TS2-*exoRe*][‡]).

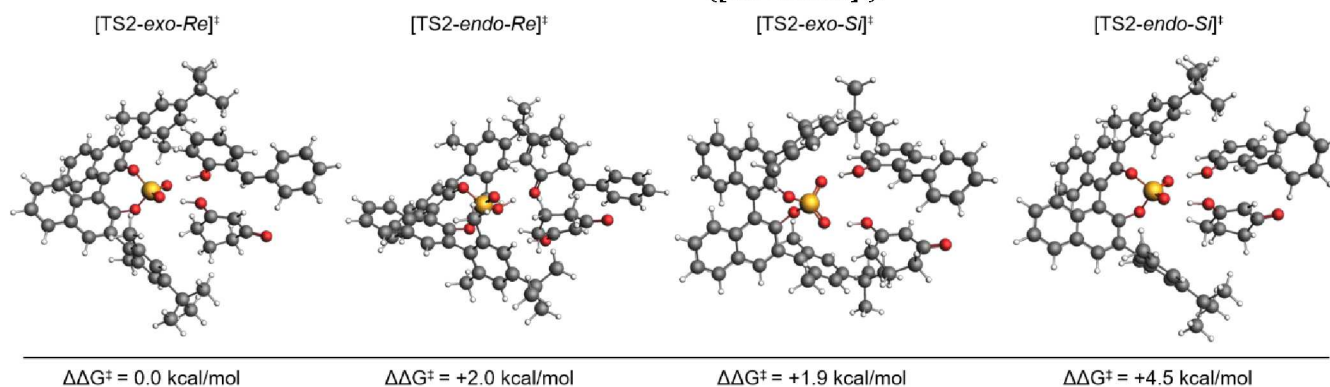


Figure 8 Enantiomeric and diastereomeric transition state structures with their corresponding relative Gibbs free activation energies ($\Delta\Delta G^\ddagger$).

In this regard, an *exo*-like assembly of the reactants inside the catalyst pocket with the enol-tautomer of **2** attacking from the *Re*-face was calculated to have the lowest energy barrier ($\Delta G^\ddagger = +13.0$ kcal/mol). A possible explanation for this result is assumed to be an attractive CH- π -interaction between one methyl group of the *para-tert*-butyl substituent in **5** and the π -system of the *ortho*-quinone methide which is located directly underneath the *tert*-butyl substituent. This assumption was supported by investigating the density of states (DOS) projected on the corresponding atoms, where states at a similar energy indicate a possible constructive overlap between the molecular orbitals.

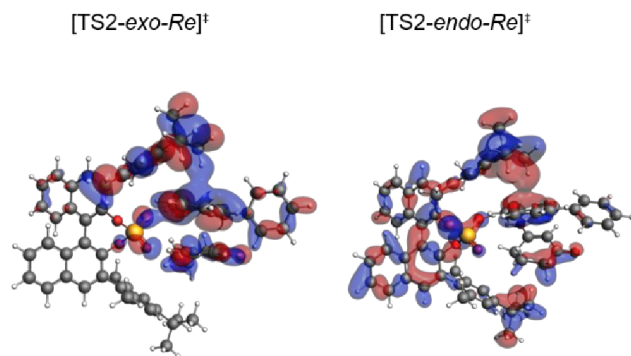


Figure 9 Representation of the orbital overlap attributed to a CH- π -interaction for *Re*-transition states

For both *Re*-face attacks such a constructive orbital overlap was found, illustrating the proposed CH- π -interaction (see Figure 9). The distance between the corresponding methyl group and the *ortho*-quinone methide- π -system was calculated to be only 2.8 Å.

It is worth emphasizing that the experimentally determined enantioselectivity of the reaction is heavily influenced by the *para*-substituent of the BINOL-phosphoric acid catalyst and increases from *para*-H (56:44 *er*) over *para*-Me (78:22 *er*) to *para*-*t*Bu (95:5 *er*).²⁶ This observation is also in good agreement with the proposed CH- π -interaction. Since no such interaction could be established for the *Si*-face attack, this is most likely the reason for the lower activation energy for [TS2-*exoRe*][‡] and thus for the highly enantioselective reaction.

A comparison of the activation energies for the *ortho*-quinone methide-formation ($\Delta G^\ddagger = +23.8$ kcal/mol) and the cycloaddition ($\Delta G^\ddagger = +13.0$ kcal/mol) clearly shows that the former represents the rate-determining step of the investigated reaction, as already expected from our kinetic experiments.

According to the calculated energy profile for the *exo-Re*-reaction, only the C-C-bond is formed within the calculated transition state. However, no second transition state was found and no significant activation barrier for the formation of the C-O-bond could be calculated. In combination with

the highly exergonic and exothermic nature of the previous C-C-bond formation we therefore propose a concerted yet highly asynchronous pathway for the formation of lactol *cis*-**3** via an *exo-Re*-transition state.

Finally, lactol *cis*-**3** undergoes epimerization to the thermodynamically more stable *trans* isomer **3** ($\Delta G_{\text{rel}} = -4.3$ kcal/mol) which releases the chiral catalyst thereby completing the catalytic cycle. The relative configuration of **3** was verified by X-ray crystallography of suitable single crystals.³¹ Finally, **3** is subjected to acid-catalyzed dehydration to form the target 1*H*-xanthen-1-one **4**.

In the course of this dehydration the two stereocenters at C4 and C5 of lactol **3** are destroyed. The stereoselectivity of the formation of the remaining stereocenter at C3 is therefore exclusively determined by *Re*- or *Si*-face attack and thus, both *endo* and *exo* transition states contribute to the overall enantioselectivity. The overall enantioselectivity was therefore calculated considering all four lactol isomers according to their relative rate constants deduced from the activation energies of the corresponding pathways. Given an experimental *er* of 95:5, the computed value of 96:4 (at $T = 298.15$ K) is in excellent agreement (see supporting information for further details).

Proposed catalytic cycle. By merging the information from the online experiments, the RPKA, and the DFT-calculations the following mechanistic pathway is proposed (Figure 10). The reaction starts with the formation of the *ortho*-quinone methide by dehydration of the corresponding *ortho*-hydroxy benzhydryl alcohol **1** catalyzed through the BINOL-phosphoric acid **5** which according to the RPKA is the rate-limiting step. A hydrogen-bonded phosphoric acid – *ortho*-quinone methide complex **A** is thus formed as evidenced by MS analysis. Upon further coordination of the enol tautomer of 1,3-diketone **2a**, a ternary complex **B** is formed as proved again by mass spectrometric evidence which then undergoes a rapid, concerted, yet highly asynchronous [4+2]-cycloaddition to produce lactol **3** after epimerization. In addition to the productive reaction, the phosphoric acid – *ortho*-quinone methide complex **A** exhibits an off-cycle equilibrium and reversibly generates the dimer **C** which is also a suitable substrate for the title reaction as indicated by control experiments. We assume that this dimer provides a reservoir for the otherwise unstable *ortho*-quinone methide to prevent it from undergoing side reactions. Finally, the phosphoric acid catalyst dissociates from the lactol and water is eliminated to furnish the target 1*H*-xanthen-1-one **4**. This dehydration occurs slowly in situ, but can be accelerated through the addition of a stronger Brønsted acid upon completion of the cycloaddition. The catalyst was not affected by deactivation or product inhibition during the reaction. By comparing kinetic data of electronically different *ortho*-hydroxy benzhydryl alcohols a clear correlation to the reaction rate of the cycloaddition can be drawn.

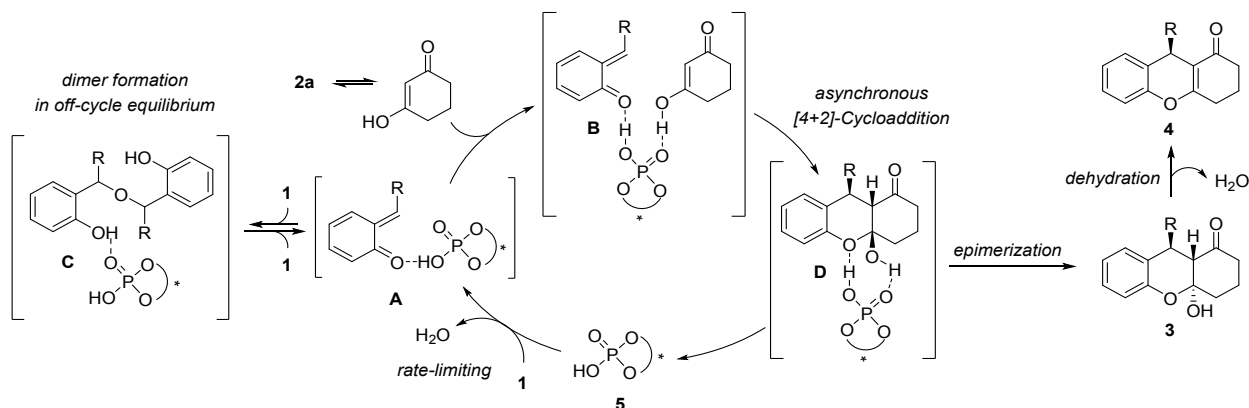


Figure 10 Proposed catalytic cycle.

CONCLUSION

We have developed a broadly applicable [4+2]-cycloaddition of β -dicarbonyl compounds with in situ generated *ortho*-quinone methides. Following this strategy a straightforward, catalytic, and highly enantioselective synthesis of valuable 4*H*-chromenes and 1*H*-xanthen-1-ones has been established which furnished a large variety of products with typically high yields and enantioselectivities. Careful mechanistic analysis on the basis of NMR- and MS-experiments, reaction progress kinetic analysis, Hammett plots, and DFT-calculations provided a complete picture of the reaction pathway. *Ortho*-quinone methide formation was proven to be the rate-limiting step of the catalytic cycle with electronrich substrates reacting faster than electronpoor ones. The actual bond-forming event took place in a concerted, yet highly asynchronous [4+2]-cycloaddition between the two substrates both hydrogen-bonded to the phosphoric acid catalyst in a highly ordered transition state assembly. The calculations show an attractive CH- π -interaction between the catalyst's *t*Bu-group and the π -system of the *ortho*-quinone methide in the *exo-Re*-transition state as the important stereochemical control element. Moreover, an off-cycle equilibrium between the *ortho*-quinone methide and its dimer was detected which presumably provides a reservoir for the unstable *ortho*-quinone methide. We believe that the detailed mechanistic analysis described herein provides useful information for the development of further reactions of *ortho*-quinone methides and related transient intermediates.

EXPERIMENTAL SECTION

General Information. ^1H and ^{13}C NMR spectra were recorded in CDCl_3 using Varian MERCURYplus 300 (300 MHz), Varian MERCURYplus 400 (400 MHz), Bruker AVANCE III HD 400 (400 MHz) and Bruker Fourier 300 (300 MHz) spectrometer. The signals were referenced to residual chloroform (7.26 ppm, ^1H , 77.16 ppm, ^{13}C). Chemical shifts are reported in ppm, multiplicities are indicated by s (singlet), d (doublet), t (triplet), q (quartet), dd (doublet of doublet), ddd (doublet of doublet of doublets) and m (multiplet). Melting points are uncorrected and were

determined on a Boetius heating table. IR spectra were obtained with FTIR spectrometer Genesis ATI Mattson/Unicam and JASCO FT/IR-4100. Optical rotations were measured using a Polarotronic polarimeter (Schmidt & Haensch). ESI mass spectra were recorded on a Bruker ESI-TOF microTOF and Bruker APEX II FT-ICR. HPLC analyses were carried out on a Jasco MD-2010 plus instrument with chiral stationary phase column (Daicel Chiralcel OD-H column, Daicel Chiralpak IA column, Daicel Chiralpak AS-H column) and Jasco MD-4015 instrument with chiral stationary phase column (Daicel Chiralpak IA column, Daicel Chiralpak IB column, Daicel Chiralpak IE column). THF, CH_2Cl_2 , and toluene for reactions were purified and dried by a Solvent Purification System MB SPS-800 (Braun). The solvents for column chromatography and TLC were distilled from indicated drying agents: hexane (KOH), ethyl acetate (KOH), *tert*-butyl methyl ether (KOH), dichloromethane (CaH_2). All reactions that required heating were heated using an oil bath. Flash column chromatography was performed by using Merck silica gel 60 230-400 mesh (0.040-0.063 mm). All reactions were monitored by thin layer chromatography using precoated silica gel plates. Spots were visualized by UV ($\lambda = 254 \text{ nm}$) and were treated with a vanillin solution in methanol (technical grade). The assignment of absolute configurations of enantioenriched products is supported by X-ray crystallographic structure determination. Compounds **1** were prepared according to reported literature procedures.^{26,27,29} Compound names were generated by the computer program ChemDraw according to the guidelines specified by the International Union of Pure and Applied Chemistry (IUPAC).

DFT Calculations

All calculations presented in this paper were carried out with the molecular ADF program, version 2018.107.³⁸ Molecular geometries were optimized in solution using the PBE functional in conjunction with the D3 version of Grimme's dispersion correction with Becke-Johnson damping and the COSMO solvation model employing CHCl_3 as solvent.³⁷ The TZP basis set was used for all atoms during geometry optimization, frequency analysis and for single point calculations. Analytic frequency calculations were performed to verify the nature of all stationary points (i.e. minima and transition states) and to calculate Gibbs free energies at 298.15 K. More accurate enantio- and diastereoselectivities were calculated by computing single-

point solution phase energies at the PBE0-D3(BJ)/TZP+COSMO(CHCl₃) level (see supporting information for further details).

General Procedure for Enantioselective Addition of 1,3-Cyclohexanedione.

Ortho-hydroxy benzyl alcohol **1** (0.2 mmol, 1.0 equiv.), 1,3-cyclohexanedione **2a** (33.6 mg, 0.30 mmol, 1.5 equiv.) and catalyst **5** (6.7 mg, 0.01 mmol, 5 mol %) were dissolved in chloroform (1.6 mL) at RT, 10°C or 0°C. The reaction mixture was stirred for 1-2 days at the same temperature until complete consumption of the starting material. Then *p*-toluenesulfonic acid monohydrate (7.6 mg, 0.04 mmol, 20 mol%) was added and the reaction mixture was further stirred for 4 h at 40°C. The crude reaction mixture was purified by short flash chromatography (hexane/MTBE 9:1) to afford the desired xanthenones. The enantiomeric ratios were determined by HPLC on a chiral stationary phase.

(*R*)-9-(4-Methoxyphenyl)-2,3,4,9-tetrahydro-1*H*-xanthen-1-one (**4aa**). Hexane/MTBE (9:1) as eluent, 95 % yield (58.2 mg), as a white solid, er 95:5, $[\alpha]_D^{24} = -54^\circ$ ($c = 1.0$, CHCl₃), mp = 113 - 116°C, ¹H NMR (400 MHz, CDCl₃) δ [ppm] = 7.21 - 6.99 (m, 6H), 6.86 - 6.65 (m, 2H), 5.02 (s, 1H), 3.73 (s, 3H), 2.80 - 2.59 (m, 2H), 2.45 - 2.31 (m, 2H), 2.17 - 1.92 (m, 2H), ¹³C{¹H} NMR (100MHz, CDCl₃) δ [ppm] = 197.2, 166.1, 158.1, 149.6, 138.8, 130.3, 129.0, 127.6, 125.8, 125.2, 116.5, 115.1, 113.9, 55.3, 37.2, 37.0, 28.0, 20.5, IR (KBr) ν [cm⁻¹] = 3031, 3013, 2953, 2899, 2835, 16.58, 1640, 1612, 1582, 1509, 1487, 1458, 1375, 1260, 1243, 1223, 1181, 1172, 1128, 1030, 996, HR-MS (ESI): calc. for: ([M+Na]⁺): 329.1154; found: 329.1148, HPLC: ODH Column (95% hexane: 5% *i*-propanol, 1 mL/min, 270 nm) R_{t1} = 15.1 min and R_{t2} = 18.6 min.

(*R*)-9-(4-(tert-Butyl)phenyl)-2,3,4,9-tetrahydro-1*H*-xanthen-1-one (**4ab**). Hexane/MTBE (9:1) as eluent, Yield 92% (61.2 mg) as a white solid, er 95:5, $[\alpha]_D^{24} = -42^\circ$ ($c = 1.0$, CHCl₃), mp = 50 - 53°C, ¹H NMR (400 MHz, CDCl₃) δ [ppm] = 7.24 - 7.20 (m, 2H), 7.20 - 7.10 (m, 4H), 7.10 - 7.00 (m, 2H), 5.05 (s, 1H), 2.82 - 2.55 (m, 2H), 2.52 - 2.24 (m, 2H), 2.16 - 1.90 (m, 2H), 1.25 (s, 9H), ¹³C{¹H} NMR (100 MHz, CDCl₃) δ [ppm] = 197.2, 166.4, 149.7, 149.0, 143.2, 130.2, 127.6, 127.5, 125.8, 125.4, 125.1, 116.5, 115.1, 37.4, 37.2, 34.5, 31.5, 28.1, 20.5, IR (KBr) ν [cm⁻¹] = 3044, 3026, 2960, 2901, 2868, 1663, 1646, 1639, 1613, 1581, 1485, 1456, 1375, 1236, 1177, 1132, 994, HR-MS (ESI): calc. for: ([M+Na]⁺): 355.1674; found: 355.1668, HPLC ODH Column (95% hexane: 5% *i*-propanol, 1 mL/min, 270 nm) R_{t1} = 8.2 min and R_{t2} = 9.6 min.

(*R*)-9-([1,1'-Biphenyl]-4-yl)-2,3,4,9-tetrahydro-1*H*-xanthen-1-one (**4ac**). Hexane/MTBE (9:1) as eluent, Yield 91% (64.1 mg) as a white solid, er 94:6, $[\alpha]_D^{25} = -8^\circ$ ($c = 1.0$, CHCl₃), mp = 169 - 171°C, ¹H NMR (400 MHz, CDCl₃) δ [ppm] = 7.54 - 7.48 (m, 2H), 7.48 - 7.42 (m, 2H), 7.42 - 7.35 (m, 2H), 7.34 - 7.27 (m, 3H), 7.23 - 7.02 (m, 4H), 5.12 (s, 1H), 2.82 - 2.59 (m, 2H), 2.50 - 2.32 (m, 2H), 2.15 - 1.95 (m, 2H), ¹³C{¹H} NMR (100 MHz, CDCl₃) δ [ppm] = 197.2, 166.5, 149.6, 145.4, 141.1, 139.4, 130.2, 128.8, 128.4, 127.8, 127.3, 127.2, 125.4, 125.3, 116.7, 114.8, 37.6, 37.2, 28.1, 20.5, IR (KBr) ν [cm⁻¹] = 3057, 3054, 3027, 2944, 2894, 1660, 1639, 1579, 1485, 1374, 1236, 1226, 1177, 1131, 996, 758, HR-MS (ESI): calc. for: ([M+Na]⁺): 375.1361; found: 375.1356, HPLC ODH

Column (95% hexane: 5% *i*-propanol, 1 mL/min, 270 nm) R_{t1} = 14.2 min and R_{t2} = 17.9 min.

(*R*)-9-(*p*-Tolyl)-2,3,4,9-tetrahydro-1*H*-xanthen-1-one (**4ad**). Hexane/MTBE (9:1) as eluent, Yield 97% (56.3 mg) as a white solid, er 92.5:7.5, $[\alpha]_D^{25} = -55^\circ$ ($c = 1.0$, CHCl₃), mp = 148 - 150°C, ¹H NMR (400 MHz, CDCl₃) δ [ppm] = 7.21 - 6.96 (m, 8H), 5.03 (s, 1H), 2.79 - 2.55 (m, 2H), 2.47 - 2.30 (m, 2H), 2.25 (s, 3H), 2.11 - 1.93 (m, 2H), ¹³C{¹H} NMR (100 MHz, CDCl₃) δ [ppm] = 197.1, 166.2, 149.6, 143.5, 136.0, 130.01, 129.3, 127.9, 127.7, 125.8, 125.2, 116.6, 115.0, 37.5, 37.2, 28.0, 21.2, 20.5, IR (KBr) ν [cm⁻¹] = 1661, 1644, 1611, 1486, 1458, 1376, 1239, 1222, 1203, 1179, 1157, 1130, 994, 823, 722, 642, 526, HR-MS (ESI): calc. for: ([M+Na]⁺): 313.1199; found: 313.1197, HPLC ODH Column (95% hexane: 5% *i*-propanol, 1 mL/min, 270 nm) R_{t1} = 9.5 min and R_{t2} = 10.7 min.

(*R*)-9-(4-Propylphenyl)-2,3,4,9-tetrahydro-1*H*-xanthen-1-one (**4ae**). Hexane/MTBE (9:1) as eluent, Yield 89% (56.7 mg) as a white solid, er 92:8, $[\alpha]_D^{26} = -40^\circ$ ($c = 1.0$, CHCl₃), mp = 71 - 75°C, ¹H NMR (300 MHz, CDCl₃) δ [ppm] = 7.24 - 6.96 (m, 8H), 5.04 (s, 1H), 2.81 - 2.57 (m, 2H), 2.54 - 2.46 (m, 2H), 2.45 - 2.28 (m, 2H), 2.11 - 1.94 (m, 2H), 1.66 - 1.50 (m, 2H), 0.91 (t, $J = 7.3$ Hz, 3H), ¹³C{¹H} NMR (100 MHz, CDCl₃) δ [ppm] = 197.1, 166.3, 149.6, 143.6, 140.7, 130.2, 128.6, 127.8, 127.6, 125.8, 125.1, 116.5, 115.1, 37.8, 37.5, 37.1, 28.0, 24.5, 20.5, 14.1, IR (KBr) ν [cm⁻¹] = 2955, 2929, 2868, 1642, 1580, 1510, 1486, 1455, 1375, 1238, 1179, 1130, 995, 919, 754, 603, HR-MS (ESI): calc. for: ([M+Na]⁺): 341.1518; found: 341.1552, HPLC IB Column (95% hexane: 5% *i*-propanol, 1 mL/min, 270 nm) R_{t1} = 7.6 min and R_{t2} = 8.4 min.

(*R*)-9-(4-Fluorophenyl)-2,3,4,9-tetrahydro-1*H*-xanthen-1-one (**4af**). Hexane/MTBE (9:1) as eluent, Yield 92% (54.2 mg) as a white solid, er 98:2, $[\alpha]_D^{24} = -73^\circ$ ($c = 0.41$, CHCl₃), mp = 108 - 110°C, ¹H NMR (400 MHz, CDCl₃) δ [ppm] = 7.23 - 7.15 (m, 3H), 7.12 - 7.00 (m, 3H), 6.96 - 6.85 (m, 2H), 5.05 (s, 0H), 2.80 - 2.55 (m, 2H), 2.50 - 2.30 (m, 2H), 2.15 - 1.92 (m, 2H), ¹³C{¹H} NMR (100 MHz, CDCl₃) δ [ppm] = 197.1, 166.4, 161.5 (d, ¹J_{C-F} = 244.5 Hz), 149.5, 142.18, 142.15, 130.1, 129.6 (d, ³J_{C-F} = 8.0 Hz), 127.9, 125.3, 116.7, 115.3 (d, ²J_{C-F} = 21.3 Hz), 114.8, 37.2, 37.1, 28.0, 20.5, IR (KBr) ν [cm⁻¹] = 3071, 3042, 3015, 2960, 2936, 2893, 2876, 1656, 1600, 1580, 1506, 1375, 1237, 1177, 997, 845, 754, HR-MS (ESI): calc. for: ([M+Na]⁺): 317.0954; found: 317.0948, HPLC ODH Column (95% hexane: 5% *i*-propanol, 1 mL/min, 270 nm) R_{t1} = 9.7 min and R_{t2} = 11.3 min.

(*R*)-9-(4-Bromophenyl)-2,3,4,9-tetrahydro-1*H*-xanthen-1-one (**4ag**). Hexane/MTBE (9:1) as eluent, Yield 79% (56.1 mg) as a white solid, er 93:7, $[\alpha]_D^{25} = -20^\circ$ ($c = 2.6$, CHCl₃), mp = 119 - 121°C, ¹H NMR (400 MHz, CDCl₃) δ [ppm] = 7.38 - 7.30 (m, 2H), 7.23 - 7.15 (m, 1H), 7.14 - 7.01 (m, 5H), 5.03 (s, 1H), 2.80 - 2.58 (m, 2H), 2.48 - 2.30 (m, 2H), 2.14 - 1.90 (m, 2H), ¹³C{¹H} NMR (100 MHz, CDCl₃) δ [ppm] = 197.0, 166.5, 149.5, 145.3, 131.6, 130.1, 129.9, 128.0, 125.3, 124.8, 120.4, 116.7, 114.5, 37.5, 37.1, 28.0, 20.5, IR (KBr) ν [cm⁻¹] = 1659, 1644, 1581, 1485, 1455, 1374, 1238, 1175, 1130, 1070, 1010, 994, 843, 757, 526, HR-MS (ESI): calc. for: ([M+Na]⁺): 377.0181/379.0181; found: 377.0146/379.0146, HPLC ODH Column (95% hexane: 5%

i-propanol, 1 mL/min, 270 nm) R_{t1} = 11.4 min and R_{t2} = 13.3 min.

(*R*)-Methyl-4-(1-oxo-2,3,4,9-tetrahydro-1*H*-xanthen-9-yl)benzoate (**4ah**). Hexane/MTBE (9:1) as eluent, Yield 70% (46.8 mg) as a white solid, er 93:7, $[\alpha]_D^{26} = +4^\circ$ ($c = 1.0$, CHCl_3), mp = 171 - 173°C, $^1\text{H NMR}$ (400 MHz, CDCl_3) δ [ppm] = 7.93 - 7.86 (m, 2H), 7.33 - 7.28 (m, 2H), 7.20 (ddd, $J = 8.6$, 6.7, 2.1 Hz, 1H), 7.13 - 7.00 (m, 3H), 5.12 (s, 1H), 3.86 (s, 3H), 2.80 - 2.59 (m, 2H), 2.47 - 2.30 (m, 2H), 2.12 - 1.92 (m, 2H), $^{13}\text{C}\{^1\text{H}\}$ NMR (100 MHz, CDCl_3) δ [ppm] = 197.0, 167.0, 166.6, 151.3, 149.5, 130.1, 130.0, 128.4, 128.2, 128.1, 125.3, 124.6, 116.8, 114.3, 52.1, 38.1, 37.1, 28.0, 20.5, IR (KBr) ν [cm^{-1}] = 3057, 2957, 2925, 1720, 1666, 1645, 1607, 1578, 1487, 1455, 1433, 1373, 1281, 1234, 1178, 1138, 1112, 1100, 1018, 1001, 859, 768, 757, 723, 703, 527, 488, HR-MS (ESI): calc. for: $[\text{M}+\text{Na}]^+$: 357.1103; found: 357.1111, HPLC IB Column (95% hexane: 5% *i*-propanol, 1 mL/min, 270 nm) R_{t1} = 7.6 min and R_{t2} = 8.4 min.

(*R*)-9-(Benzo[d][1,3]dioxol-5-yl)-2,3,4,9-tetrahydro-1*H*-xanthen-1-one (**4b**). Hexane/MTBE (9:1) as eluent, Yield 92% (58.9 mg) as a white solid, er 95:5, $[\alpha]_D^{24} = -44^\circ$ ($c = 1.0$, CHCl_3), mp = 121-124°C, $^1\text{H NMR}$ (300 MHz, CDCl_3) δ [ppm] = 7.22 - 6.98 (m, 4H), 6.75 (dd, $J = 8.0$, 1.5 Hz, 1H), 6.71 - 6.62 (m, 2H), 5.89 - 5.80 (m, 2H), 4.98 (s, 1H), 2.82 - 2.56 (m, 2H), 2.52 - 2.23 (m, 2H), 2.17 - 1.83 (m, 2H), $^{13}\text{C}\{^1\text{H}\}$ NMR (75 MHz, CDCl_3) δ [ppm] = 197.2, 166.3, 149.4, 147.8, 146.1, 140.5, 130.0, 127.8, 125.6, 125.2, 121.1, 116.6, 114.9, 108.5, 108.2, 101.0, 37.6, 37.2, 28.0, 20.5, IR (KBr) ν [cm^{-1}] = 2952, 2928, 2889, 1664, 1645, 1580, 1500, 1484, 1375, 1234, 1182, 1138, 1039, 996, 929, 761, HR-MS (ESI): calc. for: $[\text{M}+\text{Na}]^+$: 343.0946; found: 343.0941, HPLC ODH Column (80% hexane: 20% *i*-propanol, 1 mL/min, 270 nm) R_{t1} = 7.9 min and R_{t2} = 16.8 min.

(*R*)-7-Methoxy-9-(4-methoxyphenyl)-2,3,4,9-tetrahydro-1*H*-xanthen-1-one (**4c**). Hexane/MTBE (9:1) as eluent, Yield 97% (65.3 mg) as a white solid, er 96:4, $[\alpha]_D^{24} = +34^\circ$ ($c = 1.0$, CHCl_3), mp = 149 - 147°C, $^1\text{H NMR}$ (300 MHz, CDCl_3) δ [ppm] = 7.19 - 7.09 (m, 2H), 7.01 (d, $J = 9.0$ Hz, 1H), 6.71 (dd, $J = 9.0$, 3.0 Hz, 1H), 6.80 - 6.74 (m, 2H), 6.57 (d, $J = 3.0$ Hz, 1H), 4.98 (s, 1H), 3.69 (s, 3H), 3.73 (s, 3H), 2.66 (d, $J = 4.5$ Hz, 2H), 2.78 - 2.55 (m, 2H), 2.49 - 2.25 (m, 2H), 2.17 - 1.85 (m, 2H), $^{13}\text{C}\{^1\text{H}\}$ NMR (75 MHz, CDCl_3) δ [ppm] = 197.2, 166.3, 158.2, 156.7, 143.8, 138.7, 129.0, 126.6, 117.4, 114.4, 113.9, 113.8, 104.9, 55.7, 55.3, 37.5, 37.2, 28.0, 20.6, IR (KBr) ν [cm^{-1}] = 2954, 2946, 1659, 1639, 1511, 1496, 1377, 1256, 1222, 1197, 1028, 998, 832, HR-MS (ESI): calc. for: $[\text{M}+\text{Na}]^+$: 359.1259; found: 359.1254, HPLC: ODH Column (95% hexane: 5% *i*-propanol, 1 mL/min, 274 nm) R_{t1} = 18.0 min and R_{t2} = 23.4 min.

(*R*)-6-Methyl-9-phenyl-2,3,4,9-tetrahydro-1*H*-xanthen-1-one (**4da**). Hexane/MTBE (9:1) as eluent, Yield 79% (45.9 mg) as a white solid, er 95:5, $[\alpha]_D^{25} = -34^\circ$ ($c = 1.0$, CHCl_3), mp = 169 - 171°C, $^1\text{H NMR}$ (400 MHz, CDCl_3) δ [ppm] = 7.24 - 7.18 (m, 4H), 7.16 - 7.06 (m, 1H), 6.98 (d, $J = 7.8$ Hz, 1H), 6.90 (s, 1H), 6.84 (d, $J = 7.8$ Hz, 1H), 5.02 (s, 1H), 2.78 - 2.58 (m, 2H), 2.47 - 2.33 (m, 2H), 2.30 (s, 3H), 2.13 - 1.93 (m, 2H), $^{13}\text{C}\{^1\text{H}\}$ NMR (100 MHz, CDCl_3) δ [ppm] = 197.1, 166.4, 149.4, 146.5, 137.8, 129.8, 128.5, 128.0, 126.4, 126.1, 122.5, 116.9, 115.0, 37.7, 37.2, 28.1, 21.2, 20.5, IR (KBr) ν [cm^{-1}] = 1661, 1643,

1587, 1490, 1455, 1375, 1253, 1223, 1213, 1202, 1190, 1131, 996, 828, 700, 690, 530, HR-MS (ESI): calc. for: $[\text{M}+\text{Na}]^+$: 313.1199; found: 313.1199, HPLC: ODH Column (95% hexane: 5% *i*-propanol, 1 mL/min, 270 nm) R_{t1} = 7.95 min and R_{t2} = 9.03 min.

(*R*)-6-Fluoro-9-phenyl-2,3,4,9-tetrahydro-1*H*-xanthen-1-one (**4db**). Hexane/MTBE (9:1) as eluent, Yield 83% (48.9 mg) as a white solid, er 90:10, $[\alpha]_D^{26} = -34^\circ$ ($c = 1.0$, CHCl_3), mp = 135 - 137°C, $^1\text{H NMR}$ (400 MHz, CDCl_3) δ [ppm] = 7.29 - 7.16 (m, 4H), 7.17 - 7.09 (m, 1H), 7.06 (ddd, $J = 8.4$, 6.2, 0.7 Hz, 1H), 6.84 - 6.69 (m, 2H), 5.02 (s, 1H), 2.80 - 2.55 (m, 2H), 2.49 - 2.27 (m, 2H), 2.13 - 1.96 (m, 2H), $^{13}\text{C}\{^1\text{H}\}$ NMR (100 MHz, CDCl_3) δ [ppm] = 196.9, 165.8, 161.7 (d, $^1J_{\text{C-F}} = 246$ Hz), 150.0 (d, $^3J_{\text{C-F}} = 11.8$ Hz), 146.1, 131.2 (d, $^4J_{\text{C-F}} = 9.3$ Hz), 128.6, 128.0, 126.6, 121.4 (d, $^2J_{\text{C-F}} = 3.4$ Hz), 115.0, 112.5 (d, $^2J_{\text{C-F}} = 21.5$ Hz), 104.9 (d, $^3J_{\text{C-F}} = 25.3$ Hz), 37.5, 37.1, 27.9, 20.5, IR (KBr) ν [cm^{-1}] = 2948, 1646, 1597, 1501, 1378, 1272, 1210, 1185, 1137, 1000, 970, 852, 698, 526, HR-MS (ESI): calc. for: $[\text{M}+\text{Na}]^+$: 317.0954; found: 317.0957, HPLC: IB Column (95% hexane: 5% *i*-propanol, 1 mL/min, 270 nm) R_{t1} = 9.3 min and R_{t2} = 10.5 min.

(*R*)-6-Bromo-9-phenyl-2,3,4,9-tetrahydro-1*H*-xanthen-1-one (**4dc**). Hexane/MTBE (9:1) as eluent, Yield 98% (69.6 mg) as a white solid, er 84:16, $[\alpha]_D^{25} = -23^\circ$ ($c = 1.0$, CHCl_3), mp = 169 - 171°C, $^1\text{H NMR}$ (400 MHz, CDCl_3) δ [ppm] = 7.26 - 7.17 (m, 5H), 7.17 - 7.10 (m, 2H), 6.96 (d, $J = 8.2$ Hz, 1H), 4.99 (s, 1H), 2.77 - 2.55 (m, 2H), 2.47 - 2.29 (m, 2H), 2.13 - 1.92 (m, 2H), $^{13}\text{C}\{^1\text{H}\}$ NMR (100 MHz, CDCl_3) δ [ppm] = 196.9, 165.9, 150.1, 145.7, 131.5, 128.7, 128.3, 128.0, 126.7, 124.7, 120.5, 119.9, 114.9, 37.7, 37.1, 27.9, 20.5, IR (KBr) ν [cm^{-1}] = 1654, 1637, 1601, 1492, 1452, 1372, 1238, 1223, 1202, 1175, 1133, 995, 825, 705, 679, 535, HR-MS (ESI): calc. for: $[\text{M}+\text{Na}]^+$: 377.0148/379.0148; found: 377.0145/379.0145, HPLC: ODH Column (95% hexane: 5% *i*-propanol, 1 mL/min, 270 nm) R_{t1} = 11.9 min and R_{t2} = 14.9 min.

(*R*)-9-(4-Methoxy-3,5-dimethylphenyl)-2,3,4,9-tetrahydro-1*H*-xanthen-1-one (**4e**). Hexane/MTBE (9:1) as eluent, Yield 97% (64.9 mg) as a white solid, er 95:5, $[\alpha]_D^{24} = -52^\circ$ ($c = 1.0$, CHCl_3), mp = 61 - 63°C, $^1\text{H NMR}$ (400 MHz, CDCl_3) δ [ppm] = 7.22 - 6.95 (m, 4H), 6.83 (s, 2H), 4.93 (s, 1H), 3.63 (s, 3H), 2.79 - 2.60 (m, 2H), 2.46 - 2.31 (m, 2H), 2.19 (s, 6H), 1.98 - 2.10 (m, 2H), $^{13}\text{C}\{^1\text{H}\}$ NMR (100 MHz, CDCl_3) δ [ppm] = 197.2, 166.3, 155.5, 149.5, 141.5, 130.6, 130.1, 128.2, 127.6, 125.9, 125.1, 116.6, 115.0, 59.6, 37.3, 37.2, 28.1, 20.5, 16.4, IR (KBr) ν [cm^{-1}] = 3028, 2948, 2897, 2870, 2824, 1662, 1644, 1581, 1485, 1456, 1375, 1235, 1225, 1181, 1127, 1016, 995, 911, 757, 732, HR-MS (ESI): calc. for: $[\text{M}+\text{Na}]^+$: 357.1467; found: 357.1461, HPLC ODH Column (95% hexane: 5% *i*-propanol, 1 mL/min, 270 nm) R_{t1} = 10.2 min and R_{t2} = 12.1 min.

(*R*)-7-Bromo-9-(4-methoxyphenyl)-2,3,4,9-tetrahydro-1*H*-xanthen-1-one (**4f**). Hexane/MTBE (9:1) as eluent, Yield 89% (68.6 mg) as a white solid, er 97:3, $[\alpha]_D^{24} = +82^\circ$ ($c = 1.0$, CHCl_3), mp = 182 - 184°C, $^1\text{H NMR}$ (400 MHz, CDCl_3) δ [ppm] = 7.26 (dd, $J = 2.5$, 9.0 Hz, 1H), 7.21 (d, $J = 2.5$ Hz, 1H), 7.19 - 7.05 (m, 2H), 6.95 (d, $J = 9.0$ Hz, 1H), 6.82 - 6.68 (m, 2H), 4.95 (s, 1H), 3.74 (s, 3H), 2.84 - 2.50 (m, 2H), 2.48 - 2.20 (m, 2H), 2.13 - 1.83 (m, 2H), $^{13}\text{C}\{^1\text{H}\}$ NMR (100 MHz, CDCl_3) δ [ppm] = 196.9, 165.8, 158.4, 148.6, 138.1, 132.8, 130.7, 129.0,

128.0, 118.4, 117.5, 114.8, 114.1, 55.3, 37.1, 37.1, 27.9, 20.5, IR (KBr) ν [cm⁻¹] = 2948, 2934, 2890, 2876, 2834, 1663, 1645, 1611, 1509, 1375, 1256, 1237, 1176, 1129, 1027, 997, 831, HR-MS (ESI): calc. for: ([M+Na]⁺): 407.0259; found: 407.0253, HPLC ODH Column (95% hexane: 5% *i*-propanol, 1 mL/min, 270 nm) R_{t1} = 14.7 min and R_{t2} = 20.6 min.

(*R*)-9-Phenyl-2,3,4,9-tetrahydro-1*H*-xanthen-1-one (**4ga**). Hexane/MTBE (9:1) as eluent, Yield 94% (52.0 mg) as a white solid, er: 95:5, [α]_D²⁴ = -68° (c = 1.0, CHCl₃), mp = 130 - 131°C, ¹H NMR (400 MHz, CDCl₃) δ [ppm] = 7.25 - 6.99 (m, 9H), 5.07 (s, 1H), 2.79 - 2.58 (m, 2H), 2.46 - 2.29 (m, 2H), 2.11 - 1.94 (m, 2H), ¹³C{¹H} NMR (100 MHz, CDCl₃) δ [ppm] = 197.1, 166.4, 149.6, 146.3, 130.2, 128.5, 128.0, 127.7, 126.5, 125.6, 125.2, 116.6, 114.9, 37.9, 37.1, 28.0, 20.5, IR (KBr) ν [cm⁻¹] = 3059, 3025, 2954, 2889, 2869, 1662, 1644, 1486, 1455, 1374, 1237, 1226, 1177, 1130, 996, 759, HR-MS (ESI): calc. for: ([M+Na]⁺): 299.1048; found: 299.1043, HPLC ODH Column (95% hexane: 5% *i*-propanol, 1 mL/min, 274 nm) R_{t1} = 11.0 min and R_{t2} = 13.4 min.

(*R*)-7-Fluoro-9-phenyl-2,3,4,9-tetrahydro-1*H*-xanthen-1-one (**4gb**). Hexane/MTBE (9:1) as eluent, Yield 80% (47.1 mg) as a white solid, er: 93:7, [α]_D²⁶ = -68° (c = 1.0, CHCl₃), mp = 167 - 169°C, ¹H NMR (400 MHz, CDCl₃) δ [ppm] = 7.27 - 7.19 (m, 4H), 7.17 - 7.12 (m, 1H), 7.05 (dd, *J* = 9.0, 4.7 Hz, 1H), 6.87 (ddd, *J* = 8.9, 7.8, 3.0 Hz, 1H), 6.79 (ddd, *J* = 8.6, 3.0, 0.7 Hz, 1H), 5.02 (s, 1H), 2.79 - 2.57 (m, 2H), 2.47 - 2.29 (m, 2H), 2.11 - 1.92 (m, 2H), ¹³C{¹H} NMR (100 MHz, CDCl₃) δ [ppm] = 196.9, 166.3, 159.5 (d, ¹J_{C-F} = 243.5 Hz), 145.7, 145.6 (d, ⁴J_{C-F} = 2.4 Hz), 128.7, 128.0, 127.1 (d, ³J_{C-F} = 7.7 Hz), 126.8, 118.0 (d, ³J_{C-F} = 8.6 Hz), 116.1 (d, ²J_{C-F} = 23.0 Hz), 114.8 (d, ²J_{C-F} = 23.8 Hz), 114.0, 38.3 (d, ⁴J_{C-F} = 1.3 Hz), 37.1, 28.0, 20.5, IR (KBr) ν [cm⁻¹] = 2967, 2890, 1664, 1645, 1588, 1486, 1455, 1257, 1215, 1195, 1135, 1098, 999, 918, 878, 834, 805, 731, 709, 622, 530, HR-MS (ESI): calc. for: ([M+Na]⁺): 317.0954; found: 317.0954, HPLC IB Column (95% hexane: 5% *i*-propanol, 1 mL/min, 270 nm) R_{t1} = 9.2 min and R_{t2} = 10.9 min.

(*R*)-7-Methyl-9-phenyl-2,3,4,9-tetrahydro-1*H*-xanthen-1-one (**4gc**). Hexane/MTBE (9:1) as eluent, Yield 83% (48.2 mg) as a white solid, er: 89:11, [α]_D²⁴ = -26° (c = 0.5, CHCl₃), mp = 130 - 131°C, ¹H NMR (400 MHz, CDCl₃) δ [ppm] = 7.25 - 7.19 (m, 4H), 7.16 - 7.09 (m, 1H), 6.99 - 6.94 (m, 2H), 6.89 (s, 1H), 5.01 (s, 1H), 2.77 - 2.57 (m, 2H), 2.45 - 2.28 (m, 2H), 2.21 (s, 3H), 2.11 - 1.92 (m, 2H). ¹³C{¹H} NMR (100 MHz, CDCl₃) δ [ppm] = 197.1, 166.4, 147.6, 146.5, 134.7, 130.3, 128.5, 128.4, 128.1, 126.4, 125.1, 116.3, 114.8, 38.0, 37.2, 28.1, 20.9, 20.6, IR (KBr) ν [cm⁻¹] = 1638, 1503, 1491, 1454, 1375, 1244, 1214, 1176, 1137, 1009, 991, 738, 724, 701, HR-MS (ESI): calc. for: ([M+H]⁺): 291.1380; found: 291.1381, HPLC ODH Column (95% hexane: 5% *i*-propanol, 1 mL/min, 270 nm) R_{t1} = 8.2 min and R_{t2} = 9.4 min.

(*R*)-7-Methoxy-9-phenyl-2,3,4,9-tetrahydro-1*H*-xanthen-1-one (**4gd**). Hexane/MTBE (9:1) as eluent, Yield 93% (57.0 mg) as a white solid, er 98:2, [α]_D²⁴ = -132° (c = 1.0, CHCl₃), mp = 102-105°C, ¹H NMR (400 MHz, CDCl₃) δ [ppm] = 7.24 - 7.17 (m, 4H), 7.16 - 7.06 (m, 1H), 7.02 (d, *J* = 9.0 Hz, 1H), 6.72 (dd, *J* = 9.0, 3.0 Hz, 1H), 6.59 (d, *J* = 3.0 Hz, 1H), 5.02 (s, 1H), 3.69 (s, 3H), 2.79 - 2.50 (m, 2H), 2.49 - 2.20 (m, 2H), 2.11 - 1.83 (m, 2H), ¹³C{¹H} NMR (100 MHz, CDCl₃) δ [ppm] = 197.1, 166.5, 156.7, 146.2, 143.8, 128.5, 128.0, 126.5,

126.3, 117.4, 114.2, 114.0, 113.9, 55.7, 38.4, 37.1, 28.1, 20.5, IR (KBr) ν [cm⁻¹] = 3061, 3032, 3013, 2956, 2945, 2926, 1659, 1639, 1587, 1491, 1374, 1216, 1197, 997, 835, 823, 702, HR-MS (ESI): calc. for: ([M+Na]⁺): 329.1154; found: 329.1148, HPLC ODH Column (95% hexane: 5% *i*-propanol, 1 mL/min, 274 nm) R_{t1} = 13.5 and R_{t2} = 15.1 min.

(*R*)-7-(tert-Butyl)-9-(4-methoxyphenyl)-2,3,4,9-tetrahydro-1*H*-xanthen-1-one (**4h**). Hexane/MTBE (9:1) as eluent, Yield 97% (70.3 mg) as a white solid, er 96:4, [α]_D²⁴ = +74° (c = 1.0, CHCl₃), mp = 119 - 122°C, ¹H NMR (400 MHz, CDCl₃) δ [ppm] = 7.20 (dd, *J* = 8.5, 2.5 Hz, 1H), 7.16 - 7.11 (m, 2H), 7.09 (d, *J* = 2.5 Hz, 1H), 7.01 (d, *J* = 8.5 Hz, 1H), 6.80 - 6.70 (m, 2H), 5.02 (s, 1H), 3.74 (s, 3H), 2.78 - 2.53 (m, 2H), 2.49 - 2.23 (m, 2H), 2.13 - 1.84 (m, 2H), 1.23 (s, 9H), ¹³C{¹H} NMR (100 MHz, CDCl₃) δ [ppm] = 197.2, 166.5, 158.0, 148.2, 147.7, 138.8, 128.9, 126.6, 125.0, 124.8, 116.0, 115.3, 113.8, 55.3, 37.2, 37.2, 34.5, 31.5, 28.1, 20.6, IR (KBr) ν [cm⁻¹] = 2960, 2903, 2869, 2831, 1660, 1641, 1587, 1509, 1498, 1376, 1256, 1175, 1132, 1034, 997, 828, HR-MS (ESI): calc. for: ([M+Na]⁺): 385.1780; found: 385.1774, HPLC ODH Column (95% hexane: 5% *i*-propanol, 1 mL/min, 220 nm) R_{t1} = 8.7 min and R_{t2} = 10.5 min.

(*R*)-9-(2-Ethylphenyl)-2,3,4,9-tetrahydro-1*H*-xanthen-1-one (**4i**). Hexane/MTBE (9:1) as eluent, Yield 98% (59.7 mg) as a white solid, er 96:4, [α]_D²⁴ = -78° (c = 1.0, CHCl₃), mp = 133-134°C, ¹H NMR (400 MHz, CDCl₃) δ [ppm] = 7.22 - 6.90 (m, 8H), 5.33 (s, 1H), 3.16 (qd, *J* = 7.5, 4.2 Hz, 2H), 2.83 - 2.58 (m, 2H), 2.45 - 2.30 (m, 2H), 2.16 - 1.95 (m, 2H), 1.41 (t, *J* = 7.5 Hz, 3H), ¹³C{¹H} NMR (100 MHz, CDCl₃) δ [ppm] = 197.1, 166.3, 149.2, 144.7, 140.9, 129.9, 129.2, 128.5, 127.5, 126.44, 126.39, 126.29, 125.1, 116.7, 115.6, 37.2, 33.4, 28.1, 25.5, 20.6, 15.5, IR (KBr) ν [cm⁻¹] = 2963, 2928, 2892, 2878, 2847, 1644, 1580, 1485, 1373, 1234, 1177, 1132, 994, 762, HR-MS (ESI): calc. for: ([M+Na]⁺): 327.1361; found: 327.1356, HPLC ODH Column (95% hexane: 5% *i*-propanol, 1 mL/min, 240 nm) R_{t1} = 8.0 min and R_{t2} = 9.8 min.

(*R*)-9-(*p*-Tolylethynyl)-2,3,4,9-tetrahydro-1*H*-xanthen-1-one (**4j**). Hexane/MTBE (9:1) as eluent, Yield 98% (61.6 mg) as a white solid, er 89:11, [α]_D²³ = +12° (c = 1.00, CHCl₃), mp = 47 - 49°C, ¹H NMR (400 MHz, CDCl₃) δ [ppm] = 7.46 (dd, *J* = 7.7, 1.7 Hz, 1H), 7.27 - 7.20 (m, 3H), 7.19 - 7.12 (m, 2H), 7.06 - 6.99 (m, 3H), 5.02 (s, 1H), 2.70 (dt, *J* = 17.6, 5.4 Hz, 1H), 2.64 - 2.52 (m, 2H), 2.49 - 2.37 (m, 1H), 2.29 (s, 3H), 2.19 - 2.01 (m, 2H), ¹³C{¹H} NMR (100 MHz, CDCl₃) δ [ppm] = 196.6, 166.7, 149.0, 137.9, 131.8, 130.2, 128.9, 128.5, 125.3, 121.9, 120.4, 116.8, 111.3, 90.5, 80.6, 37.0, 28.0, 24.5, 21.5, 20.5, IR (KBr) ν [cm⁻¹] = 3445, 1666, 1647, 1583, 1509, 1489, 1455, 1372, 1249, 1233, 1173, 1132, 997, 818, 758, 529, HR-MS (ESI): calc. for: ([M+Na]⁺): 337.1205; found: 337.1220, HPLC IA Column (95% hexane: 5% *i*-propanol, 1 mL/min, 250 nm) R_{t1} = 12.7 min and R_{t2} = 16.8 min.

(*R*)-9-Isobutyl-2,3,4,9-tetrahydro-1*H*-xanthen-1-one (**4k**). Hexane/MTBE (9:1) as eluent, Yield 99% (50.8 mg) as a yellowish solid, er 91.5:8.5, [α]_D²⁵ = -128° (c = 0.5, CHCl₃), mp = 79 - 81°C, ¹H NMR (400 MHz, CDCl₃) δ [ppm] = 7.22 - 7.14 (m, 2H), 7.14 - 7.06 (m, 1H), 7.02 (dd, *J* = 8.0, 1.3 Hz, 1H), 3.93 (t, *J* = 6.5 Hz, 1H), 2.65 (dt, *J* = 17.7, 5.0 Hz, 1H), 2.60 - 2.46 (m, 2H), 2.42 - 2.28 (m, 1H), 2.13 - 1.96 (m, 2H), 1.61 - 1.45 (m, 1H), 1.40 - 1.32 (m, 2H), 0.93 (d, *J* = 6.6 Hz, 3H), 0.84 (d, *J* = 6.5 Hz, 3H), ¹³C{¹H} NMR (100 MHz, CDCl₃)

δ [ppm] = 197.5, 167.6, 150.7, 129.3, 127.3, 126.9, 124.6, 116.4, 116.0, 48.1, 37.3, 29.7, 28.1, 24.8, 23.8, 22.4, 20.7, IR (KBr) ν [cm⁻¹] = 1659, 1644, 1578, 1483, 1456, 1384, 1368, 1240, 1221, 1181, 1132, 1122, 994, 757, HR-MS (ESI): calc. for: ([M+Na]⁺): 279.1361; found: 279.1386, HPLC ODH Column (98% hexane: 2% *i*-propanol, 1 mL/min, 270 nm) R_{t1} = 8.8 min and R_{t2} = 17.6 min.

(*R*)-9-Vinyl-2,3,4,9-tetrahydro-1*H*-xanthen-1-one (**4l**). Hexane/MTBE (9:1) as eluent, Yield 68% (30.8 mg) as a colorless liquid, er 88:12, [α]_D²⁵ = -65° (c = 0.43, CHCl₃), ¹H NMR (400 MHz, CDCl₃) δ [ppm] = 7.24 - 7.16 (m, 2H), 7.14 - 7.08 (m, 1H), 7.02 (d, *J* = 8.1 Hz, 1H), 5.87 (ddd, *J* = 16.8, 10.0, 6.5 Hz, 1H), 4.97 (d, *J* = 10.0 Hz, 1H), 4.89 (d, *J* = 17.0 Hz, 1H), 4.53 (d, *J* = 6.4 Hz, 1H), 2.72 - 2.47 (m, 3H), 2.45 - 2.33 (m, 1H), 2.15 - 2.00 (m, 2H), ¹³C{¹H} NMR (100 MHz, CDCl₃) δ [ppm] = 197.3, 167.1, 149.9, 140.6, 130.0, 127.9, 124.9, 123.7, 116.5, 114.2, 113.0, 37.2, 35.6, 28.1, 20.7, IR (film) ν [cm⁻¹] = 1662, 1644, 1580, 1486, 1445, 1376, 1236, 1180, 1134, 993, 915, 756, HR-MS (ESI): calc. for: ([M+H]⁺): 249.0886; found: 249.0887, HPLC IA Column (98% hexane: 2% *i*-propanol, 1 mL/min, 270 nm) R_{t1} = 10.1 min and R_{t2} = 11.8 min.

(*R*)-9-Ethyl-2,3,4,9-tetrahydro-1*H*-xanthen-1-one (**4m**). Hexane/MTBE (9:1) as eluent, Yield 97% (44.3 mg) as a colorless liquid, er 91:9, [α]_D²⁵ = -112° (c = 0.5, CHCl₃), ¹H NMR (400 MHz, Chloroform-*d*) δ [ppm] = 7.21 - 7.14 (m, 2H), 7.13 - 7.07 (m, 1H), 6.99 (d, *J* = 8.2 Hz, 1H), 3.95 (t, *J* = 4.9 Hz, 1H), 2.66 (dt, *J* = 17.6, 5.0 Hz, 1H), 2.61 - 2.47 (m, 2H), 2.42 - 2.32 (m, 1H), 2.12 - 1.99 (m, 2H), 1.76 - 1.56 (m, 2H), 0.67 (t, *J* = 7.5 Hz, 3H), ¹³C{¹H} NMR (101 MHz, CDCl₃) δ [ppm] = 197.8, 168.0, 150.8, 129.1, 127.3, 125.6, 124.8, 116.1, 113.8, 37.3, 32.4, 30.1, 28.0, 20.8, 9.3, IR (KBr) ν [cm⁻¹] = 1660, 1644, 1581, 1486, 1455, 1387, 1235, 1184, 1135, 991, 756, HR-MS (ESI): calc. for: ([M+H]⁺): 251.1043; found: 251.1043, HPLC ODH Column (98% hexane: 2% *i*-propanol, 1 mL/min, 270 nm) R_{t1} = 10.1 min and R_{t2} = 11.8 min.

(*R*)-6-(*tert*-Butyl)-9-phenyl-2,3,4,9-tetrahydro-1*H*-xanthen-1-one (**4n**). Hexane/MTBE (9:1) as eluent, Yield 91% (60.5 mg) as a white solid, er 50:50, mp = 169 - 171°C, ¹H NMR (300 MHz, CDCl₃) δ [ppm] = 7.25 - 7.18 (m, 4H), 7.16 - 7.07 (m, 2H), 7.06 - 7.00 (m, 2H), 5.03 (s, 1H), 2.79 - 2.57 (m, 2H), 2.47 - 2.28 (m, 2H), 2.11 - 1.91 (m, 2H), 1.29 (s, 9H), ¹³C{¹H} NMR (100 MHz, CDCl₃) δ [ppm] = 197.1, 166.6, 151.4, 149.2, 146.4, 129.6, 128.5, 128.0, 126.4, 122.5, 122.4, 115.0, 113.4, 37.7, 37.2, 34.7, 31.4, 28.1, 20.6, IR (KBr) ν [cm⁻¹] = 1644, 1376, 1269, 1225, 1180, 1136, 997, 700. 528, HR-MS (ESI): calc. for: ([M+K]⁺): 371.1413; found: 371.1391.

(*R*)-5-Methyl-9-phenyl-2,3,4,9-tetrahydro-1*H*-xanthen-1-one (**4o**). Hexane/MTBE (9:1) as eluent, Yield 74% (43.0 mg) as a white solid, er 57:43, mp = 159 - 161°C, ¹H NMR (400 MHz, CDCl₃) δ [ppm] = 7.24 - 7.18 (m, 4H), 7.15 - 7.08 (m, 1H), 7.05 - 6.99 (m, 1H), 6.97 - 6.89 (m, 2H), 5.08 - 5.02 (m, 1H), 2.82 - 2.57 (m, 2H), 2.47 - 2.37 (m, 2H), 2.35 (s, 3H), 2.11 - 1.96 (m, 2H), ¹³C{¹H} NMR (75 MHz, CDCl₃) δ [ppm] = 197.1, 166.3, 148.0, 146.4, 129.1, 128.5, 128.0, 127.7, 126.4, 125.8, 125.2, 124.6, 115.0, 38.1, 37.2, 28.1, 20.6, 16.0, IR (KBr) ν [cm⁻¹] = 1660, 1646, 1589, 1468, 1455, 1374, 1265, 1219, 1183, 1127, 1074, 765, 747, 732, 698, HR-MS (ESI): calc. for:

([M+Na]⁺): 313.1199; found: 313.1201, HPLC ODH Column (95% hexane: 5% *i*-propanol, 1 mL/min, 270 nm) R_{t1} = 7.7 min and R_{t2} = 8.9 min.

(*S*)-6,8-Dimethyl-9-phenyl-2,3,4,9-tetrahydro-1*H*-xanthen-1-one (**4p**). Hexane/MTBE (9:1) as eluent, Yield 83% (50.5 mg) as a white solid, er 85:15, [α]_D²⁵ = -9° (c = 1.6, CHCl₃), mp = 151 - 153°C, ¹H NMR (400 MHz, CDCl₃) δ [ppm] = 7.24 - 7.15 (m, 4H), 7.13 - 7.05 (m, 1H), 6.82 (s, 1H), 6.74 (s, 1H), 5.09 (s, 1H), 2.71 - 2.51 (m, 2H), 2.44 - 2.31 (m, 2H), 2.30 (s, 3H), 2.08 (s, 3H), 2.05 - 1.85 (m, 2H), ¹³C{¹H} NMR (100 MHz, CDCl₃) δ [ppm] = 197.1, 166.2, 150.4, 145.0, 137.8, 137.6, 128.8, 128.3, 127.8, 126.2, 121.1, 116.1, 114.6, 37.1, 35.3, 28.0, 21.1, 20.4, 19.0, IR (KBr) ν [cm⁻¹] = 1659, 1644, 1575, 1490, 1452, 1380, 1368, 1310, 1285, 1244, 1230, 1219, 1186, 1129, 1030, 1006, 843, 719, 698, HR-MS (ESI): calc. for: ([M+Na]⁺): 305.1536; found: 305.1539, HPLC IA Column (98% hexane: 2% *i*-propanol, 1 mL/min, 270 nm) R_{t1} = 9.4 min and R_{t2} = 11.6 min.

(*R*)-10-(4-Methoxyphenyl)-6,7,8,10-tetrahydro-9*H*-[1,3]dioxolo[4,5-*b*]xanthen-9-one (**14**). Hexane/MTBE (9:1) as eluent, Yield 80% (51.3 mg) as a white solid, er 94:6, [α]_D²⁵ = +20° (c = 0.50, CHCl₃), mp = 52 - 54°C, ¹H NMR (300 MHz, CDCl₃) δ [ppm] = 7.18 - 7.08 (m, 2H), 6.84 - 6.71 (m, 2H), 6.58 (s, 1H), 6.47 (s, 1H), 5.91 (d, *J* = 1.3 Hz, 1H), 5.87 (d, *J* = 1.3 Hz, 1H), 4.88 (s, 1H), 3.74 (s, 3H), 2.76 - 2.53 (m, 2H), 2.46 - 2.24 (m, 2H), 2.13 - 1.90 (m, 2H), ¹³C{¹H} NMR (100 MHz, CDCl₃) δ [ppm] = 197.2, 166.0, 158.2, 146.8, 144.8, 144.0, 138.8, 128.9, 117.9, 114.4, 113.9, 108.4, 101.6, 98.2, 55.3, 37.3, 37.1, 27.9, 20.5, IR (KBr) ν [cm⁻¹] = 1650, 1618, 1509, 1482, 1383, 1255, 1241, 1215, 1183, 1142, 1035, 998, 936, 532, HR-MS (ESI): calc. for: ([M+H]⁺): 373.1046; found: 373.1042, HPLC ODH Column (90% hexane: 10% *i*-propanol, 1 mL/min, 270 nm) R_{t1} = 18.9 min and R_{t2} = 22.9 min.

Gramm-Scale Synthesis of 4f. *Ortho*-hydroxy benzyl alcohol **1f** (1.24 g, 4.00 mmol, 1.0 equiv.), 1,3-cyclohexanedione **2a** (0.673 g, 6.00 mmol, 1.5 equiv.) and catalyst **5** (80.3 mg, 0.120 mmol, 3 mol %) were dissolved in chloroform (20 mL) at RT. The reaction mixture was stirred for 1 day until complete consumption of the starting material. Then *p*-toluenesulfonic acid monohydrate (0.152 g, 0.800 mmol, 20 mol%) was added and the reaction mixture was further stirred for 4 h at 40°C. The crude reaction mixture was purified by short flash chromatography (hexane/MTBE 9:1) to afford the desired xanthenone **4f** (1.37 g, 3.56 mmol, 89 %, er 97:3).

General Procedure for Enantioselective Addition of 3,5-Pyridandione.

Ortho-hydroxy benzyl alcohol **1** (0.1 mmol, 1.0 equiv.), 3,5-pyridandione **2b** (17.1 mg, 0.15 mmol, 1.5 equiv.) and catalyst **5** (3.4 mg, 0.005 mmol, 5 mol %) were dissolved in chloroform (0.8 mL) at 0°C. The reaction mixture was stirred for 1 day at 0°C until complete consumption of the starting material and then 1 day at RT. The crude reaction mixture was purified by short flash chromatography (hexane/MTBE 9:1) to afford the desired oxaxanthenones. The enantiomeric ratios were determined by HPLC on a chiral stationary phase.

(*R*)-9-Phenyl-3-oxo-2,3,4,9-tetrahydro-1*H*-xanthen-1-one (**6a**). Hexane/MTBE (9:1) as eluent, Yield 94% (26.2 mg) as

a white solid, er 91.5:8.5, $[\alpha]_D^{25} = -68^\circ$ ($c = 0.5$, CHCl_3), mp = 120 - 122°C, $^1\text{H NMR}$ (300 MHz, CDCl_3) δ [ppm] = 7.29 - 7.02 (m, 9H), 5.09 (s, 1H), 4.61 (d, $J = 16.3$ Hz, 1H), 4.49 (dt, $J = 16.3$, 1.5 Hz, 1H), 4.19 (d, $J = 16.2$ Hz, 1H), 4.07 (dd, $J = 16.1$, 1.7 Hz, 1H), $^{13}\text{C}\{^1\text{H}\}$ NMR (75 MHz, CDCl_3) δ [ppm] = 192.9, 163.5, 149.1, 145.1, 130.6, 128.7, 128.2, 128.1, 126.9, 125.8, 125.0, 116.8, 112.6, 71.9, 64.7, 36.7, IR (KBr) ν [cm^{-1}] = 1676, 1656, 1485, 1391, 1353, 1242, 1173, 1124, 763, 710, HR-MS (ESI): calc. for: $[\text{M}+\text{Na}]^+$: 301.0835; found: 301.0835, HPLC ODH Column (95% hexane: 5% *i*-propanol, 1 mL/min, 270 nm) $R_{t1} = 13.4$ min and $R_{t2} = 17.0$ min.

(*R*)-9-(4-Methoxyphenyl)-3-oxo-2,3,4,9-tetrahydro-1H-xanthen-1-one (**6b**). Hexane/MTBE (9:1) as eluent, Yield 88% (27.1 mg) as a yellow solid, er 92:8, $[\alpha]_D^{25} = -38^\circ$ ($c = 0.5$, CHCl_3), mp = 35 - 37°C, $^1\text{H NMR}$ (400 MHz, CDCl_3) δ [ppm] = 7.23 - 7.05 (m, 6H), 6.82 - 6.75 (m, 2H), 5.04 (s, 1H), 4.59 (d, $J = 16.3$ Hz, 1H), 4.49 (dt, $J = 16.3$, 1.5 Hz, 1H), 4.18 (d, $J = 16.1$ Hz, 1H), 4.06 (dd, $J = 16.1$, 1.8 Hz, 1H), 3.74 (s, 3H), $^{13}\text{C}\{^1\text{H}\}$ NMR (100 MHz, CDCl_3) δ [ppm] = 193.0, 163.3, 158.4, 149.1, 137.6, 130.6, 129.2, 128.0, 125.8, 125.3, 116.8, 114.1, 112.8, 71.9, 64.6, 55.3, 35.9, IR (KBr) ν [cm^{-1}] = 3442, 1673, 1652, 1509, 1394, 1255, 1241, 1173, 1032, 756, HR-MS (ESI): calc. for: $[\text{M}+\text{Na}]^+$: 331.0941; found: 331.0942, HPLC ODH Column (95% hexane: 5% *i*-propanol, 1 mL/min, 270 nm) $R_{t1} = 18.3$ min and $R_{t2} = 21.2$ min.

(*R*)-9-([1,1'-Biphenyl]-3-oxo-2,3,4,9-tetrahydro-1H-xanthen-1-one (**6c**). Hexane/MTBE (9:1) as eluent, Yield 91% (32.3 mg) as a white solid, er 99:1, $[\alpha]_D^{24} = +28^\circ$ ($c = 0.5$, CHCl_3), mp = 170 - 173°C, $^1\text{H NMR}$ (300 MHz, CDCl_3) δ [ppm] = 7.57 - 7.44 (m, 4H), 7.44 - 7.35 (m, 2H), 7.35 - 7.28 (m, 3H), 7.25 - 7.03 (m, 4H), 5.15 (s, 1H), 4.63 (d, $J = 16.0$ Hz, 1H), 4.51 (dt, $J = 16.0$, 1.5 Hz, 1H), 4.22 (d, $J = 16.0$ Hz, 1H), 4.09 (dd, $J = 16.0$, 1.5 Hz, 1H), $^{13}\text{C}\{^1\text{H}\}$ NMR (100 MHz, CDCl_3) δ [ppm] = 193.0, 163.6, 149.1, 144.2, 141.0, 139.8, 130.6, 128.8, 128.6, 128.2, 127.5, 127.3, 127.2, 125.9, 124.9, 116.9, 112.5, 71.9, 64.7, 36.4, IR (KBr) ν [cm^{-1}] = 3444, 1672, 1651, 1581, 1485, 1394, 1355, 1243, 1172, 758, HR-MS (ESI): calc. for: $[\text{M}+\text{Na}]^+$: 377.1148; found: 377.1149, HPLC ODH Column (95% hexane: 5% *i*-propanol, 1 mL/min, 270 nm) $R_{t1} = 17.3$ min and $R_{t2} = 22.3$ min.

(*R*)-9-(4-Fluorophenyl)-3-oxo-2,3,4,9-tetrahydro-1H-xanthen-1-one (**6d**). Hexane/MTBE (9:1) as eluent, Yield 84% (24.9 mg) as a yellow solid, er 92:8, $[\alpha]_D^{25} = -36^\circ$ ($c = 0.5$, CHCl_3), mp = 48 - 50°C, $^1\text{H NMR}$ (400 MHz, CDCl_3) δ [ppm] = 7.25 - 7.16 (m, 3H), 7.13 - 7.07 (m, 3H), 6.98 - 6.89 (m, 2H), 5.08 (s, 1H), 4.60 (d, $J = 16.3$ Hz, 1H), 4.49 (dt, $J = 16.3$, 1.5 Hz, 1H), 4.19 (d, $J = 16.2$ Hz, 1H), 4.07 (dd, $J = 16.1$, 1.8 Hz, 1H), $^{13}\text{C}\{^1\text{H}\}$ NMR (100 MHz, CDCl_3) δ [ppm] = 193.0, 163.5, 161.7 (d, $J = 245.3$ Hz), 149.0, 140.9 (^4d , $J = 3.1$ Hz), 130.5, 129.8 (^3d , $J = 8.1$ Hz), 128.3, 125.9, 124.7, 117.0, 115.5 (d, $J = 21.4$ Hz), 112.5, 71.9, 64.6, 36.0, IR (film) ν [cm^{-1}] = 1674, 1654, 1507, 1485, 1394, 1242, 1172, 845, 788, 757, HR-MS (ESI): calc. for: $[\text{M}+\text{Na}]^+$: 319.0741; found: 319.0740, HPLC ODH Column (95% hexane: 5% *i*-propanol, 1 mL/min, 270 nm) $R_{t1} = 11.9$ min and $R_{t2} = 15.4$ min.

(*R*)-9-(4-Methoxy-3,5-dimethylphenyl)-3-oxo-2,3,4,9-tetrahydro-1H-xanthen-1-one (**6e**). Hexane/MTBE (9:1) as eluent, Yield 87% (29.3 mg) as a white solid, er 93:7, $[\alpha]_D^{25} = -72^\circ$ ($c = 0.5$, CHCl_3), mp = 162 - 164°C, $^1\text{H NMR}$ (300 MHz, CDCl_3) δ [ppm] = 7.24 - 7.17 (m, 1H), 7.16 - 7.04 (m, 3H),

6.84 (s, 2H), 4.96 (s, 1H), 4.63 (d, $J = 16.3$ Hz, 1H), 4.49 (dt, $J = 16.3$, 1.5 Hz, 1H), 4.21 (d, $J = 16.2$ Hz, 1H), 4.06 (dd, $J = 16.1$, 1.8 Hz, 1H), 3.65 (s, 3H), 2.20 (s, 6H), $^{13}\text{C}\{^1\text{H}\}$ NMR (100 MHz, CDCl_3) δ [ppm] = 193.0, 163.4, 155.8, 149.0, 140.3, 130.9, 130.5, 128.4, 128.0, 125.7, 125.4, 116.8, 112.8, 71.9, 64.7, 59.7, 36.1, 16.3, IR (KBr) ν [cm^{-1}] = 3443, 1658, 1646, 1484, 1391, 1252, 1240, 1172, 1132, 756, HR-MS (ESI): calc. for: $[\text{M}+\text{Na}]^+$: 359.1254; found: 359.1254, HPLC ODH Column (95% hexane: 5% *i*-propanol, 1 mL/min, 270 nm) $R_{t1} = 11.7$ min and $R_{t2} = 12.9$ min.

(*R*)-7-(tert-Butyl)-9-(4-methoxyphenyl)-3-oxo-2,3,4,9-tetrahydro-1H-xanthen-1-one (**6f**). Hexane/MTBE (9:1) as eluent, Yield 91% (33.2 mg) as a yellow solid, er 92.5:7.5, $[\alpha]_D^{25} = 57^\circ$ ($c = 0.5$, CHCl_3), mp = 34 - 36°C, $^1\text{H NMR}$ (300 MHz, CDCl_3) δ [ppm] = 7.23 (dd, $J = 8.6$, 2.4 Hz, 1H), 7.18 - 7.12 (m, 2H), 7.10 (d, $J = 2.3$ Hz, 1H), 7.02 (d, $J = 8.6$ Hz, 1H), 6.83 - 6.73 (m, 2H), 5.04 (s, 1H), 4.58 (d, $J = 16.3$ Hz, 1H), 4.45 (dt, $J = 16.3$, 1.4 Hz, 1H), 4.18 (d, $J = 16.1$ Hz, 1H), 4.04 (dd, $J = 16.1$, 1.8 Hz, 1H), 3.75 (s, 3H), 1.23 (s, 9H), $^{13}\text{C}\{^1\text{H}\}$ NMR (100 MHz, CDCl_3) δ [ppm] = 193.1, 163.5, 158.3, 148.9, 147.2, 137.6, 129.1, 127.1, 125.2, 124.5, 116.2, 114.0, 112.9, 71.9, 64.7, 55.3, 36.1, 34.6, 31.5, IR (KBr) ν [cm^{-1}] = 3434, 2961, 1674, 1651, 1509, 1395, 1252, 1243, 1175, 841, HR-MS (ESI): calc. for: $[\text{M}+\text{Na}]^+$: 387.1568; found: 387.1567, HPLC ODH Column (95% hexane: 5% *i*-propanol, 1 mL/min, 270 nm) $R_{t1} = 9.7$ min and $R_{t2} = 11.0$ min.

(*R*)-7-Methoxy-9-phenyl-3-oxo-2,3,4,9-tetrahydro-1H-xanthen-1-one (**6g**). Hexane/MTBE (9:1) as eluent, Yield 81% (25.0 mg) as a yellow solid, er 95:5, $[\alpha]_D^{24} = +16^\circ$ ($c = 0.5$, CHCl_3) mp = 84 - 86°C, $^1\text{H NMR}$ (400 MHz, CDCl_3) δ [ppm] = 7.28 - 7.21 (m, 4H), 7.20 - 7.13 (m, 1H), 7.04 (d, $J = 9.0$ Hz, 1H), 6.75 (dd, $J = 9.0$, 3.0 Hz, 1H), 6.59 (d, $J = 2.9$ Hz, 1H), 5.06 (s, 1H), 4.58 (d, $J = 16.2$ Hz, 1H), 4.48 (dt, $J = 16.2$, 1.5 Hz, 1H), 4.17 (d, $J = 16.1$ Hz, 1H), 4.06 (dd, $J = 16.1$, 1.8 Hz, 1H), 3.70 (s, 3H), $^{13}\text{C}\{^1\text{H}\}$ NMR (100 MHz, CDCl_3) δ [ppm] = 192.9, 163.6, 157.1, 145.0, 143.3, 128.7, 128.2, 126.9, 125.8, 117.7, 114.3, 114.2, 111.8, 71.9, 64.7, 55.7, 37.2, IR (KBr) ν [cm^{-1}] = 3441, 1671, 1647, 1614, 1597, 1494, 1396, 1231, 1194, 1030, HR-MS (ESI): calc. for: $[\text{M}+\text{Na}]^+$: 331.0941; found: 331.0942, HPLC IA Column (95% hexane: 5% *i*-propanol, 1 mL/min, 270 nm) $R_{t1} = 19.0$ min and $R_{t2} = 23.8$ min.

(*R*)-9-(2-Ethylphenyl)-3-oxo-2,3,4,9-tetrahydro-1H-xanthen-1-one (**6h**). Hexane/MTBE (9:1) as eluent, Yield 62% (19.0 mg) as a yellow solid, er 99:1, $[\alpha]_D^{24} = -21^\circ$ ($c = 0.3$, CHCl_3), mp = 64 - 66°C, $^1\text{H NMR}$ (300 MHz, CDCl_3) δ [ppm] = 7.23 - 6.96 (m, 8H), 5.34 (s, 1H), 4.62 (d, $J = 16.0$ Hz, 1H), 4.50 (dt, $J = 16.0$, 1.5 Hz, 1H), 4.15 (d, $J = 16.0$ Hz, 1H), 4.05 (dd, $J = 16.0$, 1.5 Hz, 1H), 3.24 - 2.98 (m, 2H), 1.39 (t, $J = 7.5$ Hz, 3H), $^{13}\text{C}\{^1\text{H}\}$ NMR (100 MHz, CDCl_3) δ [ppm] = 192.9, 163.5, 148.7, 143.3, 141.1, 130.2, 129.7, 128.7, 127.9, 126.8, 126.5, 125.9, 125.7, 116.9, 113.2, 71.9, 64.7, 32.4, 25.7, 15.6, IR (KBr) ν [cm^{-1}] = 3443, 1676, 1654, 1486, 1455, 1394, 1354, 1240, 1173, 755, HR-MS (ESI): calc. for: $[\text{M}+\text{Na}]^+$: 339.1148; found: 329.1147, HPLC ODH Column (95% hexane: 5% *i*-propanol, 1 mL/min, 270 nm) $R_{t1} = 10.1$ min and $R_{t2} = 13.2$ min.

(*R*)-9-(5-Methoxyphenyl)-3-oxo-2,3,4,9-tetrahydro-1H-xanthen-1-one (**6i**). Hexane/MTBE (9:1) as eluent, Yield 90% (27.7 mg) as a white solid, er 95:5, $[\alpha]_D^{24} = -116^\circ$ ($c =$

0.5, CHCl₃), mp = 116 - 118°C, ¹H NMR (300 MHz, CDCl₃) δ [ppm] = 7.25 - 7.19 (m, 2H), 7.19 - 7.09 (m, 2H), 7.06 - 6.96 (m, 2H), 6.92 - 6.82 (m, 2H), 5.42 (s, 1H), 4.62 (d, *J* = 16.0 Hz, 1H), 4.51 (dt, *J* = 16.0, 1.5 Hz, 1H), 4.17 (d, *J* = 16.0 Hz, 1H), 4.06 (dd, *J* = 16.0, 1.5 Hz, 1H), 3.82 (s, 3H), ¹³C{¹H} NMR (75 MHz, CDCl₃) δ [ppm] = 192.8, 164.3, 156.9, 149.1, 133.4, 130.0, 129.6, 128.2, 127.7, 125.5, 125.4, 121.0, 116.3, 111.8, 111.5, 72.0, 64.7, 55.9, 31.3, IR (KBr) ν [cm⁻¹] = 3443, 2834, 1655, 1491, 1456, 1394, 1254, 1173, 1127, 756, HR-MS (ESI): calc. for: ([M+Na]⁺): 331.0941; found: 331.0941, HPLC ODH Column (95% hexane: 5% *i*-propanol, 1 mL/min, 270 nm) R_{t1} = 20.1 min and R_{t2} = 24.0 min.

(*R*)-9-(2-Ethylphenyl)-7-methyl-3-oxo-2,3,4,9-tetrahydro-1*H*-xanthen-1-one (**6j**). Hexane/MTBE (9:1) as eluent, Yield 93% (29.8 mg) as a yellow oil, er 98:2, [α]_D²⁴ = -20 (c = 1.1, CHCl₃), ¹H NMR (300 MHz, CDCl₃) δ [ppm] = 7.22 - 7.17 (m, 1H), 7.15 - 7.00 (m, 3H), 6.96 (d, *J* = 1.0 Hz, 2H), 6.81 (s, 1H), 5.29 (s, 1H), 4.61 (d, *J* = 16.0 Hz, 1H), 4.49 (dt, *J* = 16.0, 1.5 Hz, 1H), 4.14 (d, *J* = 16.0 Hz, 1H), 4.04 (dd, *J* = 16.0, 1.5 Hz, 1H), 3.21 - 2.98 (m, 2H), 2.24 (s, 3H), 1.39 (t, *J* = 7.5 Hz, 3H), ¹³C{¹H} NMR (100 MHz, CDCl₃) δ [ppm] = 192.9, 163.6, 146.8, 143.4, 141.1, 135.3, 130.3, 129.7, 128.6, 126.8, 126.5, 125.5, 116.6, 113.2, 72.0, 64.7, 32.4, 25.6, 21.0, 15.6, IR (film) ν [cm⁻¹] = 2964, 1651, 1494, 1393, 1351, 1253, 1200, 1131, 816, 752, HR-MS (ESI): calc. for: ([M+H]⁺): 321.1485; found: 321.1486, HPLC ODH Column (95% hexane: 5% *i*-propanol, 1 mL/min, 270 nm) R_{t1} = 8.5 min and R_{t2} = 10.9 min.

General Procedure for Enantioselective Addition of 3,5-Thiopyrandione.

Ortho-hydroxy benzyl alcohol **1** (0.2 mmol, 1.0 equiv.) and catalyst **5** (6.7 mg, 0.01 mmol, 5 mol %) were dissolved in chloroform (1.0 mL) at RT. Then 3,5-thiopyrandione **2c** (31 mg, 0.24 mmol, 1.2 equiv.) was added in one portion, whereupon the reaction mixture was stirred for 36 h at RT. The crude reaction mixture was filtered over pad of silica gel (2 cm) using 25% of ethyl acetate in hexane to remove the water and the excess of the diketone. The solvents were removed in vacuo and the crude white solid was dissolved in chloroform (1.0 mL). Then *p*-toluenesulfonic acid monohydrate (7.6 mg, 0.04 mmol, 20 mol %) was added and the reaction mixture was further stirred for 2 h at 40°C. The crude reaction mixture was purified by short flash chromatography (hexane/MTBE 8:1) to afford the desired thioxanthenones. The enantiomeric ratios were determined by HPLC on a chiral stationary phase.

(*R*)-9-(4-(*tert*-Butyl)phenyl)-3-thio-2,3,4,9-tetrahydro-1*H*-xanthen-1-one (**7a**). Hexane/MTBE (8:1) as eluent, Yield 69% (48.4 mg) as a white solid, er 97:3, [α]_D²⁵ = +85° (c = 1.0, CHCl₃), mp = 51 - 53°C, ¹H NMR (400 MHz, CDCl₃) δ [ppm] = 7.27 - 7.20 (m, 5H), 7.18 - 7.11 (m, 2H), 7.02 (d, *J* = 8.6 Hz, 1H), 5.11 (s, 1H), 3.74 (ddd, *J* = 17.5, 2.1, 1.2 Hz, 1H), 3.51 (dd, *J* = 17.5, 2.0 Hz, 1H), 3.39 (dd, *J* = 16.0, 2.0 Hz, 1H), 3.17 (dd, *J* = 16.0, 2.0 Hz, 1H), 1.24 (s, 9H), ¹³C{¹H} NMR (100 MHz, CDCl₃) δ [ppm] = 191.3, 163.5, 148.7, 147.3, 145.6, 128.6, 127.8, 126.6, 126.4, 125.0, 124.6, 116.0, 114.5, 38.5, 34.6, 34.6, 31.5, 27.4, IR (KBr) ν [cm⁻¹] = 2962, 1636, 1589, 1495, 1362, 1230, 1190, 1127, 1009, HR-MS (ESI): calc. for: ([M+Na]⁺): 373.1238; found: 373.1234, HPLC ODH Column (95% hexane: 5% *i*-propanol, 1 mL/min, 270 nm) R_{t1} = 7.6 min and R_{t2} = 10.5 min.

(*R*)-9-(4-Methoxyphenyl)-3-thio-2,3,4,9-tetrahydro-1*H*-xanthen-1-one (**7b**). Hexane/MTBE (8:1) as eluent, Yield 59% (38.3 mg) as a colorless oil, er 99:1, [α]_D²⁴ = -78° (c = 1.0, CHCl₃), ¹H NMR (400 MHz, CDCl₃) δ [ppm] = 7.22 - 7.10 (m, 4H), 7.09 - 7.01 (m, 2H), 6.83 - 6.72 (m, 2H), 5.05 (s, 1H), 3.79 - 3.70 (m, 1H), 3.73 (s, 3H), 3.52 (dd, *J* = 17.5, 2.0 Hz, 1H), 3.39 (dd, *J* = 16.0, 2.0 Hz, 1H), 3.17 (dd, *J* = 16.0, 2.0 Hz, 1H), ¹³C{¹H} NMR (100 MHz, CDCl₃) δ [ppm] = 191.3, 163.0, 158.3, 149.2, 138.1, 129.9, 128.9, 127.8, 125.6, 125.5, 116.5, 114.5, 114.0, 55.3, 37.5, 34.6, 27.4, IR (film) ν [cm⁻¹] = 2955, 2905, 2834, 1659, 1637, 1608, 1581, 1509, 1485, 1456, 1360, 1253, 1228, 1177, 1119, 1032, 1007, 910, 840, HR-MS (ESI): calc. for: ([M+Na]⁺): 347.0718; found: 347.0713, HPLC ODH Column (90% hexane: 10% *i*-propanol, 1 mL/min, 220 nm) R_{t1} = 16.1 min and R_{t2} = 18.3 min.

(*R*)-9-([1,1'-Biphenyl]-3-thio-2,3,4,9-tetrahydro-1*H*-xanthen-1-one (**7c**). Hexane/MTBE (8:1) as eluent, Yield 68% (50.4 mg) as a white solid, er 97:3, [α]_D²⁴ = +19.2° (c = 0.5, CHCl₃), mp = 161 - 165°C, ¹H NMR (400 MHz, CDCl₃) δ [ppm] = 7.55 - 7.50 (m, 2H), 7.49 - 7.44 (m, 2H), 7.44 - 7.36 (m, 2H), 7.35 - 7.29 (m, 3H), 7.25 - 7.16 (m, 2H), 7.13 - 7.04 (m, 2H), 5.16 (s, 1H), 3.78 (ddd, *J* = 17.5, 2.0, 1.0 Hz, 1H), 3.55 (dd, *J* = 17.5, 2.0 Hz, 1H), 3.42 (dd, *J* = 16.0, 2.0 Hz, 1H), 3.20 (dd, *J* = 16.0, 2.0 Hz, 1H), ¹³C{¹H} NMR (100 MHz, CDCl₃) δ [ppm] = 191.3, 163.3, 149.2, 144.7, 141.0, 139.6, 130.0, 128.8, 128.3, 128.0, 127.5, 127.21, 127.15, 125.6, 125.3, 116.6, 114.3, 38.0, 34.6, 27.4, IR (KBr) ν [cm⁻¹] = 3026, 2889, 1638, 1580, 1485, 1456, 1358, 1229, 1188, 1121, 1007, 851, 754, HR-MS (ESI): calc. for: ([M+Na]⁺): 393.0925; found: 393.0919, HPLC ODH Column (90% hexane: 10% *i*-propanol, 1 mL/min, 220 nm) R_{t1} = 15.8 min and R_{t2} = 19.4 min.

(*R*)-9-(4-Methoxy-3,5-dimethylphenyl)-3-thio-2,3,4,9-tetrahydro-1*H*-xanthen-1-one (**7d**). Hexane/MTBE (8:1) as eluent, Yield 60% (42.3 mg) as a colorless oil, er 96:4, [α]_D²⁴ = -36° (c = 1.0, CHCl₃), ¹H NMR (400 MHz, CDCl₃) δ [ppm] = 7.22 - 7.10 (m, 2H), 7.10 - 7.01 (m, 2H), 6.85 (dd, *J* = 1.0, 0.5 Hz, 2H), 4.98 (s, 1H), 3.75 (ddd, *J* = 17.5, 2.0, 1.0 Hz, 1H), 3.64 (s, 3H), 3.55 (dd, *J* = 17.5, 1.0 Hz, 1H), 3.39 (dd, *J* = 16.0, 2.0 Hz, 1H), 3.19 (dd, *J* = 16.0, 2.0 Hz, 1H), 2.20 (s, 6H), ¹³C{¹H} NMR (100 MHz, CDCl₃) δ [ppm] = 191.4, 163.1, 155.7, 149.1, 140.8, 130.8, 129.9, 128.1, 127.7, 125.7, 125.5, 116.5, 114.5, 59.6, 37.7, 34.6, 27.4, 16.4, IR (film) ν [cm⁻¹] = 2925, 2824, 1639, 1581, 1509, 1484, 1456, 1360, 1298, 1225, 1181, 1120, 1008, 922, 872, HR-MS (ESI): calc. for: ([M+Na]⁺): 375.1031; found: 375.1027, HPLC ODH Column (95% hexane: 5% *i*-propanol, 1 mL/min, 220 nm) R_{t1} = 13.1 min and R_{t2} = 14.8 min.

(*R*)-9-(2-Methoxyphenyl)-3-thio-2,3,4,9-tetrahydro-1*H*-xanthen-1-one (**7e**). Hexane/MTBE (8:1) as eluent, Yield 65% (42.2 mg) as a white solid, er 96:4, [α]_D²⁴ = -72° (c = 1.0, CHCl₃), mp = 43 - 45°C, ¹H NMR (400 MHz, CDCl₃) δ [ppm] = 7.30 - 7.26 (m, 1H), 7.21 (dd, *J* = 8.0, 2.0 Hz, 1H), 7.17 - 7.09 (m, 2H), 7.03 - 6.96 (m, 2H), 6.87 (ddd, *J* = 8.0, 6.0, 1.5 Hz, 2H), 5.49 (s, 1H), 3.87 (s, 3H), 3.76 (ddd, *J* = 17.5, 2.0, 1.5 Hz, 1H), 3.55 (dd, *J* = 17.5, 2.0 Hz, 1H), 3.38 (dd, *J* = 16.0, 2.0 Hz, 1H), 3.15 (dd, *J* = 16.0, 2.0 Hz, 1H), ¹³C{¹H} NMR (100 MHz, CDCl₃) δ [ppm] = 191.1, 163.8, 156.7, 149.1, 134.1, 129.6, 129.0, 128.0, 127.5, 125.6, 125.2, 121.0, 116.0, 113.2, 111.8, 56.0, 34.6, 32.5, 27.4, IR (KBr) ν [cm⁻¹] = 2935, 2835,

1638, 1580, 1487, 1457, 1362, 1229, 1192, 1126, 1029, 1009, 755, HR-MS (ESI): calc. for: $[(M+Na)^+]$: 347.0718; found: 347.0711, HPLC ODH Column (95% hexane: 5% *i*-propanol, 1 mL/min, 220 nm) R_{t1} = 23.5 min and R_{t2} = 30.4 min.

General Procedure for Enantioselective Addition of 1,3-Cyclopentanedione.

Ortho-hydroxy benzyl alcohol **1** (0.1 mmol, 1.0 equiv.), 1,3-cyclopentanedione **2d** (17.1 mg, 0.15 mmol, 1.5 equiv.) and catalyst **5** (3.4 mg, 0.005 mmol, 5 mol %) were dissolved in chloroform (0.8 mL) at 0°C. The reaction mixture was stirred for 1 day at 0°C until complete consumption of the starting material. The crude reaction mixture was purified by short flash chromatography (hexane/MTBE 2:1) to afford the desired chromenes. The enantiomeric ratios were determined by HPLC on a chiral stationary phase.

(*R*)-9-(4-Methoxyphenyl)-3,9-dihydrocyclopenta[*b*]chromen-1(2*H*)-one (**8a**). Hexane/MTBE (2:1) as eluent, Yield 62% (18.1 mg) as a white solid, er 95:5, $[\alpha]_D^{24}$ = +5° (*c* = 0.37, CHCl₃), mp = 133 - 135°C, ¹H NMR (400 MHz, CDCl₃) δ [ppm] = 7.25 - 7.20 (m, 1H), 7.16 - 7.04 (m, 5H), 6.83 - 6.76 (m, 2H), 4.89 (s, 1H), 3.75 (s, 3H), 2.86 - 2.70 (m, 2H), 2.54 - 2.41 (m, 2H), ¹³C{¹H} NMR (75 MHz, CDCl₃) δ [ppm] = 202.6, 177.8, 158.5, 150.6, 136.9, 131.2, 129.4, 128.2, 125.6, 124.5, 118.1, 117.2, 114.0, 55.3, 37.7, 33.6, 25.7, IR (KBr) ν [cm⁻¹] = 3441, 2929, 1700, 1652, 1610, 1509, 1383, 1247, 1031, 756, HR-MS (ESI): calc. for: $[(M+Na)^+]$: 315.0991; found: 315.0992, HPLC ODH Column (90% hexane: 10% *i*-propanol, 1 mL/min, 270 nm) R_{t1} = 16.9 min and R_{t2} = 27.7 min.

(*R*)-9-(*p*-Tolyl)-3,9-dihydrocyclopenta[*b*]chromen-1(2*H*)-one (**8b**). Hexane/MTBE (2:1) as eluent, Yield 92% (25.4 mg) as a white solid, er 90.5:9.5, $[\alpha]_D^{25}$ = +28° (*c* = 0.50, CHCl₃), mp = 148 - 150°C, ¹H NMR (300 MHz, CDCl₃) δ [ppm] = 7.25 - 7.18 (m, 1H), 7.18 - 7.00 (m, 7H), 4.90 (s, 1H), 2.94 - 2.64 (m, 2H), 2.55 - 2.40 (m, 2H), 2.27 (s, 3H), ¹³C{¹H} NMR (100 MHz, CDCl₃) δ [ppm] = 202.6, 177.9, 150.6, 141.6, 136.4, 131.2, 129.3, 128.3, 128.2, 125.6, 124.4, 118.0, 117.2, 38.1, 33.6, 25.7, 21.2, IR (KBr) ν [cm⁻¹] = 1702, 1656, 1576, 1509, 1482, 1455, 1382, 1248, 1164, 1116, 1014, 755, 525, HR-MS (ESI): calc. for: $[(M+Na)^+]$: 299.1040; found: 299.1043, HPLC ODH Column (90% hexane: 10% *i*-propanol, 1 mL/min, 270 nm) R_{t1} = 11.0 min and R_{t2} = 14.0 min.

(*R*)-9-(4-(*tert*-Butyl)phenyl)-3,9-dihydrocyclopenta[*b*]chromen-1(2*H*)-one (**8c**). Hexane/MTBE (2:1) as eluent, Yield 91% (29.0 mg) as a white solid, er 90:10, $[\alpha]_D^{25}$ = +25° (*c* = 0.50, CHCl₃), mp = 148 - 150°C, ¹H NMR (300 MHz, CDCl₃) δ [ppm] = 7.29 - 7.26 (m, 1H), 7.25 - 7.19 (m, 2H), 7.16 - 7.04 (m, 5H), 4.92 (s, 1H), 2.89 - 2.66 (m, 2H), 2.54 - 2.43 (m, 2H), 1.26 (s, 9H), ¹³C{¹H} NMR (100 MHz, CDCl₃) δ [ppm] = 202.6, 178.0, 150.7, 149.4, 141.4, 131.3, 128.2, 127.9, 125.5, 124.4, 118.1, 117.2, 37.9, 34.5, 33.6, 31.5, 25.7, IR (KBr) ν [cm⁻¹] = 3445, 2958, 2359, 1701, 1654, 1578, 1482, 1455, 1382, 1248, 1120, 1013, 841, 749, 691, 606, 555, HR-MS (ESI): calc. for: $[(M+Na)^+]$: 341.1512; found: 341.1511, HPLC ODH Column (90% hexane: 10% *i*-propanol, 1 mL/min, 270 nm) R_{t1} = 8.8 min and R_{t2} = 11.0 min.

(*R*)-9-([1,1'-Biphenyl]-3,9-dihydrocyclopenta[*b*]chromen-1(2*H*)-one (**8d**). Hexane/MTBE (2:1) as eluent, Yield 62% (21.0 mg) as a white solid, er 93:7, $[\alpha]_D^{24}$ = +51° (*c* = 0.82, CHCl₃), mp = 216 - 218°C, ¹H NMR (300 MHz, CDCl₃) δ [ppm] = 7.57 - 7.45 (m, 4H), 7.44 - 7.35 (m, 2H), 7.34 - 7.27 (m, 2H), 7.26 - 7.22 (m, 2H), 7.20 - 7.05 (m, 3H), 5.00 (s, 1H), 2.97 - 2.66 (m, 2H), 2.61 - 2.41 (m, 2H), ¹³C{¹H} NMR (100 MHz, CDCl₃) δ [ppm] = 202.6, 178.1, 150.7, 143.5, 141.0, 139.8, 131.3, 128.81, 128.80, 128.4, 127.4, 127.3, 127.2, 125.7, 124.1, 117.8, 117.3, 38.2, 33.7, 25.7, IR (KBr) ν [cm⁻¹] = 3444, 1701, 1653, 1576, 1483, 1383, 1245, 1164, 756, 698, HR-MS (ESI): calc. for: $[(M+Na)^+]$: 361.1200; found: 361.1199, HPLC ODH Column (90% hexane: 10% *i*-propanol, 1 mL/min, 270 nm) R_{t1} = 17.5 min and R_{t2} = 23.0 min.

(*R*)-7-Bromo-9-(4-methoxyphenyl)-3,9-dihydrocyclopenta[*b*]chromen-1(2*H*)-one (**8e**). Hexane/MTBE (2:1) as eluent, Yield 43% (16.0 mg) as a white solid, er 91.5:8.5, $[\alpha]_D^{25}$ = +50° (*c* = 0.50, CHCl₃), mp = 165 - 167°C, ¹H NMR (300 MHz, CDCl₃) δ [ppm] = 7.32 (ddd, *J* = 8.7, 2.4, 0.5 Hz, 1H), 7.19 (dd, *J* = 2.4, 0.7 Hz, 1H), 7.15 - 7.05 (m, 2H), 7.02 (d, *J* = 8.7 Hz, 1H), 6.87 - 6.73 (m, 2H), 4.84 (s, 1H), 3.76 (s, 3H), 2.87 - 2.68 (m, 2H), 2.55 - 2.43 (m, 2H), ¹³C{¹H} NMR (75 MHz, CDCl₃) δ [ppm] = 202.3, 177.4, 158.6, 149.7, 136.1, 133.8, 131.3, 129.4, 126.7, 119.0, 118.1, 117.8, 114.2, 55.3, 37.6, 33.7, 25.6, IR (KBr) ν [cm⁻¹] = 1698, 1649, 1611, 1509, 1470, 1377, 1240, 1176, 1159, 1119, 1034, 1019, 844, 823, HR-MS (ESI): calc. for: $[(M+Na)^+]$: 393.0097/395.0097; found: 393.0098/395.0098, HPLC ODH Column (90% hexane: 10% *i*-propanol, 1 mL/min, 270 nm) R_{t1} = 19.3 min and R_{t2} = 32.6 min.

(*R*)-9-(2-Ethylphenyl)-7-methyl-3,9-dihydrocyclopenta[*b*]chromen-1(2*H*)-one (**8f**). Hexane/MTBE (2:1) as eluent, Yield 78% (23.7 mg) as a white solid, er 97:3, $[\alpha]_D^{24}$ = +208° (*c* = 0.34, CHCl₃), mp = 118 - 120°C, ¹H NMR (300 MHz, CDCl₃) δ [ppm] = 7.19 (dd, *J* = 7.5, 1.5 Hz, 1H), 7.15 - 6.95 (m, 4H), 6.89 (d, *J* = 7.5 Hz, 1H), 6.74 (s, 1H), 5.15 (s, 1H), 3.18 - 2.89 (m, 2H), 2.89 - 2.68 (m, 2H), 2.48 - 2.38 (m, 2H), 2.19 (s, 3H), 1.35 (t, *J* = 7.5 Hz, 3H), ¹³C{¹H} NMR (75 MHz, CDCl₃) δ [ppm] = 202.3, 177.9, 148.6, 142.6, 141.7, 135.2, 131.0, 129.9, 128.8, 128.7, 126.8, 126.4, 124.8, 118.4, 116.9, 34.0, 33.5, 26.1, 25.7, 20.9, 15.8, IR (film) ν [cm⁻¹] = 2927, 1703, 1656, 1491, 1378, 1253, 1231, 1188, 813, 787, 760, HR-MS (ESI): calc. for: $[(M+Na)^+]$: 327.1356; found: 327.1356, HPLC ODH Column (90% hexane: 10% *i*-propanol, 1 mL/min, 270 nm) R_{t1} = 8.5 min and R_{t2} = 10.9 min.

(*R*)-7-Methoxy-9-(2-methoxyphenyl)-3,9-dihydrocyclopenta[*b*]chromen-1(2*H*)-one (**8g**). Hexane/MTBE (2:1) as eluent, Yield 92% (29.7 mg) as a white solid, er 93.5:6.5, $[\alpha]_D^{25}$ = -25° (*c* = 0.50, CHCl₃), mp = 114 - 116°C, ¹H NMR (300 MHz, CDCl₃) δ [ppm] = 7.21 - 7.09 (m, 1H), 7.09 - 6.96 (m, 2H), 6.92 - 6.79 (m, 2H), 6.76 - 6.63 (m, 2H), 5.31 (s, 1H), 3.83 (s, 3H), 3.68 (s, 3H), 2.92 - 2.67 (m, 2H), 2.48 (t, *J* = 5.0 Hz, 2H), ¹³C{¹H} NMR (75 MHz, CDCl₃) δ [ppm] = 202.3, 179.2, 156.8, 156.7, 144.6, 132.6, 129.4, 128.1, 126.0, 121.0, 117.5, 116.5, 114.8, 113.4, 111.7, 55.9, 55.6, 33.6, 32.4, 25.7, IR (KBr) ν [cm⁻¹] = 3442, 2925, 1702, 1655, 1492, 1386, 1244, 1179, 1030, HR-MS (ESI): calc. for: $[(M+Na)^+]$: 345.1097; found: 345.1096, HPLC ODH

Column (90% hexane: 10% *i*-propanol, 1 mL/min, 270 nm) $R_{t1} = 20.9$ min and $R_{t2} = 29.3$ min.

(*R*)-7-Methyl-9-(*o*-tolyl)-3,9-dihydrocyclopenta[*b*]chromen-1(2*H*)-one (**8h**). Hexane/MTBE (2:1) as eluent, Yield 86% (25.0 mg) as a yellow solid, er 98:2, $[\alpha]_D^{24} = +74^\circ$ ($c = 1.3$, CHCl_3), mp = 59 - 61°C, $^1\text{H NMR}$ (300 MHz, CDCl_3) δ [ppm] = 7.17 - 6.88 (m, 6H), 6.72 (s, 1H), 5.11 (s, 1H), 2.88 - 2.68 (m, 2H), 2.57 (s, 3H), 2.48 - 2.40 (m, 2H), 2.19 (s, 3H), $^{13}\text{C}\{^1\text{H}\}$ NMR (75 MHz, CDCl_3) δ [ppm] = 202.4, 177.9, 148.6, 143.1, 135.8, 135.2, 131.0, 130.6, 129.9, 128.8, 126.6, 126.5, 124.5, 118.3, 116.8, 34.8, 33.5, 25.8, 20.8, 20.3, IR (film) ν [cm^{-1}] = 2924, 1703, 1655, 1491, 1377, 1253, 1189, 787, 761, 735, HR-MS (ESI): calc. for: $[\text{M}+\text{Na}]^+$: 313.1199; found: 313.1200, HPLC ODH Column (90% hexane: 10% *i*-propanol, 1 mL/min, 270 nm) $R_{t1} = 10.6$ min and $R_{t2} = 14.9$ min.

(*R*)-9-(2-Methoxyphenyl)-3,9-dihydrocyclopenta[*b*]chromen-1(2*H*)-one (**8i**). Hexane/MTBE (2:1) as eluent, Yield 69% (20.2 mg) as a white solid, er 95:5, $[\alpha]_D^{25} = +20^\circ$ ($c = 0.50$, CHCl_3), mp = 119 - 121°C, $^1\text{H NMR}$ (300 MHz, CDCl_3) δ [ppm] = 7.20 - 7.11 (m, 3H), 7.11 - 7.05 (m, 2H), 7.03 - 6.96 (m, 1H), 6.90 - 6.82 (m, 2H), 5.32 (s, 1H), 3.80 (s, 3H), 2.92 - 2.71 (m, 2H), 2.48 (t, $J = 5.0$ Hz, 2H), $^{13}\text{C}\{^1\text{H}\}$ NMR (75 MHz, CDCl_3) δ [ppm] = 202.4, 178.9, 156.9, 150.5, 132.8, 130.5, 129.7, 128.1, 127.8, 125.3, 125.1, 121.0, 117.2, 116.8, 111.8, 55.9, 33.6, 32.3, 25.7, IR (KBr) ν [cm^{-1}] = 3442, 2924, 1708, 1658, 1482, 1387, 1247, 1122, 1026, 759, HR-MS (ESI): calc. for: $[\text{M}+\text{Na}]^+$: 315.0992; found: 315.0992, HPLC ODH Column (90% hexane: 10% *i*-propanol, 1 mL/min, 270 nm) $R_{t1} = 18.3$ min and $R_{t2} = 23.2$ min.

(*R*)-9-(2-Ethylphenyl)-7-methoxy-3,9-dihydrocyclopenta[*b*]chromen-1(2*H*)-one (**8j**). Hexane/MTBE (2:1) as eluent, Yield 94% (30.1 mg) as a white solid, er 96:4, $[\alpha]_D^{24} = +76^\circ$ ($c = 0.50$, CHCl_3), mp = 122 - 124°C, $^1\text{H NMR}$ (300 MHz, CDCl_3) δ [ppm] = 7.17 (dd, $J = 7.5$, 1.5 Hz, 1H), 7.14 - 7.00 (m, 3H), 6.89 (d, $J = 7.5$ Hz, 1H), 6.74 (dd, $J = 9.0$, 3.0 Hz, 1H), 6.45 (d, $J = 3.0$ Hz, 1H), 5.16 (s, 1H), 3.66 (s, 3H), 3.15 - 2.87 (m, 2H), 2.87 - 2.68 (m, 2H), 2.52 - 2.35 (m, 2H), 1.34 (t, $J = 7.5$ Hz, 3H), $^{13}\text{C}\{^1\text{H}\}$ NMR (75 MHz, CDCl_3) δ [ppm] = 202.3, 178.0, 156.9, 144.7, 142.2, 141.7, 129.8, 128.8, 126.8, 126.4, 126.2, 117.9, 117.8, 115.2, 113.6, 55.6, 33.5, 26.1, 25.7, 15.84, IR (KBr) ν [cm^{-1}] = 3445, 2963, 2927, 1702, 1654, 1490, 1381, 1235, 1180, 1035, 1017, 814, HR-MS (ESI): calc. for: $[\text{M}+\text{Na}]^+$: 343.1305; found: 343.1302, HPLC ODH Column (90% hexane: 10% *i*-propanol, 1 mL/min, 270 nm) $R_{t1} = 13.4$ min and $R_{t2} = 16.6$ min.

General Procedure for Enantioselective Addition of Acetylacetone.

Ortho-hydroxy benzyl alcohol **1** (0.10 mmol, 1.0 equiv.) and catalyst **5** (3.4 mg, 0.005 mmol, 5 mol %) were dissolved in chloroform (1.0 mL). Acetylacetone (15.6 μL , 15.2 mg, 0.15 mmol, 1.5 equiv.) was added in portion and the reaction mixture was stirred for 1 day at RT until complete consumption of the starting material. Then *p*-toluenesulfonic acid monohydrate (3.8 mg, 0.02 mmol, 20 mol%) was added and the reaction mixture was further stirred for 4 h at 40°C. The crude reaction mixture was purified by short flash chromatography (hexane/MTBE 9:1)

to afford the desired chromenes. The enantiomeric ratios were determined by HPLC on a chiral stationary phase.

(*R*)-1-(6-Methoxy-2-methyl-4-(*o*-tolyl)-4*H*-chromen-3-yl)ethan-1-one (**9a**). Hexane/MTBE (9:1) as eluent, Yield 91% (28.1 mg) as a yellow oil, er 94:6, $[\alpha]_D^{25} = +22^\circ$ ($c = 0.50$, CHCl_3), $^1\text{H NMR}$ (400 MHz, CDCl_3) δ [ppm] = 7.16 - 6.99 (m, 4H), 6.93 (d, $J = 9.0$ Hz, 1H), 6.67 (dd, $J = 9.0$, 3.0 Hz, 1H), 6.51 (d, $J = 3.0$ Hz, 1H), 5.30 (s, 1H), 3.67 (s, 3H), 2.56 (s, 3H), 2.40 (d, 3H), 2.11 (s, 3H), $^{13}\text{C}\{^1\text{H}\}$ NMR (100 MHz, CDCl_3) δ [ppm] = 199.2, 158.3, 156.2, 144.2, 143.4, 134.6, 131.2, 129.3, 126.9, 126.8, 125.8, 117.1, 114.2, 113.3, 113.2, 55.6, 38.6, 30.2, 20.2, 12.0, IR (film) ν [cm^{-1}] = 2931, 1682, 1613, 1584, 1496, 1379, 1216, 1151, 1036, 787, 758, 733, HR-MS (ESI): calc. for: $[\text{M}+\text{Na}]^+$: 333.1305; found: 331.1304, HPLC ODH Column (98% hexane: 2% *i*-propanol, 1 mL/min, 270 nm) $R_{t1} = 11.3$ min and $R_{t2} = 14.0$ min.

(*R*)-1-(6-Methoxy-4-(2-methoxyphenyl)-2-methyl-4*H*-chromen-3-yl)ethan-1-one (**9b**). Hexane/MTBE (9:1) as eluent, Yield 96% (31.1 mg) as a yellow oil, er 91.5:8.5, $[\alpha]_D^{25} = -21^\circ$ ($c = 1.25$, CHCl_3), $^1\text{H NMR}$ (400 MHz, CDCl_3) δ [ppm] = 7.18 - 7.11 (m, 1H), 7.07 (dd, $J = 7.6$, 1.6 Hz, 1H), 6.94 - 6.80 (m, 4H), 6.65 (dd, $J = 8.9$, 3.0 Hz, 1H), 5.59 (s, 1H), 3.96 (s, 3H), 3.70 (s, 3H), 2.45 (s, 3H), 2.08 (s, 3H), $^{13}\text{C}\{^1\text{H}\}$ NMR (100 MHz, CDCl_3) δ [ppm] = 199.6, 160.1, 156.2, 155.4, 143.6, 134.5, 129.3, 128.0, 126.4, 121.6, 116.9, 113.2, 113.1, 112.5, 110.8, 55.7, 55.6, 34.5, 29.3, 20.1, IR (KBr) ν [cm^{-1}] = 2932, 1683, 1599, 1496, 1379, 1219, 1033, 933, HR-MS (ESI): calc. for: $[\text{M}+\text{Na}]^+$: 347.1254; found: 347.1252, HPLC ODH Column (98% hexane: 2% *i*-propanol, 1 mL/min, 270 nm) $R_{t1} = 11.3$ min and $R_{t2} = 15.8$ min.

(*R*)-1-(4-(2-Ethylphenyl)-2,6-dimethyl-4*H*-chromen-3-yl)ethan-1-one (**9c**). Hexane/MTBE (9:1) as eluent, Yield 74% (22.7 mg) as a yellow oil, er 93.5:6.5, $[\alpha]_D^{25} = +43^\circ$ ($c = 0.97$, CHCl_3), $^1\text{H NMR}$ (400 MHz, CDCl_3) δ [ppm] = 7.21 (d, $J = 7.4$ Hz, 1H), 7.17 - 7.06 (m, 3H), 6.94 - 6.85 (m, 2H), 6.77 (s, 1H), 5.34 (s, 1H), 3.05 - 2.88 (m, 2H), 2.38 (s, 3H), 2.17 (s, 3H), 2.11 (s, 3H), 1.31 (t, $J = 7.5$ Hz, 3H), $^{13}\text{C}\{^1\text{H}\}$ NMR (100 MHz, CDCl_3) δ [ppm] = 199.6, 157.6, 147.1, 143.7, 140.6, 133.9, 129.6, 129.1, 128.8, 128.4, 126.9, 126.6, 124.7, 116.1, 115.5, 37.8, 30.6, 24.9, 21.0, 20.2, 15.2, IR (film) ν [cm^{-1}] = 1762, 1683, 1625, 1578, 1382, 1354, 1251, 1213, 815, 787, 757, 601, 460, 452, HR-MS (ESI): calc. for: $[\text{M}+\text{Na}]^+$: 329.1512; found: 329.1147, HPLC ODH Column (98% hexane: 2% *i*-propanol, 1 mL/min, 270 nm) $R_{t1} = 6.5$ min and $R_{t2} = 8.6$ min.

(*R*)-1-(4-(2-Methoxyphenyl)-2,6-dimethyl-4*H*-chromen-3-yl)ethan-1-one (**9d**). Hexane/MTBE (9:1) as eluent, Yield 78% (24.1 mg) as a yellow oil, er 93.5:6.5, $[\alpha]_D^{25} = -7^\circ$ ($c = 0.90$, CHCl_3), $^1\text{H NMR}$ (400 MHz, CDCl_3) δ [ppm] = 7.14 (t, $J = 7.8$ Hz, 1H), 7.07 (d, $J = 7.5$ Hz, 1H), 7.03 (s, 1H), 6.93 - 6.82 (m, 4H), 5.56 (s, 1H), 3.95 (s, 3H), 2.43 (s, 3H), 2.20 (s, 3H), 2.09 (s, 3H), $^{13}\text{C}\{^1\text{H}\}$ NMR (100 MHz, CDCl_3) δ [ppm] = 199.8, 159.8, 155.4, 147.3, 134.8, 133.9, 129.5, 129.0, 128.2, 127.9, 125.2, 121.6, 115.9, 113.3, 110.9, 55.7, 34.2, 29.3, 21.0, 20.1, IR (film) ν [cm^{-1}] = 2924, 1761, 1682, 1583, 1498, 1463, 1381, 1247, 1215, 1097, 1050, 1026, 935, 815, 754, 626, 598, HR-MS (ESI): calc. for: $[\text{M}+\text{Na}]^+$: 331.1305; found: 331.1302, HPLC ODH Column (98% hexane: 2% *i*-propanol, 1 mL/min, 270 nm) $R_{t1} = 7.8$ min and $R_{t2} = 9.3$ min.

(*R*)-1-(4-(2-Methoxyphenyl)-2-methyl-4*H*-chromen-3-yl)ethan-1-one (**9e**). Hexane/MTBE (9:1) as eluent, Yield 90% (26.5 mg) as a yellow oil, er 90.5:9.5, $[\alpha]_D^{25} = -49^\circ$ ($c = 0.85$, CHCl₃, ¹H NMR (400 MHz, CDCl₃) δ [ppm] = 7.30 – 7.23 (m, 1H), 7.18 – 7.05 (m, 3H), 6.98 – 6.92 (m, 2H), 6.91 – 6.82 (m, 2H), 5.62 (s, 1H), 3.95 (s, 3H), 2.45 (s, 3H), 2.09 (s, 3H), ¹³C{¹H} NMR (100 MHz, CDCl₃) δ [ppm] = 199.7, 159.6, 155.5, 149.4, 134.6, 129.4, 128.9, 128.0, 127.5, 125.6, 124.5, 121.6, 116.2, 113.4, 110.9, 55.7, 34.2, 29.2, 20.0, IR (KBr) ν [cm⁻¹] = 2925, 1685, 1577, 1488, 1381, 1245, 1097, 1027, 939, 754, HR-MS (ESI): calc. for: ([M+Na]⁺): 317.1148; found: 317.1147, HPLC ODH Column (98% hexane: 2% *i*-propanol, 1 mL/min, 270 nm) R_{t1} = 9.0 min and R_{t2} = 10.0 min.

(*R*)-1-(6-(tert-Butyl)-4-(3-methoxyphenyl)-2-methyl-4*H*-chromen-3-yl)ethan-1-one (**9f**). Hexane/MTBE (9:1) as eluent, Yield 86% (30.1 mg) as a yellow oil, er 95:5, $[\alpha]_D^{25} = +68^\circ$ ($c = 1.00$, CHCl₃, ¹H NMR (400 MHz, CDCl₃) δ [ppm] = 7.22 – 7.12 (m, 3H), 6.93 (dd, $J = 8.0, 1.0$ Hz, 1H), 6.87 (ddd, $J = 7.5, 1.5, 1.0$ Hz, 1H), 6.79 (dd, $J = 2.5, 1.5$ Hz, 1H), 6.71 (ddd, $J = 8.0, 2.5, 1.0$ Hz, 1H), 4.97 (s, 1H), 3.76 (s, 3H), 2.45 (s, 3H), 2.18 (s, 3H), 1.24 (s, 9H), ¹³C{¹H} NMR (100 MHz, CDCl₃) δ [ppm] = 199.0, 160.1, 159.9, 152.8, 147.6, 147.2, 129.9, 125.4, 124.9, 124.1, 112.0, 115.9, 114.1, 113.8, 111.7, 55.3, 42.7, 34.5, 31.5, 30.3, 20.3, IR (film) ν [cm⁻¹] = 2963, 1766, 1680, 1597, 1582, 1489, 1261, 1226, 1045, 912, 732, HR-MS (ESI): calc. for: ([M+Na]⁺): 373.1774; found: 373.1777, HPLC ODH Column (98% hexane: 2% *i*-propanol, 1 mL/min, 280 nm) R_{t1} = 7.4 min and R_{t2} = 12.7 min.

General Procedure for Enantioselective Addition of Ethyl Acetoacetate.

Ortho-hydroxy benzyl alcohol **1** (0.10 mmol, 1.0 equiv.) and catalyst **5** (3.4 mg, 0.005 mmol, 5 mol %) were dissolved in chloroform (0.8 mL). Ethyl acetoacetate (18.9 μ L, 19.5 mg, 0.15 mmol, 1.5 equiv.) was added in portion and the reaction mixture was stirred for 3 days at RT until complete consumption of the starting material. The crude reaction mixture was purified by short flash chromatography (hexane/MTBE 19:1) to afford the desired chromenes. The enantiomeric ratios were determined by HPLC on a chiral stationary phase.

(*R*)-Ethyl 2-methyl-4-(naphthalen-1-yl)-4*H*-chromene-3-carboxylate (**10a**). Hexane/MTBE (19:1) as eluent, Yield 74% (25.5 mg) as a white solid, er 89:11, $[\alpha]_D^{25} = -18^\circ$ ($c = 1.01$, CHCl₃), mp = 77 – 79°C, ¹H NMR (400 MHz, CDCl₃) δ [ppm] = 8.53 (d, $J = 8.6$ Hz, 1H), 7.84 (d, $J = 8.1$ Hz, 1H), 7.66 (dd, $J = 7.0, 2.0$ Hz, 1H), 7.60 (t, $J = 7.6$ Hz, 1H), 7.49 (t, $J = 7.5$ Hz, 1H), 7.39 – 7.32 (m, 2H), 7.09 (t, $J = 7.6$ Hz, 1H), 7.02 (d, $J = 7.9$ Hz, 2H), 6.83 (t, $J = 7.4$ Hz, 1H), 5.98 (s, 1H), 3.93 – 3.77 (m, 2H), 2.56 (s, 3H), 0.75 (t, $J = 7.1$ Hz, 3H), ¹³C{¹H} NMR (100 MHz, CDCl₃) δ [ppm] = 167.3, 160.1, 148.9, 144.1, 133.9, 131.2, 128.9, 128.7, 127.6, 127.02, 126.99, 126.3, 126.0, 125.5, 125.3, 124.5, 123.7, 116.5, 106.4, 60.1, 35.6, 19.5, 13.8, IR (film) ν [cm⁻¹] = 1710, 1645, 1584, 1487, 1382, 1253, 1216, 1187, 1105, 1065, 786, 773, 757, HR-MS (ESI): calc. for: ([M+Na]⁺): 367.1305; found: 367.1301, HPLC ODH Column (99% hexane: 1% *i*-propanol, 1 mL/min, 270 nm) R_{t1} = 16.3 min and R_{t2} = 17.6 min.

(*R*)-Ethyl 4-(2-ethylphenyl)-2,6-dimethyl-4*H*-chromene-3-carboxylate (**10b**). Hexane/MTBE (19:1) as eluent, Yield

50% (16.8 mg) as a yellow oil, er 95.5:4.5, $[\alpha]_D^{25} = +39^\circ$ ($c = 0.68$, CHCl₃, ¹H NMR (400 MHz, CDCl₃) δ [ppm] = 7.21 – 7.15 (m, 1H), 7.15 – 7.03 (m, 3H), 6.93 – 6.85 (m, 2H), 6.75 (s, 1H), 5.31 (s, 1H), 4.09 – 3.97 (m, 2H), 3.08 – 2.90 (m, 2H), 2.45 (s, 3H), 2.17 (s, 3H), 1.32 (t, $J = 7.5$ Hz, 3H), 1.09 (t, $J = 7.1$ Hz, 3H), ¹³C{¹H} NMR (100 MHz, CDCl₃) δ [ppm] = 167.6, 159.6, 147.3, 144.8, 140.6, 133.9, 129.6, 129.3, 128.3, 128.2, 126.5, 126.3, 124.9, 116.1, 106.5, 60.1, 36.9, 25.1, 21.0, 19.7, 15.2, 14.2, IR (film) ν [cm⁻¹] = 1708, 1642, 1592, 1499, 1377, 1318, 1290, 1261, 1236, 1210, 1118, 1068, 984, 827, 749, 712, HR-MS (ESI): calc. for: ([M+Na]⁺): 359.1618; found: 359.1620, HPLC IA Column (99% hexane: 1% *i*-propanol, 1 mL/min, 270 nm) R_{t1} = 5.1 min and R_{t2} = 5.7 min.

(*R*)-Ethyl 6-methoxy-4-(2-methoxyphenyl)-2-methyl-4*H*-chromene-3-carboxylate (**10c**). Hexane/MTBE (19:1) as eluent, Yield 72% (25.5 mg) as a white solid, er 90:10, $[\alpha]_D^{25} = -6^\circ$ ($c = 1.07$, CHCl₃), mp = 92 – 94°C, ¹H NMR (400 MHz, CDCl₃) δ [ppm] = 7.16 – 7.08 (m, 2H), 6.91 – 6.80 (m, 3H), 6.77 (d, $J = 2.9$ Hz, 1H), 6.63 (dd, $J = 8.9, 3.0$ Hz, 1H), 5.53 (s, 1H), 4.09 – 3.93 (m, 2H), 3.89 (s, 3H), 3.68 (s, 3H), 2.50 (s, 3H), 1.08 (t, $J = 7.1$ Hz, 3H), ¹³C{¹H} NMR (100 MHz, CDCl₃) δ [ppm] = 167.5, 161.2, 156.2, 156.1, 143.8, 135.4, 129.0, 127.6, 126.2, 121.0, 116.7, 113.3, 113.0, 110.9, 104.3, 60.0, 55.7, 55.6, 34.6, 19.6, 14.1, IR (film) ν [cm⁻¹] = 1708, 1636, 1593, 1496, 1463, 1442, 1432, 1376, 1339, 1280, 1243, 1217, 1207, 1121, 1099, 1073, 1038, 838, 810, 751, HR-MS (ESI): calc. for: ([M+Na]⁺): 377.1359; found: 377.1358, HPLC ODH Column (99% hexane: 1% *i*-propanol, 1 mL/min, 270 nm) R_{t1} = 9.5 min and R_{t2} = 10.7 min.

(*R*)-Ethyl 2-methyl-4-(*p*-tolyl)-4*H*-chromene-3-carboxylate (**10d**). Hexane/MTBE (19:1) as eluent, Yield 84% (25.9 mg) as a colorless oil, er 9.1:5:8:5, $[\alpha]_D^{25} = +70^\circ$ ($c = 0.60$, CHCl₃, ¹H NMR (400 MHz, CDCl₃) δ [ppm] = 7.17 – 7.08 (m, 3H), 7.08 – 6.94 (m, 5H), 4.98 (s, 1H), 4.16 – 4.03 (m, 2H), 2.48 (s, 3H), 2.26 (s, 3H), 1.20 (t, $J = 7.1$ Hz, 3H), ¹³C{¹H} NMR (100 MHz, CDCl₃) δ [ppm] = 167.4, 160.1, 149.5, 143.9, 136.1, 129.3, 129.2, 127.8, 127.5, 125.2, 124.6, 116.3, 106.4, 60.3, 41.2, 21.2, 19.7, 14.3, IR (film) ν [cm⁻¹] = 1713, 1644, 1585, 1510, 1487, 1456, 1381, 1338, 1288, 1252, 1218, 1194, 1105, 1064, 985, 754, 505, HR-MS (ESI): calc. for: ([M+Na]⁺): 331.1305; found: 331.1306, HPLC ODH Column (99% hexane: 1% *i*-propanol, 1 mL/min, 270 nm) R_{t1} = 7.6 min and R_{t2} = 8.6 min.

(*R*)-Ethyl 4-(4-(tert-butyl)phenyl)-2-methyl-4*H*-chromene-3-carboxylate (**10e**). Hexane/MTBE (19:1) as eluent, Yield 65% (22.8 mg) as a colorless oil, er 92:8, $[\alpha]_D^{25} = +23^\circ$ ($c = 0.77$, CHCl₃, ¹H NMR (400 MHz, CDCl₃) δ [ppm] = 7.25 – 7.20 (m, 2H), 7.18 – 7.10 (m, 3H), 7.10 – 7.05 (m, 1H), 7.04 – 6.94 (m, 2H), 4.99 (s, 1H), 4.19 – 4.02 (m, 2H), 2.48 (s, 3H), 1.25 (s, 9H), 1.18 (t, $J = 7.1$ Hz, 3H), ¹³C{¹H} NMR (100 MHz, CDCl₃) δ [ppm] = 167.4, 160.1, 149.7, 149.2, 143.7, 129.4, 127.52, 127.45, 125.4, 125.3, 124.6, 116.3, 106.5, 60.3, 41.1, 34.5, 31.5, 19.7, 14.3, IR (film) ν [cm⁻¹] = 1714, 1644, 1585, 1487, 1457, 1380, 1365, 1337, 1288, 1251, 1236, 1217, 1190, 1105, 1064, 984, 754, 619, HR-MS (ESI): calc. for: ([M+Na]⁺): 373.1774; found: 373.1776, HPLC IA Column (99% hexane: 1% *i*-propanol, 1 mL/min, 270 nm) R_{t1} = 6.4 min and R_{t2} = 7.1 min.

(R)-Ethyl 4-(4-methoxyphenyl)-2-methyl-4H-chromene-3-carboxylate (**10f**). Hexane/MTBE (19:1) as eluent, Yield 70% (22.7 mg) as a colorless oil, er 92:8, $[\alpha]_D^{25} = -2^\circ$ ($c = 1.11$, CHCl_3), $^1\text{H NMR}$ (400 MHz, CDCl_3) δ [ppm] = 7.17 – 7.10 (m, 3H), 7.07 – 6.95 (m, 3H), 6.76 (d, $J = 8.6$ Hz, 2H), 4.97 (s, 1H), 4.18 – 4.02 (m, 2H), 3.74 (s, 3H), 2.47 (s, 3H), 1.20 (t, $J = 7.1$ Hz, 3H), $^{13}\text{C}\{^1\text{H}\}$ NMR (100 MHz, CDCl_3) δ [ppm] = 167.4, 159.9, 158.2, 149.5, 139.3, 129.3, 128.9, 127.5, 125.2, 124.6, 116.3, 113.9, 106.5, 60.3, 55.3, 40.7, 19.7, 14.3, IR (film) ν [cm^{-1}] = 1702, 1635, 1585, 1509, 1486, 1457, 1379, 1288, 1256, 1217, 1105, 1068, 1036, 849, 765, 754, HR-MS (ESI): calc. for: $[\text{M}+\text{Na}]^+$: 347.1254; found: 347.1253, HPLC ODH Column (99% hexane: 1% *i*-propanol, 1 mL/min, 270 nm) $R_{t1} = 8.7$ min and $R_{t2} = 9.8$ min.

(R)-Ethyl 6-bromo-4-(4-methoxyphenyl)-2-methyl-4H-chromene-3-carboxylate (**10g**). Hexane/MTBE (19:1) as eluent, Yield 94% (37.9 mg) as a white solid, er 91:9, $[\alpha]_D^{25} = +107^\circ$ ($c = 1.15$, CHCl_3), mp = 77 – 79°C, $^1\text{H NMR}$ (400 MHz, CDCl_3) δ [ppm] = 7.23 (dd, $J = 8.6, 2.3$ Hz, 1H), 7.15 (d, $J = 2.2$ Hz, 1H), 7.14 – 7.08 (m, 2H), 6.89 (d, $J = 8.7$ Hz, 1H), 6.81 – 6.75 (m, 2H), 4.92 (s, 1H), 4.16 – 4.02 (m, 2H), 3.75 (s, 3H), 2.46 (s, 3H), 1.19 (t, $J = 7.1$ Hz, 3H), $^{13}\text{C}\{^1\text{H}\}$ NMR (100 MHz, CDCl_3) δ [ppm] = 167.0, 159.6, 158.5, 148.6, 138.5, 132.0, 130.6, 128.9, 127.4, 118.2, 116.8, 114.1, 106.4, 60.4, 55.4, 40.7, 19.5, 14.3, IR (film) ν [cm^{-1}] = 1642, 1608, 1509, 1480, 1376, 1321, 1278, 1252, 1234, 1219, 1176, 1068, 1030, 810, HR-MS (ESI): calc. for: $[\text{M}+\text{Na}]^+$: 425.0359/427.0359; found: 425.0362/427.0362, HPLC ODH Column (99% hexane: 1% *i*-propanol, 1 mL/min, 270 nm) $R_{t1} = 7.3$ min and $R_{t2} = 8.8$ min.

General Procedure for Enantioselective Addition of 3-Oxobutanitrile.

Ortho-hydroxy benzyl alcohol **1** (0.10 mmol, 1.0 equiv.) and catalyst **5** (3.4 mg, 0.005 mmol, 5 mol %) were dissolved in chloroform (0.8 mL). 3-Oxobutanitrile (12.5 mg, 0.15 mmol, 1.5 equiv.) was added in portion and the reaction mixture was stirred for 3 days at 0°C until complete consumption of the starting material. Then *p*-toluenesulfonic acid monohydrate (22.8 mg, 0.12 mmol, 1.2 equiv.) was added and the reaction mixture was further stirred for 4 h at reflux. The crude reaction mixture was purified by short flash chromatography (hexane/MTBE 19:1) to afford the desired chromenes. The enantiomeric ratios were determined by HPLC on a chiral stationary phase.

(R)-6-(tert-Butyl)-4-(2-methoxyphenyl)-2-methyl-4H-chromene-3-carbonitrile (**11a**). Hexane/MTBE (19:1) as eluent, Yield 85% (28.3 mg) as a white solid, er 95:5, $[\alpha]_D^{25} = +131^\circ$ ($c = 1.02$, CHCl_3), mp = 107 – 109°C, $^1\text{H NMR}$ (400 MHz, CDCl_3) δ [ppm] = 7.25 – 7.15 (m, 2H), 7.05 (d, $J = 2.2$ Hz, 1H), 6.99 (dd, $J = 7.5, 1.5$ Hz, 1H), 6.95 – 6.86 (m, 3H), 5.27 (s, 1H), 3.88 (s, 3H), 2.29 (s, 3H), 1.19 (s, 9H), $^{13}\text{C}\{^1\text{H}\}$ NMR (100 MHz, CDCl_3) δ [ppm] = 161.9, 156.8, 148.1, 147.5, 132.3, 129.7, 128.6, 125.8, 125.3, 121.4, 121.3, 118.8, 115.8, 111.3, 88.3, 55.7, 35.0, 34.5, 31.4, 19.4, IR (KBr) ν [cm^{-1}] = 2963, 2210, 1655, 1596, 1588, 1490, 1463, 1387, 1271, 1253, 1135, 1028, 828, 758, HR-MS (ESI): calc. for: $[\text{M}+\text{Na}]^+$: 356.1621; found: 356.1619, HPLC ODH Column (98% hexane: 2% *i*-propanol, 1 mL/min, 270 nm) $R_{t1} = 6.9$ min and $R_{t2} = 8.1$ min.

(R)-4-(2-Ethylphenyl)-2,6-dimethyl-4H-chromene-3-carbonitrile (**11b**). Hexane/MTBE (19:1) as eluent, Yield 78% (22.6 mg) as a yellow oil, er 94.5:5.5, $[\alpha]_D^{25} = +92^\circ$ ($c = 0.52$, CHCl_3), $^1\text{H NMR}$ (400 MHz, CDCl_3) δ [ppm] = 7.25 – 7.11 (m, 3H), 7.05 – 6.95 (m, 2H), 6.91 (d, $J = 8.3$ Hz, 1H), 6.61 (s, 1H), 5.06 (s, 1H), 2.95 – 2.76 (m, 2H), 2.29 (s, 3H), 2.17 (s, 3H), 1.29 (t, $J = 7.5$ Hz, 3H), $^{13}\text{C}\{^1\text{H}\}$ NMR (100 MHz, CDCl_3) δ [ppm] = 161.0, 147.2, 141.7, 141.6, 134.9, 130.3, 129.6, 129.2, 129.1, 127.6, 127.0, 121.9, 118.6, 116.4, 89.0, 37.1, 26.0, 20.9, 19.4, 16.2, IR (KBr) ν [cm^{-1}] = 2324, 2200, 1680, 1615, 1592, 1569, 1500, 1433, 1416, 1390, 1253, 1280, 1132, 1105, 990, 947, HR-MS (ESI): calc. for: $[\text{M}+\text{Na}]^+$: 312.1359; found: 312.1357, HPLC ODH Column (98% hexane: 2% *i*-propanol, 1 mL/min, 270 nm) $R_{t1} = 14.1$ min and $R_{t2} = 15.1$ min.

(R)-6-Methoxy-4-(2-methoxyphenyl)-2-methyl-4H-chromene-3-carbonitrile (**11c**). Hexane/MTBE (19:1) as eluent, Yield 72% (22.1 mg) as a white solid, er 94:6, $[\alpha]_D^{25} = +123^\circ$ ($c = 0.80$, CHCl_3), mp = 131 – 133°C, $^1\text{H NMR}$ (400 MHz, CDCl_3) δ [ppm] = 7.25 – 7.17 (m, 1H), 7.09 – 6.97 (m, 1H), 6.98 – 6.84 (m, 3H), 6.71 (dd, $J = 8.9, 2.9$ Hz, 1H), 6.53 (d, $J = 2.9$ Hz, 1H), 5.25 (s, 1H), 3.86 (s, 3H), 3.67 (s, 3H), 2.29 (d, $J = 1.0$ Hz, 3H), $^{13}\text{C}\{^1\text{H}\}$ NMR (100 MHz, CDCl_3) δ [ppm] = 161.8, 156.7, 156.6, 143.7, 132.0, 129.8, 128.8, 123.0, 121.3, 118.8, 117.3, 114.0, 113.3, 111.4, 87.4, 55.8, 55.6, 35.2, 19.3, IR (KBr) ν [cm^{-1}] = 2214, 1653, 1587, 1494, 1430, 1385, 1327, 1288, 1246, 1205, 1031, 996, 820, 751, HR-MS (ESI): calc. for: $[\text{M}+\text{Na}]^+$: 330.1101; found: 330.1102, HPLC ASH Column (90% hexane: 10% *i*-propanol, 1 mL/min, 270 nm) $R_{t1} = 10.1$ min and $R_{t2} = 12.3$ min.

(R)-4-(2-Methoxyphenyl)-2,6-dimethyl-4H-chromene-3-carbonitrile (**11d**). Hexane/MTBE (19:1) as eluent, Yield 86% (25.1 mg) as a white solid, er 94:6, $[\alpha]_D^{25} = +134^\circ$ ($c = 0.93$, CHCl_3), mp = 51 – 53°C, $^1\text{H NMR}$ (400 MHz, CDCl_3) δ [ppm] = 7.25 – 7.19 (m, 1H), 7.01 (d, $J = 7.3$ Hz, 1H), 6.98 – 6.85 (m, 4H), 6.78 (s, 1H), 5.22 (s, 1H), 3.85 (s, 3H), 2.28 (s, 3H), 2.19 (s, 3H), $^{13}\text{C}\{^1\text{H}\}$ NMR (100 MHz, CDCl_3) δ [ppm] = 161.6, 156.8, 147.6, 134.6, 132.3, 129.9, 129.5, 128.9, 128.7, 121.7, 121.3, 118.8, 116.1, 111.4, 88.2, 55.8, 34.9, 20.9, 19.4, IR (KBr) ν [cm^{-1}] = 2209, 1654, 1579, 1492, 1461, 1438, 1386, 1327, 1261, 1242, 1213, 1132, 1102, 1026, 822, 814, 754, HR-MS (ESI): calc. for: $[\text{M}+\text{Na}]^+$: 314.1152; found: 314.1149, HPLC ODH Column (98% hexane: 2% *i*-propanol, 0.5 mL/min, 270 nm) $R_{t1} = 19.5$ min and $R_{t2} = 20.9$ min.

(R)-2-Methyl-4-(*p*-tolyl)-4H-chromene-3-carbonitrile (**11e**). Hexane/MTBE (19:1) as eluent, Yield 75% (19.6 mg) as a white solid, er 91.5:8.5, $[\alpha]_D^{25} = +35^\circ$ ($c = 0.81$, CHCl_3), mp = 83 – 85°C, $^1\text{H NMR}$ (400 MHz, CDCl_3) δ [ppm] = 7.23 – 7.16 (m, 1H), 7.14 (d, $J = 8.0$ Hz, 2H), 7.08 (d, $J = 8.1$ Hz, 2H), 7.06 – 6.99 (m, 2H), 6.99 – 6.89 (m, 1H), 4.70 (s, 1H), 2.32 (s, 3H), 2.30 (d, $J = 1.1$ Hz, 3H), $^{13}\text{C}\{^1\text{H}\}$ NMR (100 MHz, CDCl_3) δ [ppm] = 160.9, 149.1, 140.9, 137.4, 129.8, 128.5, 128.2, 125.3, 121.7, 118.5, 116.7, 89.4, 41.5, 21.2, 19.4, IR (KBr) ν [cm^{-1}] = 2210, 1655, 1584, 1511, 1488, 1455, 1385, 1336, 1250, 1125, 995, 845, 758, HR-MS (ESI): calc. for: $[\text{M}+\text{Na}]^+$: 284.1046; found: 284.1049, HPLC ODH Column (98% hexane: 2% *i*-propanol, 1 mL/min, 270 nm) $R_{t1} = 9.3$ min and $R_{t2} = 12.4$ min.

(R)-4-(4-Methoxyphenyl)-2-methyl-4H-chromene-3-carbonitrile (**11f**). Hexane/MTBE (19:1) as eluent, Yield

80% (22.2 mg) as a yellow oil, er 91.5:8.5, $[\alpha]_D^{25} = +93^\circ$ ($c = 0.56$, CHCl_3), $^1\text{H NMR}$ (400 MHz, CDCl_3) δ [ppm] = 7.25 – 7.17 (m, 1H), 7.12 (d, $J = 8.7$ Hz, 2H), 7.07 – 6.99 (m, 2H), 6.97 – 6.91 (m, 1H), 6.86 (d, $J = 8.7$ Hz, 2H), 4.70 (s, 1H), 3.78 (s, 3H), 2.36 – 2.24 (m, 3H), $^{13}\text{C}\{^1\text{H}\}$ NMR (100 MHz, CDCl_3) δ [ppm] = 160.7, 159.0, 149.0, 136.1, 129.8, 129.4, 128.5, 125.3, 121.8, 118.5, 116.7, 114.4, 89.4, 55.4, 41.0, 19.4, IR (film) ν [cm^{-1}] = 2210, 1654, 1607, 1509, 1455, 1384, 1251, 1177, 1031, 756, HR-MS (ESI): calc. for: $[\text{M}+\text{Na}]^+$: 300.0995; found: 300.0994, HPLC ODH Column (98% hexane: 2% *i*-propanol, 1 mL/min, 270 nm) $R_{t1} = 13.1$ min and $R_{t2} = 19.9$ min.

(*R*)-4-(4-(*tert*-Butyl)phenyl)-2-methyl-4*H*-chromene-3-carbonitrile (**11g**). Hexane/MTBE (19:1) as eluent, Yield 87% (26.4 mg) as a yellow oil, er 90:10, $[\alpha]_D^{25} = +140^\circ$ ($c = 0.50$, CHCl_3), $^1\text{H NMR}$ (400 MHz, CDCl_3) δ [ppm] = 7.32 (d, $J = 8.3$ Hz, 2H), 7.23 – 7.17 (m, 1H), 7.10 (d, $J = 8.3$ Hz, 2H), 7.06 – 7.00 (m, 2H), 7.00 – 6.95 (m, 1H), 4.71 (s, 1H), 2.30 (d, $J = 0.9$ Hz, 3H), 1.29 (s, 9H), $^{13}\text{C}\{^1\text{H}\}$ NMR (100 MHz, CDCl_3) δ [ppm] = 160.9, 150.4, 149.2, 140.7, 129.8, 128.5, 127.9, 125.9, 125.3, 121.8, 118.6, 116.7, 89.4, 41.4, 34.6, 31.5, 19.4, IR (film) ν [cm^{-1}] = 2962, 2210, 1653, 1585, 1489, 1458, 1386, 1337, 1251, 1210, 1191, 1182, 1128, 1105, 757, HR-MS (ESI): calc. for: $[\text{M}+\text{Na}]^+$: 326.1515; found: 326.1513, HPLC ODH Column (98% hexane: 2% *i*-propanol, 1 mL/min, 270 nm) $R_{t1} = 6.3$ min and $R_{t2} = 9.2$ min.

(*R*)-4-([1,1'-Biphenyl]-4-yl)-2-methyl-4*H*-chromene-3-carbonitrile (**11h**). Hexane/MTBE (19:1) as eluent, Yield 60% (19.4 mg) as a white solid, er 90:10, $[\alpha]_D^{25} = +122^\circ$ ($c = 0.67$, CHCl_3), mp = 152 – 154°C, $^1\text{H NMR}$ (400 MHz, CDCl_3) δ [ppm] = 7.60 – 7.52 (m, 4H), 7.46 – 7.39 (m, 2H), 7.37 – 7.31 (m, 1H), 7.30 – 7.19 (m, 3H), 7.09 – 7.02 (m, 2H), 7.00 (d, $J = 8.0$ Hz, 1H), 4.80 (s, 1H), 2.33 (s, 3H), $^{13}\text{C}\{^1\text{H}\}$ NMR (100 MHz, CDCl_3) δ [ppm] = 161.2, 149.2, 142.7, 140.7, 140.6, 129.8, 128.9, 128.73, 128.65, 127.8, 127.5, 127.2, 125.4, 121.4, 118.5, 116.8, 89.09, 41.6, 19.5, IR (KBr) ν [cm^{-1}] = 2210, 1654, 1487, 1455, 1386, 1335, 1324, 1252, 1127, 995, 852, 756, 697, HR-MS (ESI): calc. for: $[\text{M}+\text{Na}]^+$: 346.1202; found: 346.1199, HPLC ODH Column (98% hexane: 2% *i*-propanol, 1 mL/min, 270 nm) $R_{t1} = 13.2$ min and $R_{t2} = 19.8$ min.

(*R*)-4-(2-Methoxyphenyl)-2-methyl-4*H*-chromene-3-carbonitrile (**11i**). Hexane/MTBE (19:1) as eluent, Yield 80% (22.2 mg) as a white solid, er 90:10, $[\alpha]_D^{25} = +77^\circ$ ($c = 0.91$, CHCl_3), mp = 79 – 81°C, $^1\text{H NMR}$ (400 MHz, CDCl_3) δ [ppm] = 7.25 – 7.19 (m, 1H), 7.20 – 7.13 (m, 1H), 7.06 – 6.96 (m, 4H), 6.94 – 6.86 (m, 2H), 5.27 (s, 1H), 3.84 (s, 3H), 2.31 (d, $J = 1.0$ Hz, 3H), $^{13}\text{C}\{^1\text{H}\}$ NMR (100 MHz, CDCl_3) δ [ppm] = 161.6, 156.8, 149.5, 132.1, 129.9, 129.3, 128.8, 128.2, 125.1, 122.2, 121.3, 118.7, 116.4, 111.4, 88.4, 55.8, 34.9, 19.4, IR (KBr) ν [cm^{-1}] = 2210, 1658, 1598, 1585, 1490, 1457, 1387, 1340, 1330, 1288, 1253, 1129, 1024, 756, HR-MS (ESI): calc. for: $[\text{M}+\text{Na}]^+$: 300.0995; found: 300.0994, HPLC ODH Column (98% hexane: 2% *i*-propanol, 0.5 mL/min, 270 nm) $R_{t1} = 23.0$ min and $R_{t2} = 24.5$ min.

(*R*)-6-(*tert*-Butyl)-2-methyl-4-(*o*-tolyl)-4*H*-chromene-3-carbonitrile (**11j**). Hexane/MTBE (19:1) as eluent, Yield 89% (28.3 mg) as a yellow oil, er 96:4, $[\alpha]_D^{25} = +126^\circ$ ($c = 0.86$, CHCl_3), $^1\text{H NMR}$ (400 MHz, CDCl_3) δ [ppm] = 7.21 (dd, $J = 8.6$, 2.2 Hz, 1H), 7.19 – 7.12 (m, 3H), 7.06 – 6.99 (m, 1H),

6.94 (d, $J = 8.6$ Hz, 1H), 6.79 (d, $J = 2.0$ Hz, 1H), 5.06 (s, 1H), 2.44 (s, 3H), 2.28 (s, 3H), 1.17 (s, 9H), $^{13}\text{C}\{^1\text{H}\}$ NMR (100 MHz, CDCl_3) δ [ppm] = 161.1, 148.4, 147.2, 141.8, 135.5, 131.1, 130.1, 127.4, 126.9, 125.8, 125.6, 121.2, 118.6, 116.1, 88.7, 39.1, 34.5, 31.4, 19.8, 19.3, IR (KBr) ν [cm^{-1}] = 2963, 2211, 1654, 1615, 1489, 1461, 1385, 1364, 1327, 1270, 1252, 1134, 829, 753, 729, HR-MS (ESI): calc. for: $[\text{M}+\text{Na}]^+$: 340.1672; found: 340.1674, HPLC ODH Column (98% hexane: 2% *i*-propanol, 1.0 mL/min, 270 nm) $R_{t1} = 5.6$ min and $R_{t2} = 6.8$ min.

Synthesis of Compound 19.

3-Methylphenol (0.260 g, 2.41 mmol, 1.0 equiv.), ^{13}C -labelled paraformaldehyde (0.500 g, 16.1 mmol, 6.7 equiv.) and anhydrous MgCl_2 (0.344 g, 3.62 mmol, 1.5 equiv.) were suspended in THF (12 mL). NEt_3 (1.23 mL, 8.90 mmol, 3.7 equiv.) was added dropwise and the reaction mixture was stirred for 2 h at 65°C. The reaction mixture was acidified to pH = 2 with 1M aq. HCl and the aqueous layer was extracted with CH_2Cl_2 . The combined organic extracts were washed with brine, dried over Na_2SO_4 , filtered and concentrated under reduced pressure. The crude reaction mixture was purified by short flash chromatography (hexane/MTBE 9:1 → 4:1) to afford the ^{13}C -labelled aldehyde (0.297 g, 2.18 mmol, 91%).

Phenylmagnesium bromide (2M in THF, 2.71 mL, 5.43 mmol, 2.5 equiv.) was added dropwise to a solution of ^{13}C -labelled aldehyde (0.297 g, 2.17 mmol, 1.0 equiv.) in THF (3 mL). The reaction mixture was stirred for 2 h at RT, then cooled to 0°C and saturated aq. NH_4Cl -solution was added. The aqueous layer was extracted with MTBE. The combined organic extracts were washed with brine, dried over Na_2SO_4 , filtered and concentrated under reduced pressure. The crude reaction mixture was purified by short flash chromatography (hexane/MTBE 9:1 → 4:1) to afford the ^{13}C -labelled *ortho*-hydroxy benzyl alcohol **19** (0.347 g, 1.63 mmol, 75%).

^{13}C -Labelled 2-(Hydroxy(phenyl)methyl)-5-methylphenol (**19**) Yield 75% (0.347 g) as a colorless liquid, $^1\text{H NMR}$ (400 MHz, CDCl_3) δ [ppm] = 7.73 (s, 1H), 7.43 – 7.27 (m, 5H), 6.77 – 6.70 (m, 2H), 6.63 (dd, $J = 7.8$, 1.7 Hz, 1H), 6.02 (dd, $^1J_{13\text{CH}} = 145.0$, $J = 3.1$ Hz, 1H), 2.75 (dd, $J = 3.3$, 2.2 Hz, 1H), 2.29 (s, 3H), IR (KBr) ν [cm^{-1}] = 1617, 1581, 1508, 1492, 1451, 1420, 1287, 1225, 1156, 1105, 985, 950, 822, 796, 753, 700, 553, HR-MS (ESI): calc. for: $[\text{M}+\text{Na}]^+$: 238.0915; found: 238.0915.

Synthesis of Compound 21.

Benzyl alcohol **20** (0.258 g, 1.00 mmol, 1.0 equiv.) was dissolved in CH_3CN (10 mL) and cooled to 0°C. Iodine (9.90 mg, 0.04 mmol, 4 mol%) was added in portion and the reaction mixture was stirred for 3 h at RT. Saturated aq. $\text{Na}_2\text{S}_2\text{O}_3$ -solution was added upon complete consumption of the starting material and the aqueous layer was extracted with CH_2Cl_2 . The combined organic extracts were dried over Na_2SO_4 , filtered and concentrated under reduced pressure. The crude reaction mixture was purified by flash chromatography (hexane/MTBE 100:1 → 50:1 → 9:1) to afford the dimer **21** (0.131 g, 0.262 mmol, 52%).

4,4'-(Oxybis(phenylmethylene))bis(3-(methoxymethoxy)-1-methylbenzene) (**21**) Yield 52% as a colorless liquid, dr 1:1 $^1\text{H NMR}$ (400 MHz, CDCl_3) δ [ppm] = 7.58 – 7.53 (m, 2H),

7.38 – 7.33 (m, 4H), 7.25 – 7.15 (m, 6H), 6.89 – 6.80 (m, 4H), 5.79 (s, 1H), 5.77 (s, 1H), 5.02 (d, $J = 6.7$ Hz, 1H), 4.99 (d, $J = 6.7$ Hz, 1H), 4.93 (d, $J = 6.8$ Hz, 1H), 4.89 (d, $J = 6.7$ Hz, 1H), 3.18 (s, 3H), 3.14 (s, 2H), 2.31 (s, 3H), 2.31 (s, 3H), $^{13}\text{C}\{^1\text{H}\}$ NMR (100MHz, CDCl_3) δ [ppm] = 154.2, 154.1, 142.9, 142.8, 138.32, 138.25, 129.0, 128.8, 128.1, 127.6, 127.5, 127.4, 127.1, 127.0, 122.80, 122.75, 114.8, 114.6, 94.11, 94.1, 74.5, 74.2, 55.9, 55.8, 21.6, IR (film) ν [cm^{-1}] = 2952, 2923, 1613, 1581, 1504, 1493, 1453, 1250, 1152, 1078, 1014, 923, 787, 699, 601, 452, HR-MS (ESI): calc. for: $[\text{M}+\text{Na}]^+$: 512.2304; found: 512.2303.

ASSOCIATED CONTENT

Supporting Information

Control Experiments, Kinetic Studies, Online NMR, ^{13}C -Labelling Experiments, HR-ESI-MS-Studies, Theoretical Calculations, Crystallographic Data (PDF)
Copies of NMR spectra and HPLC chromatograms. (PDF)
X-ray data for **4f** (CIF)
X-ray data for **4p** (CIF)
X-ray data for **3** (CIF)

This material is available free of charge via the Internet at <http://pubs.acs.org>.

AUTHOR INFORMATION

Corresponding Author

*schneider@chemie.uni-leipzig.de

Notes

The authors declare no competing financial interest.

ACKNOWLEDGMENT

This work was generously supported through the Deutsche Forschungsgemeinschaft (SCHN 441/11-1 and 11-2). F. Göricke and M. Laue are grateful for doctoral fellowships provided by the Fonds der Chemischen Industrie and the Deutsche Bundesstiftung Umwelt, respectively. We thank Dr. P. Lönnecke (University of Leipzig) for the crystal structure analyses, Dr. S. Naumov (Leibniz Institute of Surface Engineering) for preliminary calculations, Priv.-Doz. Dr. C. Baldauf (Fritz-Haber-Institute) for his support with DFT-calculations and Prof. Dr. T. Heine (TU Dresden) for providing the computational infrastructure.

REFERENCES

[1] (a) Fries, K.; Kann, K. I. Ueber die Einwirkung von Brom und von Chlor auf Phenole: Substitutionsproducte, Pseudobromide und Pseudochloride. Ueber o-Pseudohalogenide und o-Methylenchinone aus o-Oxymesitylalkohol. *Liebigs Ann. Chem.* **1907**, *353*, 335-356. (b) Fries, K.; Hübner, E. Ueber 1-Methyl-2-naphtol und chinoide Abkömmlinge desselben. *Ber. Dtsch. Chem. Ges.* **1906**, *39*, 435-453.
[2] (a) Angle, S. R.; Yang, W. Synthesis and chemistry of a quinone methide model for anthracycline antitumor antibiotics. *J. Am. Chem. Soc.* **1990**, *112*, 4524-4528. (b) Angle, S. R.; Rainier, J. D.; Woytowicz, C. Synthesis and Chemistry of Quinone Methide Models for the Anthracycline Antitumor Antibiotics. *J. Org. Chem.* **1997**, *62*, 5884-5892. (c) Li, V.-S.; Choi, D.; Tang, M.-s.; Kohn, H. Concerning in Vitro Mitomycin-DNA Alkylation. *J. Am. Chem. Soc.* **1996**, *118*, 3765.

[3] Gardner, P. D.; Sarrafizadeh R., H.; Brandon, R. L. o-QUINONE METHIDE. *J. Am. Chem. Soc.* **1959**, *81*, 5515.
[4] Arduini, A.; Pochini, A.; Ungaro, R.; Domiano, P. o-Quinone methides. Part 3. X-Ray crystal structure and reactivity of a stable o-quinone methide in the E-configuration. *J. Chem. Soc., Perkin Trans. 1* **1986**, 1391-1395.
[5] Amouri, H.; Besace, Y.; Le Bras, J.; Vaissermann, J. General Synthesis, First Crystal Structure, and Reactivity of Stable o-Quinone Methide Complexes of Cp*Ir. *J. Am. Chem. Soc.* **1998**, *120*, 6171-6172.
[6] Select reviews: (a) van de Water, R. W.; Pettus, T. R. R. o-Quinone methides: intermediates underdeveloped and underutilized in organic synthesis. *Tetrahedron* **2002**, *58*, 5367-5405. (b) Pathak, T. P.; Sigman, M. S. Applications of *ortho*-Quinone Methide Intermediates in Catalysis and Asymmetric Synthesis. *J. Org. Chem.* **2011**, *76*, 9210-9215. (c) Bai, W.-J.; David, J. G.; Feng, Z.-G.; Weaver, M. G.; Wu, K.-L.; Pettus, T. R. R. The Domestication of *ortho*-Quinone Methides. *Acc. Chem. Res.* **2014**, *47*, 3655-3664. (d) Wang, Z.; Sun, J. Recent Advances in Catalytic Asymmetric Reactions of o-Quinone Methides. *Synthesis* **2015**, *47*, 3629-3644. (e) Caruana, L.; Fochi, M.; Bernardi, L. The Emergence of Quinone Methides in Asymmetric Organocatalysis. *Molecules* **2015**, *20*, 11733-11764. (f) Jaworski, A. A.; Scheidt, K. A. Emerging Roles of in Situ Generated Quinone Methides in Metal-Free Catalysis. *J. Org. Chem.* **2016**, *81*, 10145-10153. (g) Nielsen, C. D.-T.; Abas, H.; Spivey, A. C. Stereoselective Reactions of *ortho*-Quinone Methide and *ortho*-Quinone Methide Imines and Their Utility in Natural Product Synthesis. *Synthesis* **2018**, *50*, 4008-4018.
[7] Select reviews: (a) Willis, N. J.; Bray, C. D. *ortho*-Quinone Methides in Natural Product Synthesis. *Chem. Eur. J.* **2012**, *18*, 9160-9173. (b) Yang, B.; Gao, S. Recent advances in the application of Diels-Alder reactions involving o-quinodimethanes, aza-o-quinone methides and o-quinone methides in natural product total synthesis. *Chem. Soc. Rev.* **2018**, *47*, 7926-7953.
[8] Lumb, J.-P.; Choong, K. C.; Trauner, D. *ortho*-Quinone Methides from para-Quinones: Total Synthesis of Rubioncolin B. *J. Am. Chem. Soc.* **2008**, *130*, 9230-9231.
[9] (a) Zhang, Y.; Sigman, M. S. Palladium(II)-Catalyzed Enantioselective Aerobic Dialkoxylation of 2-Propenyl Phenols: A Pronounced Effect of Copper Additives on Enantioselectivity. *J. Am. Chem. Soc.* **2007**, *129*, 3076-3077. (b) Jensen, K. H.; Pathak, T. P.; Zhang, Y.; Sigman, M. S. Palladium-Catalyzed Enantioselective Addition of Two Distinct Nucleophiles across Alkenes Capable of Quinone Methide Formation. *J. Am. Chem. Soc.* **2009**, *131*, 17074-17075. (c) Jensen, K. H.; Webb, J. D.; Sigman, M. S. Advancing the Mechanistic Understanding of an Enantioselective Palladium-Catalyzed Alkene Difunctionalization Reaction. *J. Am. Chem. Soc.* **2010**, *132*, 17471-17482.
[10] Alden-Danforth, E.; Scerba, M. T.; Lectka, T. Asymmetric Cycloadditions of o-Quinone Methides Employing Chiral Ammonium Fluoride Precatalysts. *Org. Lett.* **2008**, *10*, 4951-4953.
[11] Luan, Y.; Schaus, S. E. Enantioselective Addition of Boronates to o-Quinone Methides Catalyzed by Chiral Biphenols. *J. Am. Chem. Soc.* **2012**, *134*, 19965-19968.
[12] Lv, H.; Jia, W.-Q.; Sun, L.-H.; Ye, S. N-Heterocyclic Carbene Catalyzed [4+3] Annulation of Enals and o-Quinone Methides: Highly Enantioselective Synthesis of Benzo- ϵ -Lactones. *Angew. Chem. Int. Ed.* **2013**, *52*, 8607-8610.
[13] Izquierdo, J.; Orue, A.; Scheidt, K. A. A Dual Lewis Base Activation Strategy for Enantioselective Carbene-Catalyzed Annulations. *J. Am. Chem. Soc.* **2013**, *135*, 10634-10637.
[14] Huang, Y.; Hayashi, T. Asymmetric Synthesis of Triarylmethanes by Rhodium-Catalyzed Enantioselective Arylation of Diarylmethylamines with Arylboroxines. *J. Am. Chem. Soc.* **2015**, *137*, 7556-7559.
[15] (a) Hu, H.; Liu, Y.; Guo, J.; Lin, L.; Xu, Y.; Liu, X.; Feng, X. Enantioselective synthesis of dihydrocoumarin derivatives by chiral scandium(iii)-complex catalyzed inverse-electron-demand hetero-Diels-Alder reaction. *Chem. Commun.* **2015**, *51*, 3835-3837.

- (b) Zheng, J.; Lin, L.; Dai, L.; Yuan, X.; Liu, X.; Feng, X. Chiral *N,N'*-Dioxide-Scandium(III) Complex-Catalyzed Asymmetric Friedel-Crafts Alkylation Reaction of *ortho*-Hydroxybenzyl Alcohols with C3-Substituted *N*-Protected Indoles. *Chem. Eur. J.* **2016**, *22*, 18254-18258. (c) Zhang, J.; Lin, L.; He, C.; Xiong, Q.; Liu, X.; Feng, X. A chiral scandium-complex-catalyzed asymmetric inverse-electron-demand oxa-Diels-Alder reaction of *o*-quinone methides with fulvenes. *Chem. Commun.* **2018**, *54*, 74-77. (d) Zhang, J.; Liu, X.; Guo, S.; He, C.; Xiao, W.; Lin, L.; Feng, X. Enantioselective Formal [4 + 2] Annulation of *ortho*-Quinone Methides with *ortho*-Hydroxyphenyl α,β -Unsaturated Compounds. *J. Org. Chem.* **2018**, *83*, 10175-10185.
- [16] (a) Görlicke, F.; Schneider, C. Palladium-Catalyzed Enantioselective Addition of Chiral Metal Enolates to In Situ Generated *ortho*-Quinone Methides. *Angew. Chem. Int. Ed.* **2018**, *57*, 14736-14741. (b) An, X.-T.; Du, J.-Y.; Jia, Z.-L.; Zhang, Q.; Yu, K.-Y.; Zhang, Y.-Z.; Zhao, X.-H.; Fang, R.; Fan, C.-A. Asymmetric Catalytic [4+5] Annulation of *ortho*-Quinone Methides with Vinyl ethylene Carbonates and its Extension to Stereoselective Tandem Rearrangement. *Chem. Eur. J.* **2020**, *26*, 3803-3809.
- [17] Select recent work: (a) Caruana, L.; Mondatori, M.; Corti, V.; Morales, S.; Mazzanti, A.; Fochi, M.; Bernardi, L. Catalytic Asymmetric Addition of Meldrum's Acid, Malononitrile, and 1,3-Dicarbonyls to *ortho*-Quinone Methides Generated In Situ Under Basic Conditions. *Chem. Eur. J.* **2015**, *21*, 6037-6041. (b) Zhou, J.; Wang, M.-L.; Gao, X.; Jiang, G.-F.; Zhou, Y.-G. Bifunctional squaramide-catalyzed synthesis of chiral dihydrocoumarins via *ortho*-quinone methides generated from 2-(1-tosylalkyl)phenols. *Chem. Commun.* **2017**, *53*, 3531-3534. (c) Zhang, T.; Ma, C.; Zhou, J.-Y.; Mei, G.-J.; Shi, F. Application of Homophthalic Anhydrides as 2C Building Blocks in Catalytic Asymmetric Cyclizations of *ortho*-Quinone Methides: Diastereo- and Enantioselective Construction of Dihydrocoumarin Frameworks. *Adv. Synth. Catal.* **2018**, *360*, 1128-1137. (d) Zhou, J.; Huang, W.-J.; Jiang, G.-F. Synthesis of Chiral Pyrazolone and Spiropyrazolone Derivatives through Squaramide-Catalyzed Reaction of Pyrazolin-5-ones with *o*-Quinone Methides. *Org. Lett.* **2018**, *20*, 1158-1161. (e) Cu, L.; Lv, D.; Wang, Y.; Fan, Z.; Li, Z.; Zhou, Z. Asymmetric Formal [4 + 2] Annulation of *o*-Quinone Methides with β -Keto Acylpyrazoles: A General Approach to Optically Active *trans*-3,4-Dihydrocoumarins. *J. Org. Chem.* **2018**, *83*, 4221-4228.
- [18] (a) Wu, X.; Xue, L.; Li, D.; Jia, S.; Ao, J.; Deng, J.; Yan, H. Organocatalytic Intramolecular [4+2] Cycloaddition between In Situ Generated Vinylidene *ortho*-Quinone Methides and Benzofurans. *Angew. Chem. Int. Ed.* **2017**, *56*, 13722-13726. (b) Yang, Q.-Q.; Xiao, W.-J. Catalytic Asymmetric Synthesis of Chiral Dihydrobenzofurans through a Formal [4+1] Annulation Reaction of Sulfur Ylides and In Situ Generated *ortho*-Quinone Methides. *Eur. J. Org. Chem.* **2017**, 233-236.
- [19] (a) Barbato, K. S.; Luan, Y.; Ramella, D.; Panek, J. S.; Schaus, S. E. Enantioselective Multicomponent Condensation Reactions of Phenols, Aldehydes, and Boronates Catalyzed by Chiral Biphenols. *Org. Lett.* **2015**, *17*, 5812-5815. (b) Grayson, M. N.; Goodman, J. M. Asymmetric Boronate Addition to *o*-Quinone Methides: Ligand Exchange, Solvent Effects, and Lewis Acid Catalysis. *J. Org. Chem.* **2015**, *80*, 2056-2061.
- [20] (a) Wang, Z.; Wang, T.; Yao, W.; Lu, Y. Phosphine-Catalyzed Enantioselective [4 + 2] Annulation of *o*-Quinone Methides with Allene Ketones. *Org. Lett.* **2017**, *19*, 4126-4129. (b) Zhou, T.; Xia, T.; Liu, Z.; Liu, L.; Zhang, J. Asymmetric Phosphine-Catalyzed [4+1] Annulations of *o*-Quinone Methides with MBH Carbonates. *Adv. Synth. Catal.* **2018**, *360*, 4475-4479. (c) Cheng, Y.; Fang, Z.; Li, W.; Li, P. Phosphine-mediated enantioselective [4 + 1] annulations between *ortho*-quinone methides and Morita-Baylis-Hillman carbonates. *Org. Chem. Front.* **2018**, *5*, 2728-2733. (d) Zhang, S.; Yu, X.; Pan, J.; Jiang, C.; Zhang, H.; Wang, T. Asymmetric synthesis of spiro-structural 2,3-dihydrobenzofurans via the bifunctional phosphonium salt-promoted [4 + 1] cyclization of *ortho*-quinone methides with α -bromoketones. *Org. Chem. Front.* **2019**, *6*, 3799-3803.
- [21] (a) Adili, A.; Tao, Z.-L.; Chen, D.-F.; Han, Z.-Y. Quinine-catalyzed highly enantioselective cycloannulation of *o*-quinone methides with malononitrile. *Org. Biomol. Chem.* **2015**, *13*, 2247-2250. (b) Zhu, Y.; Zhang, L.; Luo, S. Asymmetric Retro-Claisen Reaction by Chiral Primary Amine Catalysis. *J. Am. Chem. Soc.* **2016**, *138*, 3978-3981. (c) Deng, Y.-H.; Chu, W.-D.; Zhang, X.-Z.; Yan, X.; Yu, K.-Y.; Yang, L.-L.; Huang, H.; Fan, C.-A. *Cinchona* Alkaloid Catalyzed Enantioselective [4 + 2] Annulation of Allenic Esters and *in Situ* Generated *ortho*-Quinone Methides: Asymmetric Synthesis of Functionalized Chromans. *J. Org. Chem.* **2017**, *82*, 5433-5440. (d) Zhu, Y.; Zhang, W.-Z.; Zhang, L.; Luo, S. Chiral Primary Amine Catalyzed Asymmetric α -Benzoylation with In Situ Generated *ortho*-Quinone Methides. *Chem. Eur. J.* **2017**, *23*, 1253-1257. (e) Meisinger, N.; Roiser, L.; Monkowius, U.; Himmelsbach, M.; Robiette, R.; Waser, M. Asymmetric Synthesis of 2,3-Dihydrobenzofurans by a [4+1] Annulation Between Ammonium Ylides and In Situ Generated *o*-Quinone Methides. *Chem. Eur. J.* **2017**, *23*, 5137-5142. (f) Lian, X.-L.; Adili, A.; Liu, B.; Tao, Z.-L.; Han, Z.-Y. Enantioselective [4 + 1] cycloaddition of *ortho*-quinone methides and bromomalones under phase-transfer catalysis. *Org. Biomol. Chem.* **2017**, *15*, 3670-3673. (g) Jin, J.-H.; Li, X.-Y.; Luo, X.; Fossey, J. S.; Deng, W.-P. Asymmetric Synthesis of *cis*-3,4-Dihydrocoumarins via [4 + 2] Cycloadditions Catalyzed by Amidine Derivatives. *J. Org. Chem.* **2017**, *82*, 5424-5432. (h) Zhou, D.; Yu, X.; Zhang, J.; Wang, W.; Xie, H. Organocatalytic Asymmetric Formal [4 + 2] Cycloaddition of *in Situ* Oxidation-Generated *ortho*-Quinone Methides and Aldehydes. *Org. Lett.* **2018**, *20*, 174-177. (i) Zhang, J.; Zhang, S.; Yang, H.; Zhou, D.; Yu, X.; Wang, W.; Xie, H. A general asymmetric route to *enantio*-enriched isoflavanes via an organocatalytic annulation of *o*-quinone methides and aldehydes. *Tetrahedron Lett.* **2018**, *59*, 2407-2411.
- [22] (a) Lee, A.; Scheidt, K. A. *N*-Heterocyclic carbene-catalyzed enantioselective annulations: a dual activation strategy for a formal [4+2]-addition for dihydrocoumarins. *Chem. Commun.* **2015**, *51*, 3407-3410. (b) Wang, Y.; Pan, J.; Dong, J.; Yu, C.; Li, T.; Wang, X.-S.; Shen, S.; Yao, C. *N*-Heterocyclic Carbene-Catalyzed [4 + 2] Cyclization of Saturated Carboxylic Acid with *o*-Quinone Methides through In Situ Activation: Enantioselective Synthesis of Dihydrocoumarins. *J. Org. Chem.* **2017**, *82*, 1790-1795. (c) Chen, X.; Song, R.; Liu, Y.; Ooi, C.Y.; Jin, Z.; Zhu, T.; Wang, H.; Hao, L.; Chi, Y. R. Carbene and Acid Cooperative Catalytic Reactions of Aldehydes and *o*-Hydroxybenzhydryl Amines for Highly Enantioselective Access to Dihydrocoumarins. *Org. Lett.* **2017**, *19*, 5892-5895. (d) Lu, S.; Ong, J.-Y.; Yang, H.; Poh, S. B.; Liew, X.; Seow, C. S. D.; Wong, M. W.; Zhao, Y. Diastereo- and Atroposelective Synthesis of Bridged Biaryls Bearing an Eight-Membered Lactone through an Organocatalytic Cascade. *J. Am. Chem. Soc.* **2019**, *141*, 17062-17067.
- [23] Pandit, R. P.; Kim, S. T.; Ryu, D. H. Asymmetric Synthesis of Enantioenriched 2-Aryl-2,3-Dihydrobenzofurans by a Lewis Acid Catalyzed Cyclopropanation/Intramolecular Rearrangement Sequence. *Angew. Chem. Int. Ed.* **2019**, *58*, 13427-13432.
- [24] Wilcke, D.; Herdtweck, E.; Bach, T. Enantioselective Brønsted Acid Catalysis in the Friedel-Crafts Reaction of Indoles with Secondary *ortho*-Hydroxybenzyl Alcohols. *Synlett* **2011**, 1235-1238.
- [25] Rueping, M.; Uria, U.; Lin, M. Y.; Atodiresei, I. Chiral Organic Contact Ion Pairs in Metal-Free Catalytic Asymmetric Allylic Substitutions. *J. Am. Chem. Soc.* **2011**, *133*, 3732-3735.
- [26] El-Sepelgy, O.; Haseloff, S.; Alamsetti, S. K.; Schneider, C. Brønsted Acid Catalyzed, Conjugate Addition of β -Dicarbonyls to In Situ Generated *ortho*-Quinone Methides—Enantioselective Synthesis of 4-Aryl-4*H*-Chromenes. *Angew. Chem. Int. Ed.* **2014**, *53*, 7923-7927.
- [27] Hsiao, C.-C.; Liao, H.-H.; Rueping, M. Enantio- and Diastereoselective Access to Distant Stereocenters Embedded within Tetrahydroxanthenes: Utilizing *ortho*-Quinone Methides as

Reactive Intermediates in Asymmetric Brønsted Acid Catalysis. *Angew. Chem. Int. Ed.* **2014**, *53*, 13258-13263.

[28] (a) Zhao, W.; Wang, Z.; Chu, B.; Sun, J. Enantioselective Formation of All-Carbon Quaternary Stereocenters from Indoles and Tertiary Alcohols Bearing A Directing Group. *Angew. Chem. Int. Ed.* **2015**, *54*, 1910-1913. b) Wang, Z.; Ai, F.; Wang, Z.; Zhao, W.; Zhu, G.; Lin, Z.; Sun, J. Organocatalytic Asymmetric Synthesis of 1,1-Diarylethanes by Transfer Hydrogenation. *J. Am. Chem. Soc.*, **2015**, *137*, 383-389.

[29] Select recent work, for a more comprehensive compilation see the reviews in [6]: (a) Saha, S.; Schneider, C. Brønsted Acid-Catalyzed, Highly Enantioselective Addition of Enamides to In Situ-Generated *ortho*-Quinone Methides: A Domino Approach to Complex Acetamidotetrahydroxanthenes. *Chem. Eur. J.* **2015**, *21*, 2348-2352. (b) Saha, S.; Alamsetti, S. K.; Schneider, C. Chiral Brønsted acid-catalyzed Friedel-Crafts alkylation of electron-rich arenes with *in situ*-generated *ortho*-quinone methides: highly enantioselective synthesis of diarylindolylmethanes and triarylmethanes. *Chem. Commun.* **2015**, *51*, 1461-1464. (c) Saha, S.; Schneider, C. Directing Group Assisted Nucleophilic Substitution of Propargylic Alcohols via *o*-Quinone Methide Intermediates: Brønsted Acid Catalyzed, Highly Enantio- and Diastereoselective Synthesis of 7-Alkynyl-12a-acetamido-Substituted Benzoxanthenes. *Org. Lett.* **2015**, *17*, 648-651. (d) Zhao, J. J.; Sun, S. B.; He, S. H.; Wu, Q.; Shi, F. Catalytic Asymmetric Inverse-Electron-Demand Oxa-Diels-Alder Reaction of In Situ Generated *ortho*-Quinone Methides with 3-Methyl-2-Vinylindoles. *Angew. Chem. Int. Ed.* **2015**, *54*, 5460-5463. (e) Hsiao, C. C.; Raja, S.; Liao, H. H.; Atodiressei, I.; Rueping, M. *Ortho*-Quinone Methides as Reactive Intermediates in Asymmetric Brønsted Acid Catalyzed Cycloadditions with Unactivated Alkenes by Exclusive Activation of the Electrophile. *Angew. Chem. Int. Ed.* **2015**, *54*, 5762-5765. (f) Tsui, G. C.; Liu, L.; List, B. The Organocatalytic Asymmetric Prins Cyclization. *Angew. Chem. Int. Ed.* **2015**, *54*, 7703-7706. (g) Alamsetti, S. K.; Spanka, M.; Schneider, C. Synergistic Rhodium/Phosphoric Acid Catalysis for the Enantioselective Addition of Oxonium Ylides to *ortho*-Quinone Methides. *Angew. Chem. Int. Ed.* **2016**, *55*, 2392-2396. (h) Yu, X.-Y.; Chen, J.-R.; Wei, Q.; Cheng, H.-G.; Liu, Z.-C.; Xiao, W.-J. Catalytic Asymmetric Cycloaddition of In Situ-Generated *ortho*-Quinone Methides and Azlactones by a Triple Brønsted Acid Activation Strategy. *Chem. Eur. J.* **2016**, *22*, 6774-6778. (i) Zhang, Y.-C.; Zhu, Q.-N.; Yang, X.; Zhou, L.-J.; Shi, F. Merging Chiral Brønsted Acid/Base Catalysis: An Enantioselective [4 + 2] Cycloaddition of *o*-Hydroxystyrenes with Azlactones. *J. Org. Chem.* **2016**, *81*, 1681-1688. (j) Xu, M.-M.; Wang, H.-Q.; Wan, Y.; He, G.; Yan, J.; Zhang, S.; Wang, S.-L.; Shi, F. Catalytic asymmetric substitution of *ortho*-hydroxybenzyl alcohols with tetronic acid-derived enamines: enantioselective synthesis of tetronic acid-derived diarylmethanes. *Org. Chem. Front.* **2017**, *4*, 358-368.

[30] Further select recent work: (a) Wang, Z.; Sun, J. Enantioselective [4 + 2] Cycloaddition of *o*-Quinone Methides and Vinyl Sulfides: Indirect Access to Generally Substituted Chiral Chromanes. *Org. Lett.* **2017**, *19*, 2334-2337. (b) Xie, Y.; List, B. Catalytic Asymmetric Intramolecular [4+2] Cycloaddition of In Situ Generated *ortho*-Quinone Methides. *Angew. Chem. Int. Ed.* **2017**, *56*, 4936-4940. (c) Wu, J.-L.; Wang, J.-Y.; Wu, P.; Mei, G.-J.; Shi, F. Catalytic asymmetric C2-nucleophilic substitutions of C3-substituted indoles with *ortho*-hydroxybenzyl alcohols. *Org. Chem. Front.* **2017**, *4*, 2465-2479. (d) Gebauer, K.; Reuß, F.; Spanka, M.; Schneider, C. Relay Catalysis: Manganese(III) Phosphate Catalyzed Asymmetric Addition of β -Dicarbonyls to *ortho*-Quinone Methides Generated by Catalytic Aerobic Oxidation. *Org. Lett.* **2017**, *19*, 4588-4591. (e) Spanka, M.; Schneider, C. Phosphoric Acid Catalyzed Aldehyde Addition to in Situ Generated *o*-Quinone Methides: An Enantio- and Diastereoselective Entry toward *cis*-3,4-Diaryl Dihydrocoumarins. *Org. Lett.* **2018**, *20*, 4769-4772. (f) Suneja, A.; Schneider, C. Phosphoric Acid Catalyzed [4 + 1]-

Cycloannulation Reaction of *ortho*-Quinone Methides and Diazoketones: Catalytic, Enantioselective Access toward *cis*-2,3-Dihydrobenzofurans. *Org. Lett.* **2018**, *20*, 7576-7580. (g) Sun, M.; Ma, C.; Zhou, S.-J.; Lou, S.-F.; Xiao, J.; Jiao, Y.; Shi, F. Catalytic Asymmetric (4+3) Cyclizations of In Situ Generated *ortho*-Quinone Methides with 2-Indolylmethanols. *Angew. Chem. Int. Ed.* **2019**, *58*, 8703-8708. (h) Jiang, F.; Chen, K.-W.; Wu, P.; Zhang, Y.-C.; Jiao, Y.; Shi, F. A Strategy for Synthesizing Axially Chiral Naphthyl-Indoles: Catalytic Asymmetric Addition Reactions of Racemic Substrates. *Angew. Chem. Int. Ed.* **2019**, *58*, 15104-15110. (i) Ukis, R.; Schneider, C. Brønsted Acid-Catalyzed, Diastereo- and Enantioselective, Intramolecular Oxa-Diels-Alder Reaction of *ortho*-Quinone Methides and Unactivated Dienophiles. *J. Org. Chem.* **2019**, *84*, 7175-7188. (j) Suneja, A.; Loui, H. J.; Schneider, C. Cooperative Catalysis for the Highly Diastereo- and Enantioselective [4+3]-Cycloannulation of *ortho*-Quinone Methides and Carbonyl Ylides. *Angew. Chem. Int. Ed.* **2020**, *59*, 5536-5540.

[31] CCDC 969295 (**4f**), CCDC 1561287 (**4p**) and CCDC 1997560 (**3**) contain the supplementary crystallographic data for this paper and can be obtained free of charge from The Cambridge Crystallographic Data Centre via www.ccdc.cam.ac.uk/data_request/cif. For details concerning the crystal structures of **4f**, **4p** and **3** see the Supporting Information as well.

[32] Jurd, L. Quinones and quinone-methides — I: Cyclization and dimerisation of crystalline *ortho*-quinone methides from phenol oxidation reactions. *Tetrahedron* **1977**, *33*, 163-168.

[33] (a) Blackmond, D. G. Reaction Progress Kinetic Analysis: A Powerful Methodology for Mechanistic Studies of Complex Catalytic Reactions. *Angew. Chem. Int. Ed.* **2005**, *44*, 4302-4320. (b) Mathew, J. S.; Klussmann, M.; Iwamura, H.; Valera, F.; Futran, A.; Emanuelsson, E. A. C.; Blackmond, D. G. Investigations of Pd-Catalyzed ArX Coupling Reactions Informed by Reaction Progress Kinetic Analysis. *J. Org. Chem.* **2006**, *71*, 4711-4722. (c) Blackmond, D. G. Kinetic Profiling of Catalytic Organic Reactions as a Mechanistic Tool. *J. Am. Chem. Soc.* **2015**, *137*, 10852-10866. (d) Nielsen, C. D.; Burés, J. Visual kinetic analysis. *Chem. Sci.* **2019**, *10*, 348-353.

[34] Burés, J. A Simple Graphical Method to Determine the Order in Catalyst. *Angew. Chem. Int. Ed.* **2016**, *55*, 2028-2031.

[35] For a recent insightful analysis see: Jansen, D.; Gramüller, J.; Niemeyer, F.; Schaller, T.; Letzel, M. C.; Grimme, S.; Zhu, H.; Gschwind, R. M.; Niemeyer, J. What is the role of acid-acid interactions in asymmetric phosphoric acid organocatalysis? A detailed mechanistic study using interlocked and non-interlocked catalysts. *Chem. Sci.* **2020**, *11*, 4381-4390.

[36] σ_p^+ and σ_m were taken from Hansch, C.; Leo, A.; Taft, R. W. A survey of Hammett substituent constants and resonance and field parameters. *Chem. Rev.* **1991**, *91*, 165-195.

[37] (a) Klamt, A.; Schuurmann, G. COSMO: A New Approach to Dielectric Screening in Solvents with Explicit Expressions for the Screening Energy and its Gradient. *J. Chem. Soc. Perkin Trans 2* **1993**, 799-805. (b) Ernzerhof, M.; Scuseria, G. E. Assessment of the Perdew-Burke-Ernzerhof exchange-correlation functional. *J. Chem. Phys.* **1999**, *110*, 5029-5036. (c) Grimme, S. Accurate Description of van der Waals Complexes by Density Functional Theory Including Empirical Corrections. *J. Comput. Chem.* **2004**, *25*, 1463.

[38] te Velde, G.; Bickelhaupt, F. M.; Baerends, E. J.; Fonseca Guerra, C.; van Gisbergen, S. J. A.; Snijders, J. G.; Ziegler, T. Chemistry with ADF. *J. Comput. Chem.* **2001**, *22*, 931-967.

[39] Henkelman, G.; Uberuaga, B. P.; Jónsson, H. A climbing image nudged elastic band method for finding saddle points and minimum energy paths. *J. Chem. Phys.* **2000**, *113*, 9901-9904.